THE DESIGN AND EVALUATION OF A WATER DELIVERY SYSTEM FOR EVAPORATIVE COOLING OF A PROTON EXCHANGE MEMBRANE FUEL CELL

A Thesis

by

DAWOOD KHALED ABDULLAH AL-ASAD

Submitted to the Office of Graduate Studies of
Texas A&M University
in partial fulfillment of the requirements for the degree of

MASTER OF SCIENCE

August 2006

Major Subject: Mechanical Engineering

THE DESIGN AND EVALUATION OF A WATER DELIVERY SYSTEM FOR EVAPORATIVE COOLING OF A PROTON EXCHANGE MEMBRANE FUEL CELL

A Thesis

by

DAWOOD KHALED ABDULLAH AL-ASAD

Submitted to the Office of Graduate Studies of
Texas A&M University
in partial fulfillment of the requirements for the degree of

MASTER OF SCIENCE

Approved by:

Co-Chairs of Committee,	Thomas R. Lalk
	A. J. Appleby
Committee Members,	Chii-Der S. Suh
	Terry L. Kohutek
Head of Department,	Dennis O'Neal

August 2006

Major Subject: Mechanical Engineering

ABSTRACT

The Design and Evaluation of a Water Delivery System for Evaporative Cooling of a Proton Exchange Membrane Fuel Cell. (August 2006)

Dawood Khaled Abdullah Al-Asad, B.S., Bangladesh University of Engineering & Technology

Co-Chairs of Advisory Committee: Dr. Thomas R. Lalk
Dr. A. J. Appleby

An investigation was performed to demonstrate system design for the delivery of water required for evaporative cooling of a proton exchange membrane fuel cell (PEMFC). The water delivery system uses spray nozzles capable of injecting water directly and uniformly to the nickel metal foam flow-field (element for distributing the reactant gases over the surface of the electrodes) on the anode side from which water can migrate to the cathode side of the cell via electroosmotic drag. For an effective overall cooling, water distribution over the surface of the nickel foam has to be uniform to avoid creation of hotspots within the cell. A prototype PEMFC structure was constructed modeled after a 35 kW electrical output PEMFC stack. Water was sprayed on the nickel metal foam flow-field using two types of nozzle spray, giving conical fog type flow and flat fan type flow. A detailed investigation of the distribution pattern of water over the surface of the nickel metal flow field was conducted. The motive behind the investigation was to determine if design parameters such as type of water flow from nozzles, vertical location of the water nozzles above the flowfield, area of the nozzles, or operating variables such as reactant gas flow had any effect on water distribution over the surface of the Ni-metal foam flow field. It was found that the design parameters (types of flow, area and location of the nozzle) had a direct impact on the distribution of water in the nickel metal foam. However, the operating variable, reactant gas flow, showed no effect on the water distribution pattern in the Ni-foam.

ACKNOWLEDGEMENTS

I would like to thank Dr. Thomas R. Lalk, Co-Chair of my committee, for guiding and encouraging me towards the accomplishment of my graduate studies and helping me with all the problems I faced while conducting the research. I consider myself fortunate to have had the opportunity to work under his supervision. Actually his vision has taught me to think methodically to solve problems, no matter how complicated the problem is. I believe, without his support and guidance, it would have been simply impossible for me to complete this research project.

I also thank Dr. A. J. Appleby for his extreme help and technical advice in accomplishing the research project and overall learning process of the fuel cell systems. Sometimes, I wonder how a how world renowned scientist like Dr. Appleby can be so humble. I wish more people were like him, and I will always cherish my experience of working with him.

I would also like to thank Dr. Terry L. Kohutek for taking the time to serve as a member of my committee and providing valuable suggestions. I will always remember the support you provided that helped me to sustain the hardships of graduate studies.

I would also like to thank and extend my special gratitude to Dr. Chii-Der Steve Suh for all his time and assistance toward this project.

I must thank Dr. Alan B. Palazzolo for taking time out of his extremely busy schedule to sit in my thesis presentation as a committee member. I am really grateful to you for this generosity.

Last but not the least, I would like to say a special thanks to Erik Snyder and Joy Xiaole. You people helped me whenever I needed it most. So, thanks a lot.

TABLE OF CONTENTS

Page

ABSTRACT iii

ACKNOWLEDGEMENTS iv

TABLE OF CONTENTS v

LIST OF FIGURES ix

LIST OF TABLES xii

1. INTRODUCTION 1

1.1 General interest 2
1.2 Specific interest 5
1.3 Objective 6
1.4 Scope of research 6
1.5 Organization of the thesis 7

2. BASIC UNDERSTANDING OF THE FUEL CELL 8

2.1 What is a fuel cell and how does it work 8
2.1.1 Basic structure and electrochemistry of PEM fuel cells 11
2.1.2 Thermodynamics of PEM fuel cell: maximum work and efficiency 15
2.1.3 Irreversibilities and waste thermal energy 20
2.2 Construction of PEM fuel cell stack 21
2.2.1 Design approach for fuel cell stack 22
2.2.1.1 Components of PEMFC stack 22
2.2.1.1.1 MEA (membrane electrode assembly) 22
2.2.1.1.2 Flow fields 23
2.2.1.1.3 Bipolar plates 25

3. WATER AND THERMAL MANAGEMENT OF PEM FUEL CELL 26

3.1 Water management 26

3.1.1 Typical water management methods 27
3.1.1.1 Reactant gas humidification 28
3.1.1.2 Wicking method 28

Page

3.1.2 Removal of water from the cell 28
3.2 Thermal management of PEMFC 29
3.3 Evaporative cooling, an innovative way of dealing the thermal management of PEM fuel cell stacks 32

4. EVAPORATIVE COOLING 33

4.1 What is evaporative cooling and how it can be used in PEMFC thermal management 33
4.2 Electroosmotic drag and its relevance in evaporative cooling 34
4.3 Water requirement for evaporative cooling 35
4.4 Design approach to attain a realistic design solution for water delivery system 44
4.4.1 Need statement 45
4.4.2 Need analysis 45
4.5 Means to supply water to the fuel cell 47
4.6 Critical parameters and their influence on the design 48
4.6.1 Design parameters 49
4.6.1.1 Type of water spray pattern 49
4.6.1.1.1 Flat fan flow pattern 50
4.6.1.1.2 Finely atomized conical spray pattern 51
4.6.1.1.3 Atomization of water 51
4.6.1.2 Height (H) of the nozzle 52
4.6.1.3 Area of the nozzle orifice 52
4.6.2 Operating parameters 52
4.6.2.1 Reactant gas flow 53
4.6.2.1.1 Calculation of velocity of hydrogen in the PEMFC 53
4.6.2.1.2 Calculation of terminal velocity of the water particle 56
4.6.2.1.3 Equations for water particle motion moving in a fluid 58

5. EXPERIMENTAL SET-UP AND PROCEDURES 63

5.1 General description 63
5.2 Experimental set-up 67
5.2.1 Description of experimental set-up to measure the average water mass flow output of the nozzles 67

Page

5.2.2 Description of experimental set-up to determine the water distribution over the surface of the Ni-metal foam flow field 68
5.3 Apparatus 70
5.3.1 PEMFC model structure 70
5.3.2 Nozzles 71
5.3.3 MKS 1159B mass flow controller 73
5.3.4 Watts IWTG pressure gauge 74
5.3.5 Nickel metal foam 75
5.3.6 Water collector 75
5.4 Experimental procedures 76
5.4.1 Measurement of average water mass flow output from the nozzles 76
5.4.1.1 Precautions taken for the experiment 77
5.4.1.2 Experimental procedure to measure the water mass flow rate of the nozzles 78
5.4.2 Determination of the water distribution pattern over the Ni-metal foam flow field surface 78
5.4.2.1 Experimental procedure to investigate the effect of nozzle distance (H) from the Ni-metal foam on water distribution over the Ni-metal foam surface 80
5.4.2.2 Experimental procedure to determine the effect of the nozzle area on the water distribution over the Ni-metal foam surface 80
5.4.2.3 Experimental procedure to investigate the effect of reactant gas flow on the water distribution over the Ni-metal foam surface 81

6. RESULTS AND DISCUSSION 82

6.1 Introduction 82
6.2 Mass flow rate of water from the nozzles 83
6.3 Distribution of water over the surface of the Ni-metal foam 84
6.3.1 Influence of type of flows on the distribution of water over the surface of the Ni-metal foam 85
6.3.2 Influence of nozzle tip height (H) on the distribution of water over the Ni-metal foam surface 87
6.3.2.1 Dependence of water distribution over the Ni- metal foam surface for the case of conical fog flow from PJ type nozzles 87

Page

6.3.2.2 Dependence of water distribution over the Ni- metal foam surface for the case of flat fan flow from BJ type nozzles 88
6.4 Influence of nozzle orifice area (A) on the distribution of water over the Ni- metal foam surface 89
6.4.1 Influence of nozzle orifice area (A) on the distribution of water over the Ni-metal foam surface for conical fog flow pattern from PJ nozzles 90
6.4.2 Influence of nozzle orifice area (A) on the distribution of water over the Ni-metal foam surface for flat fan type flow pattern from BJ nozzles 91
6.5 Influence of reactant gas flow on the distribution of water over the Ni-metal foam surface 92

7. FINDINGS 94

8. CONCLUSIONS 95

9. RECOMMENDATIONS 96

REFERENCES 97

APPENDIX A 99

APPENDIX B 124

VITA 128

LIST OF FIGURES

Page

Figure 1: A typical PEM fuel cell and its working principle……..... 100

Figure 2: Schematic representation of PEMFC…… 100

Figure 3a: Components of a typical PEMFC…..…… 101

Figure 3b: Extra holes in bipolar plate for running cooling air…… 101

Figure 4: Structures of sulphonated fluoroethylene..…… 102

Figure 5: Structure of Nafion^{TM} membrane and the movement of water particles in it……...……. 103

Figure 6: A typical polarization curve for a PEMFC……..... 103

Figure 7a: Side view of water cooled PEMFC stack……... 104

Figure 7b: PEMFC stack. Top view…… 104

Figure 7c: PEMFC stack. Bottom view…….. 105

Figure 8: Dismantled PEMFC stack…….. 105

Figure 9: Membrane electrode assembly by 3M Corporation...…… 106

Figure 10: Various patterns of flow fields……... 106

Figure 11: Ni-metal foam flow field used in this research project…….. 107

Figure 12: A microscopic view of the Ni-metal flow field used in this research project…….. 107

Figure 13: Various water movements in MEA…… 108

Figure 14: Temperature vs. moles of water added per mole of H_2 curve. For this plot, S = 2.5, V = 0.8 and Pt =1 atm……. 108

Figure 15: Flat fan type water spray from BJ type nozzles used in this research project…….. 109

Figure 16: Schematic of a flat fan spray pattern used in this research project……. 109

Figure 17: Datasheet containing the various aspects of the nozzle utilized for the flat fan flow pattern…… 110

Figure 18: Finely atomized conical fog spray pattern of water…… 111

Figure 19: Conical fog/mist created by the finely atomized water droplets…… 111

Page

Figure 20: Datasheet containing the overview of the nozzle used for producing finely atomized conical flow pattern (PJ type nozzle)…… 112

Figure 21: Schematic diagram of various forces acting on a water particle in reactant gas (H_2) environment…… 113

Figure 22: A schematic representation of the areas used for the calculation of distribution parameter…… 113

Figure 23: Schematic diagram of the experimental set-up to measure the average water mass flow output of the nozzles…….. 114

Figure 24: Schematic diagram of experimental set-up to find out the water distribution over the surface of the Ni-metal foam flow field...……. 114

Figure 25: Front view of the model structure used in this research project…… 115

Figure 26: Top view of the model structure used in this research project……... 115

Figure 27: Nozzles in the model structure…….…….. 115

Figure 28: Various parts of a single BJ type nozzle…… 116

Figure 29: PID mass flow controller…… 116

Figure 30: Watts pressure gauge…….. 116

Figure 31: Hose pressure gauge connection……. 117

Figure 32: Water collector used in the experiment…….. 117

Figure 33: Tracing paper image imported in the Photoshop…… 118

Figure 34: Colored water distribution in the Ni-metal foam…… 118

Figure 35: Comparison between the experimentally obtained mass flow rate values with those of supplied by the manufacturer for conical fog flow nozzles (PJ type nozzles with various areas)……...…….. 119

Figure 36: Comparison between the experimentally obtained mass flow rate values with those of supplied by the manufacturer for flat fan flow nozzles (BJ type nozzles with various areas)…… 119

Figure 37: Distribution of water over the Ni-metal foam surface obtained by using finely atomized conical flow (PJ nozzles)……... 120

Figure 38: Distribution of water over the Ni-metal foam surface obtained by using flat fan flow (from BJ nozzles)…… 120

Page

Figure 39: Effect of nozzle height from the top edge of the Ni-metal foam for the finely atomized conical fog flow (PJ type nozzle)……. 121

Figure 40: Effect of nozzle height from the top edge of the Ni-metal foam for the flat fan flow (BJ type nozzle)……. 121

Figure 41: Effect of nozzle area on the distribution of water over the Ni-metal foam surface for the conical fog flow (PJ type nozzle).…… 122

Figure 42: Effect of nozzle area on the distribution of water over the Ni-metal foam surface for the flat fan flow (BJ type nozzle)…….. 122

Figure 43: Effect of reactant gas flow (simulated by air) on the distribution of water over the Ni-metal foam surface for finely atomized conical fog flow PJ nozzles)...……... 123

Figure 44: Effect of reactant gas flow (simulated by air) on the distribution of water over the Ni-metal foam surface for flat fan flow (BJ nozzles)…..……. 123

LIST OF TABLES

Page

Table 1: Different values of temperature of PEMFC obtained through using the correlation between water added at anode, cell voltage, oxygen stoichiometry and atmospheric pressure……... 125

Table 2: Effect of moles of water added on the temperature of PEMFC…… 125

Table 3: Effect of varying total pressure on the temperature and the water requirement per mole of reactant hydrogen for evaporative cooling……. 126

Table 4: Terminal velocities of water particles in the hydrogen gas environment for the conical fog type flow from PJ nozzles……. 126

Table 5: Terminal velocities of water particles in the hydrogen gas environment for the flat fan type flow from BJ nozzles…… 127

Table 6: Listing of nozzles used in the research and their orifice diameters…….. 127

1. INTRODUCTION

1.1 General interest

For quite some time, the Proton Exchange Membrane Fuel Cell (PEMFC) has been a good prospect for providing clean and environmentally-friendly power. For its ease of construction, design, mass scale production of components and above all high energy density, the PEMFC has emerged as a potentially preeminent energy conversion device. For these reasons, PEMFCs are being considered for use in automobiles and for supplying grid electric power. Effort has been in progress for over 15 years to make that a reality. Although the development of the PEMFC was not much emphasized for these applications during the 1970s and early 1980s, the later part of the 1990s saw some significant work in these fields [1]. Some of the key players responsible for these developments were Ballard Power Systems of Canada and Los Alamos National Laboratory in US.

Although the PEMFC has been an object of interest for generating power and its attractiveness has increased significantly over the last decade, it has yet to establish itself as a commercially viable source of power for the automotive sector or for grid power due to its high capital cost. Continuous efforts are being made to reduce its cost and/or to increase its efficiency. Reducing the cost of the fuel cell is not easy to do. Many factors contribute to this and each has to be dealt with separately. Many people consider that the electrocatalyst used in the PEMFC is the sole cause of its high cost. PEMFC uses platinum as a catalyst but in amounts that have fallen with time. In the early years (before 1986), a typical platinum usage rate or loading was in the range of 28 mg/cm^2 [2]. This high loading generated a common misconception that the high cost of power generation of fuel cell was to be attributed totally to the catalyst. In fact, today the loading has been brought down to a level of 0.2 mg/cm^2, which is only a fraction of the total cost [2].

This thesis follows the style of the Journal of Power Sources.

PEMFCs have many other issues that make their total power generation very expensive.

One of these is the removal of waste thermal energy. High cost has always been a challenge for the development of this technology and efforts are continually being made to deal with this issue. Component cost is a major factor [3]. One other important issue in this case is the balance of plants (BOP) [2]. The PEMFC is only a part (though the core part) of the total fuel cell system. Other parts, such as pumps, humidifiers (in big systems), fuel processing units, etc, usually make up a large portion of the total system cost. A good way to reduce the cost of the total system is to reduce the cost related to all these "extra parts". Thus, it can be said that the thermal and water management sub-systems contribute a great deal to the total cost of the PEMFC system.

1.2 Specific interest

From the discussion so far, it is clear that, for PEMFC to be a mass marketable energy conversion device, its efficiency must be increased or cost of operation must be reduced, or both. As discussed in the previous paragraph, an effective way to reduce the cost of operation is to reduce "extra parts" related to the PEM FC operation. A major share in the extra parts of the PEMFC system is contributed by pumps and air compressors required for circulating the cooling fluid and reactants in and around the PEMFC stack. These components in conventional pressurized PEMFC systems require considerable amount of parasitic power.

Thermal management is of immense importance for operation of PEMFC systems. Only about 50% of the heating value of hydrogen fuel appears as generated power in the PEMFC. It is very important that this waste thermal energy be dissipated properly. Failure to do so may damage the internal components of the fuel cell system resulting from overheating. Moreover, this waste thermal energy may also dehydrate the Nafion™ membrane (a Teflon™-like membrane containing sulfonic acid groups manufactured by DuPont) in the MEA (Membrane electrode assembly) and cause serious

consequences as far as the performance of the cell is concerned. Therefore, thermal management has to be taken care of in some fashion to remove the waste energy. At the same time, it has to be kept in mind that if highly energy intensive heat removal techniques are employed, the efficiency of the fuel cell system will be severely affected. Typical thermal management procedures, currently in use (using water and air as the cooling fluids), are quite energy intensive and thus increase the parasitic power losses of the integrated system. To improve the efficiency and cost-effectiveness of PEM-FC, a new approach for cooling should be explored which does not require much operating energy and which is efficient in dissipating the waste thermal energy.

For this, evaporative cooling was considered as a new proposition. Although proposed in a few patents [4] [5] [6], evaporative cooling in the PEMFC has not been investigated or tried / investigated yet by developers for thermal management. The idea of the evaporative cooling is conceptually simple. All one has to do is to introduce water inside the reaction zone of the PEMFC. Once there, by the process of electroosmotic drag, this water will be transported to the cathode side of the cell through the MEA. At the cathode side of the cell, gas is relatively dry and contains a large volume of nitrogen, and therefore the water evaporates. Water has a large enthalpy of evaporation (2296 kJ/kg @ 80°C) and therefore when it evaporates it Absorbs a large amount of waste thermal energy. This process of removal of thermal energy can be especially attractive since it would require less power consumption than typical energy removal processes. There are potential benefits to this particular mode of thermal management:

I. Typically, a dielectric fluid (such as pure water) or air is circulated around the fuel cell stack (a fuel cell stack consists several individual fuel cell) to remove waste thermal energy. This process is energy extensive and increases the parasitic power losses. If evaporative cooling process is applied, much of this parasitic power loss can be reduced as the introduction of liquid water does not require much pump work.

II. As will be discussed later, without proper water content, the PEMFC electrolyte membrane cannot function properly which may cause a serious deterioration of performance. Water introduced for evaporative cooling can also serve as a humidifier of the membrane, keeping it wet. Therefore it may be said that application of an evaporative cooling method can serve as both water and thermal management of the PEMFC.

III. Most typical cooling methods are indirect, and if used, have the possibility of localized cooling effects. Whereas, evaporative cooling is a direct method which can be very effective in overall thermal energy removal. This means that if evaporative cooling is applied, there is a much less chance of localized cooling compared to conventional cooling methods [7].

Evaporative cooling is a potentially attractive technique for thermal as well as water management for a PEMFC. As already mentioned, evaporative cooling has never been tried in demonstration stacks. An attempt to examine it was made at the Center for Electrochemical Systems and Hydrogen Research (CESHR) at Texas A&M University at College Station [7]. However, that work did not show any practicable cooling effect. The failure of the project may be attributed to the fact that enough water could not be admitted to the reaction zone of the PEMFC used. As will be shown later, for evaporative cooling to occur, a minimum amount of water must be delivered to the reaction zone of the PEMFC. This amount of water depends on the power output of the PEMFC. In general, 3.4 – 3.6 moles of water per mole of hydrogen fuel is required to carry out evaporative cooling. This is a considerable amount of water and is not easy to supply to the fuel cell reaction zone, especially if water is supplied only by humidification of the reactant gases. The water in the work reported was supplied as fine droplets in the anode gas stream. However, the apparatus used could not force the water to reach the anode surface, and therefore no practicable cooling could occur. As is discussed and calculated later, evaporative cooling can be achieved. So, the failure of the research project at CESHR does not by any means prove that evaporative cooling is not possible. Rather, it would be more appropriate to say that due to design failure, enough water could not be

carried to the anode surface by the anode gas stream resulting in inefficient cooling. Had there been a better design to supply adequate water, it is possible that better cooling could have been achieved. As a result, a new design that can ensure better delivery of water in the right quantity is required to accomplish evaporative cooling. It is again stressed that evaporative cooling is very possible since the reactant gas humidification subsystem in the Ballard Power PEMFC system has shown that a Nafion™ membrane can transport water effectively across its surface without hindrance. This practical application of Nafion™ membranes in humidification has inspired the exploration of a method of evaporative cooling that utilizes this characteristic of Nafion™, which in an operating PEMFC is known as electroosmotic drag. It will be discussed in detail in a later section.

As was mentioned earlier, in the last project carried out at CESHR [7], the apparent deficiency in attempting to accomplish the cooling was the lack of water. The present research work is a follow-up work to previous one, and will address the delivery of water into the fuel cell. In other words, the current work will be solely concerned with a water delivery system that will be able to deliver the correct amount of water into the fuel cell anode zone.

Now, the question remains is what should be the desired water delivery method. By analyzing multiple options, it was decided that a direct water injection spray system would almost certainly be successful in delivering the required amount of water for the removal of waste heat, i.e., thermal management of the PEMFC. Direct injection of water is also a proven method for effective water management. Wood et al. have successfully performed an investigation on this and showed that a direct injection system can be an excellent method for water management [8]. This result also prompted the author to use the direct injection system to deal with thermal management of the PEMFC and thereby demonstrate a design for the water delivery system.

1.3 Objective

For the water delivery system to be effective, it has to meet certain performance metrics, for example, the system has to deliver the right amount of water under certain pressures and water must be distributed uniformly within the reaction zone of the PEMFC. These performance metrics will also depend on certain design and operating parameters, such as, how far the water injecting nozzles are situated, what is the orifice area of the nozzles, etc. Therefore, a thorough investigation regarding dependence on design and operating parameters is also required. Therefore the objective of the research can be summarized as:

"To determine if a direct water injection spray system can be used to deliver the required amount of water with the proper distribution for evaporative cooling of a PEM fuel cell, and how the design and operating parameters affect its performance."

1.4 Scope of research

To satisfy the objective of the research project, some questions were formulated in such a way that answering them will establish the efficacy of the proposed design. The questions are as follows:

1. What amount of water, in terms of reacting gas usage, to be evaporated to dissipate certain amount of waste thermal energy?
2. How much water should be admitted to each cell given a particular capacity of PEM FC?
3. What performance metrics need to be satisfied for a workable design solution? How they can be satisfied?
4. What are the design and operating parameters that can affect the performance metrics? In what ways?

5. Is the proposed design of water delivery system better than other conventional methods of thermal management, and if so why?

To answer the above questions, necessary calculations were performed followed by experimental setup design and conducting experiments. After the experiments were performed, a methodical analysis of results was done to see whether the proposed design could meet the objective in terms of distribution and delivery of water in the PEM FC.

1.5 Organization of the thesis

Including the introductory section, this thesis consists of eight individual sections. To understand the objective and procedures of this thesis, some basic knowledge about the PEM fuel cell and its working principle is required. Section 2 will provide that basic understanding. In this section, certain fundamental issues such as basic electrochemistry and thermodynamics, stack design, efficiency and water and thermal management of PEMFC are briefly discussed. Among these, thermal and water management of PEMFC are the most important topics and knowledge about these two are vital for understanding this thesis. Therefore a further section, Section 3, is dedicated to these two important issues regarding PEMFC operation. Section 4 discusses the evaporative cooling in detail. It describes the process and discusses how evaporative cooling can be applied to remove waste thermal energy of a PEMFC. Section 5 outlines the experimental setup and procedures for the experiments to satisfy the objective of this research project. Section 6 describes the results obtained from the experiments. This section also discusses the interpretation of the results. Section 7 includes the findings from the research project. Finally, Sections 8 and 9 give the conclusions and outline recommendations for future work respectively. All the figures and tables referred to in this thesis are placed in the Appendix A and Appendix B which can be found immediately after the Bibliography section.

2. BASIC UNDERSTANDING OF THE FUEL CELL

To fully appreciate the research work performed, a basic knowledge of the fuel cell is required. This section of the thesis is solely dedicated to the basic understanding of fuel cell theory.

2.1 What is a fuel cell and how does it work

Different people have defined "fuel cell" in various ways. Among them, the following two probably describe fuel cell in a most concise yet precise manner from the functional point of view:

"Fuel cell is a device that directly converts the chemical energy of the reactants into low voltage DC electricity" [9].

"A fuel cell is an electrochemical device that continuously converts chemical energy into electrical energy (and some heat) for as long as fuel and oxidant are supplied" [10].

Fuel cells operate like batteries with certain fundamental differences in their construction and engineering. Like a regular battery, it generates electricity via electrochemical reactions. The difference between the fuel cell and a battery is that the latter consume reactant material that is an integral part of their structure, whereas in fuel cells, the reactants are supplied from an external source to the reaction zone/areas (electrodes). The fuel cell works as an energy converter performing the same function as a Galvanic Cell [9]. The basic working principle of the fuel cell was first demonstrated by Jurist and Scientist Sir William Grove in 1839. It was already known that water can be electrolyzed to hydrogen and oxygen by passing an electric current through it. If this electrolysis is reversed, i.e., if the hydrogen and oxygen recombine, an electric current is produced. This is the working principle of a fuel cell.

At this point a little discussion on redox or oxidation-reduction reactions is required. This type of reaction solely involves the transfer of the electrons between the participating species and always involves a matching set of reactants (two redox couples). Thus a redox reaction can be described in terms of two half-reactions, first part being oxidation and the second part reduction. Loss of electrons occurs in the oxidation half reaction and a gain of electron occurs in reduction half reaction. It must be mentioned here that it is not possible to have them individually; i.e., it is not possible to have an oxidation reaction without having a reduction reaction at the same time. As an example, when Magnesium reacts with chlorine, it undergoes oxidation, since it loses electrons:

$$Mg - 2e^- \rightarrow Mg^{2+}$$

On the other hand, a chlorine molecule undergoes reduction, since it gains two electrons.

$$Cl_2 + 2e^- \rightarrow 2Cl^-$$

Therefore the overall reaction can be expressed as;

$$Mg + Cl_2 \rightarrow MgCl_2$$

The overall reaction between the magnesium and chlorine is an excellent example of coupled redox reactions. Here magnesium becomes oxidized and chlorine becomes reduced. The substance gaining electrons (Cl in the above case) and thus being reduced and causing oxidation is known as the oxidizing agent or oxidant and the substance that loses electrons (Mg in the above case) and thus being oxidized and causing reduction is called the reducing agent or reductant.

These redox reactions are the heart of the operating principle of the fuel cell. A fuel cell, as an electrochemical energy conversion device, works by making use of these redox reactions (reduction and oxidation half reactions). In case of fuel cell, the oxidizing

agent is essentially oxygen and the reducing agent is the reactant fuel (in case of PEMFC, hydrogen). Electrons are donated by the oxidizing agent and received by the reducing agent through an external electric circuit. Figure 1 depicts the process schematically. This means that the flow of electrons generates an electric current which can be used across an electrical load. However, this flow of electrons or electrical current has to be controlled otherwise useful electrical work cannot be obtained. The structure in fuel a cell has to be arranged such that the electron passes through the external circuit, not through the internal membrane. If that happens, the current generated will be short-circuited and all there will be no electrical work. This is why it is necessary to keep the anode and cathode of a fuel cell physically separated. This is accomplished by membrane electrode assembly or MEA.

Figure 2 shows the structure of a typical PEMFC system. The PEMFC is made up of an anode and a cathode separated by the ion-conducting electrolyte to prevent short-circuiting. Any substance which is capable of chemical oxidation and which can be supplied continuously can be burned galvanically as the fuel at the anode of the fuel cell. Similarly, the oxidant can be any fluid that can be reduced at a sufficient rate. For most applications, hydrogen has been a good choice as a fuel because of its high reactivity in the presence of a suitable catalyst and its high energy density when stored cryogenically. As for the oxidant in the cathode, oxygen is the most popular choice due to its easy and economic availability from air. The electrodes are connected through a load by a metallic external electric circuit. The reactant fuel and oxidant constitute redox couples and essentially two redox reactions occur (at the anode, hydrogen is oxidized and at the cathode oxygen is reduced). This enables the transport of the electronic current from anode to cathode through the electric circuit. In the meanwhile, ions make their way from anode to the cathode through the electrolyte (H^+ in acid electrolytes and OH^- in alkaline electrolytes) [9]. The type of a fuel cell generally depends on the electrolyte being used. The Nafion™ acid membrane electrolyte plays a vital role in the correct functioning of the PEM fuel cell.

2.1.1 The basic structure and electrochemistry of the PEM fuel cell

We will concentrate on the PEMFC, the type which is of sole concern in this research. In the PEMFC, the reactant fuel is gaseous hydrogen and the oxidant is oxygen. These two species of gas fundamentally form the redox couples. As mentioned above, the anode and cathode must be separated to avoid electronic short circuiting and in PEM fuel cell, this is done by putting a non-electronically conductive, relatively impervious membrane with a selective ionic conductivity. This solid polymer membrane works as the electrolyte for the PEMFC and forms a thin but sound electronic insulator. It also forms a gas barrier between the electrodes and obstructs the transport of reactant gases. The PEMFC was called the "solid polymer fuel cell" (SPE™) by its original developer, General Electric in the mid-1960s to 1984 program, the name being derived from the membrane. This polymer membrane electrolyte is the heart of the PEM fuel cell system. This membrane paved the way for the PEM fuel cell to be used without any liquid electrolyte medium. Therefore this electrolyte does not redistribute, diffuse or evaporate. So, intermittent operation or rapid load change becomes an easy option and all these make the fuel cell insensitive to special orientation [9]. Figure 3a schematically shows the positioning of the anode, cathode and the polymer electrolyte membrane.

As pointed out before, hydrogen is the reactant fuel (reducing agent) for the PEM fuel cell. The cell can produce power continuously (unlike batteries) as long as the reactant is fed to the anode side of the cell. Both electrodes in the PEMFC are electrically (both electronically and ionically) conductive. The electronic part is provided by the catalyst (platinum carried on carbon black), whereas the ionic part is provided by the inclusion of about 30 wt % of Nafion™ electrolyte to allow reaction throughout the electrode. Moreover, the electrodes are thin, porous and are capable of diffusing the reactant gas. The direction of diffusion this gas is perpendicular to the direction of the flow of the current [9]. Figure 1 shows the direction of both the current and the reactant gas. When hydrogen reaches the anode, it is oxidized (electrons are stripped off in the oxidation half reaction) and the electron is passed through the external circuit to the

cathode side. This is, in fact the, half reaction of the redox. At the anode, the following reaction takes place [9]:

$$H_2 \leftrightarrow 2H^+ + 2e^- \text{ ---------- (1)}$$

Like the anode, the cathode is also porous and assists the flow of oxygen in the same way but in a reverse direction of the reactant gas. The reduction half reaction occurs (i.e., oxygen is reduced and receives electrons):

$$\frac{1}{2}O_2 + 2H + 2e^- \leftrightarrow H_2O \text{ ---------- (2)}$$

Therefore the overall redox cell reaction becomes:

$$H_2 + \frac{1}{2}O_2 \leftrightarrow H_2O \text{ ---------- (3)}$$

In this reaction, electrical energy is produced instead of the thermal energy from combustion. Both of these half reactions must take place at the same time. To achieve usable electrical work and for these half reactions to go on continuously, electrons must go through the external circuit and hydrogen ions (or protons) must be transported through the electrolyte. An acid is a medium that has free H^+ ions and serves that purpose very well. Acid fuel cells formerly used aqueous acidic electrolyte, such as the phosphoric acid fuel cell which uses the only high temperature acid electrolyte. However, low temperature aqueous acids have been replaced by solid polymers that contain free hydrated H^+ ions and work as well as a liquid aqueous acidic medium without the disadvantage of spreading a corrosive liquid over cell components. In the PEMFC, only hydrogen ion (H^+) is allowed to pass through the electrolyte. The free electrons make their way through the electrical circuit as shown in the Figure 1. To accomplish this, the electrodes must be electronically conductive and each cell must be separated by an electronically conducting plate (the “bipolar plate”) incorporating channels for reactant

distribution and product water removal. In conventional PEMFCs, this also contains cooling channels.

At this stage of discussion, it is important to discuss the polymer electrolyte membrane and its working principle. This knowledge will prove to be useful when the transportation of H^+ ion across the Nafion membrane is considered. The polymer electrolyte membrane in the PEMFC was considered to be a major breakthrough for fuel cell industry. It was first developed in the 1960s at General Electric for the Gemini Orbital Program [10]. This used a cross-linked polystyrene sulfonic acid membrane with poor stability. The much more stable DuPont Nafion™ became available about 1968. Many companies were later engaged in the researching and manufacturing of similar polymers, but the industry leader in this sector is still DuPont [2]. The basic construction of Nafion® starts with ethylene in which the hydrogen is replaced by fluorine to give tetrafluoroethylene. This can be polymerized to give polytetrafluroethylene or PTFE (Du Pont Teflon™, Figure 4). This is also an important material in PEMFC construction, to be discussed later.

To make Nafion™, tetrafluoroethylene is reacted with sulfur trioxide, SO_3, to give a cyclic sultone with a four-membered ring which rearranges to give the acid difluoride of a difluoromethane carboxylic sulfonic acid. This can be reacted with hexafluoropropylene epoxide and tetrafluoroethylene to give a perfluorinated polyether chain with sulfonyl fluoride groups on each end, which is thermoplastic and is cast into films. This is hydrolyzed with base to give a sulfonic acid salt, which is ion-exchanged to give acid groups within the (now-Nafion™) membrane. Its structure makes Nafion™ a very interesting and unique substance, with hydrophilic regions created within a hydrophobic substrate and enables Nafion™ to absorb water. In the region where liquid water is present, the H^+ ion is hydrated and is only weakly associated with the SO_3^-group and can move about. This essentially makes Nafion™ act like an acid that is capable of transporting H^+ ion [2] [10]. Figure 5 shows the structure of Nafion™ type membrane and the movement of water particles in it.

Let us now look back at the electrochemical reactions of the PEM FC. It needs to be mentioned here that, in reality, the half-cell reactions also need several steps to be completed, and free protons are not produced, rather the following phenomenon takes place:

$$H_2 \Leftrightarrow 2\dot{H} \quad \text{---------- (4)}$$

$$2\dot{H} + 2H_2 0 \Leftrightarrow 2H_3 0 + 2e^- \quad \text{---------- (5)}$$

This is followed by electrostatic association of the hydronium (H_3O^+) ion with three water molecules to give the complex $H_9O_4^+$.

Thus, the proton (H^+) is actually transported through the electrolyte membrane with the help of water particles in the form of hydrated hydronium ions. In other words, H^+ ions are transported through the membrane with the help of a "vehicle". This is a popular theory known as "vehicle theory" for transport of H^+ ions [11].

In fact, there are two principal theories by which the transport of protons can be explained. The first one is the vehicle theory mentioned in the previous paragraph. The second one is called "proton hopping". This theory is also known as the "Grotthus mechanism" [12] because of a pre-ionic 1806 theory for conduction in electrolytes proposed by von Grotthuss where charges were supposed to hop from one site to a site of opposite charge in the solution. In case of the "proton hopping theory," the vehicles show pronounced local dynamics but generally reside in their own sites. The protons are transferred from one vehicle to another by quantum tunneling via hydrogen bonds [13].

2.1.2 Thermodynamics of PEM fuel cell: maximum work and efficiency

The electrons, as shown in Equation 5, pass through the external circuit and eventually the electrical work is done on the load. The amount of work done in this process is important to determine the efficiency of the cell. From thermodynamic analysis, it is possible to find out the amount of work that can be obtained from the redox reaction and the associated electron flow. This determination of the work employs the Gibbs free energy principle as follows:

$$G = H - TS \quad \text{----------} \quad (6)$$

Where G = Gibbs free energy

H = Enthalpy

S = Entropy

T = Temperature

Taking the differentials

$$dG = dH - SdT - TdS \quad \text{----------} \quad (7)$$

We also know that,

$$H = U + PV \quad \text{----------} \quad (8)$$

Therefore,

$$dG = dU + PdV + VdP - SdT - TdS \quad \text{----------} \quad (9)$$

From the 1st Law of Thermodynamics,

$$dU = \delta Q - \delta W \quad \text{----------} \quad (10)$$

From Equation 9 and 10, we obtain,

$$dG = \delta Q - \delta W + PdV + VdP - SdT - TdS \text{ --------(11)}$$

For a reversible process,

$$\delta Q]_{rev} = TdS \text{ ----------(12)}$$

Therefore, from equation (11) and (12), we obtain,

$$dG = -\delta W + PdV + VdP - SdT \text{ ----------(13)}$$

Now, for constant pressure and temperature dP and dT are zero. Moreover, if there is no work obtained through expansion, PdV also becomes zero. Therefore, Equation 13 becomes,

$$dG = -\delta W \text{ ----------(14)}$$

This work W is electrical work. This work is done by moving the charge "q" through a potential "V". Therefore following expression can be deduced for electrical work:

$$W = qV \text{ ---------- (15)}$$

This charge q can be expressed as the product of number of moles reacted and the Faraday's constant, F, (96,485 Coulombs).

$$q = nF \text{ ---------- (16)}$$

Therefore, equation (15) can be expressed as,

$$W = nFV \text{ ----------(17)}$$

So, from equation 15, 16 and 17, it is evident that, the reversible voltage V can be given as,

$$V = \frac{-dG}{nF} \text{ ----------(18)}$$

For a hydrogen fuel cell, n = 2 (Equation 1). From this equation the reversible or theoretical open circuit voltage can be calculated (1.229 Volts for liquid water with hydrogen and oxygen at 1.0 atm pressure at 25°C). Temperature is important here because dG changes with temperature since the Gibbs free energy for the reactants also changes with temperature.

Since the Gibbs free energy is dependent on the temperature, it is not considered to be a very good measure for efficiency calculation. And since the reactant fuels are oxidized to produce the electricity, the change in enthalpy of reaction, which is not strongly temperature-dependent, should be considered for the measurement of the efficiency, which is why the following ratio is introduced to calculate the efficiency of a hydrogen fuel cell:

Maximum possible efficiency (η_{max})

$$= \frac{Electrical\ Energy\ \mathrm{Pr}oduced\ per\ mole\ of\ fuel}{Enthalpy\ of\ \mathrm{Re}action}$$

$$= \frac{Electrical\ Energy\ \mathrm{Pr}oduced\ per\ mole\ of\ fuel}{-\Delta H_{reaction}}$$

$$= \frac{\Delta G}{\Delta H_{reaction}} \text{ ---------- (19)}$$

This $\Delta H_{reaction}$ (measured at 25°C) has two different values when the reaction produces water, one when water produced is in the liquid state and one for the situation when water vapor is produced. The following reactions should be noted:

$$H_2 + \frac{1}{2}O_2 \leftrightarrow H_2O(steam) \text{ ----------(20)}$$

$\Delta H_{reaction} = -241.83$ kJ/mol at 25°C

$$H_2 + \frac{1}{2}O_2 \leftrightarrow H_2O(liquid) \text{ ----------(21)}$$

$\Delta H_{reaction} = -285.84$ kJ/mol at 25°C

The higher figure is known as the HHV (higher heating value) and the lower figure is known as LHV (lower heating value). If these values were used instead of Gibbs free energy in Equation 18, the result would be 1.253 V for the LHV and 1.481 V for the HHV. For most cases, the LHV is used, as it is more appropriate for most applications (except condensing steam engines).

In practice, the reversible voltage (open circuit potential) is impossible to achieve due to the occurrence of irreversibilities. These irreversibilities cause the voltage to drop below the theoretical value of 1.229 V to about 0.95 to 1.0 V. Under load, the voltage obtained from most fuel cells is in the range between 0.6-0.8 V. A polarization curve is a convenient way to represent the effect of irreversibilities on the electrical performance of a fuel cell. A polarization curve, also known as performance curve, is a plot of fuel cell voltage versus current density. Figure 6 shows a typical polarization curve for the PEMFC. As discussed above, it can be seen from Figure 6 that the open current voltage (OCV) is less than the theoretical no loss value.

There are several factors that contribute to voltage losses. A brief description of these is given below [2].

1. Activation loss:

This loss occurs due to the slowness of the reaction that happens at the surface of the electrodes. Some voltage is lost to in pursuing the reaction that transfers the electrons from the electrodes. This voltage drop is highly non-linear. The first region of polarization curve in Figure 6, which represents a very sharp drop in voltage, is actually caused by activation loss.

2. Fuel crossover and internal current

As stated earlier, electrons produced at the anode must be transported in a controlled fashion. This means that the electrons must follow a path perpendicular to the direction of flow of ions to an external circuit and the electrons must not pass through the electrolyte membrane. If that happens, the potential to perform electrical work is lost and voltage drop occurs. Although in an ideal case, the electrolyte should only transport the ions through the cell, in practice, some electrons are transported through the electrolyte membrane.

3. Ohmic Losses:

This kind of drop occurs due the resistance offered to the electrons by the electrodes materials, various other interconnections and the electrolyte. The ohmic voltage drop is proportional to the current density and follows Ohm's law which is as follows:

$V_{ohmic\ loss} = I * R$

Where, I = Cell Current

R = Total internal resistance.

This kind of voltage drop is linear as can be seen in the second region of the polarization curve of Figure 6.

4. Mass transport or concentration loss:

The concentration of fuel in fuel cell (hydrogen for PEMFC fuel cell) does not stay constant throughout the cell during the time the cell is operating. Since a concentration change has a direct effect on cell voltage, voltage drops occur. In Figure 6, the last region, which shows a sudden drop in voltage, actually represents the drop caused by the mass transport inadequacy due to the reduction in concentration of the reactants.

2.1.3 Irreversibilities and waste thermal energy

The irreversibilities discussed so far have a direct effect on the fuel cell operation. These irreversibilities cause the voltage to drop and generate a considerable amount of waste thermal energy; that is, chemical energy not converted to electrical energy (almost 50% of the total power output of a cell). This waste thermal energy must be removed from the cell in some manner (thermal management of the fuel cell). Failure to do that will trigger the internal temperature beyond the safe operating temperature (usually 80°C for PEM fuel cell). The result is a high possibility of damaging the electrolyte membrane, with severe consequences as far performance is concerned.

Removal of the waste energy produced is of extreme importance for proper functioning of the fuel cell. Measures for removal of this waste energy are called “thermal management” of the fuel cell. The amount of waste thermal energy produced

due to irreversibilities during the operation of the fuel cell can be given by the following formula:

$$Q = I * (V_{reversible} - V_{cell}) \text{ ----------(22)}$$

Where,

I = Current Density

$V_{reversible}$ = Reversible voltage of the cell, ΔH_{HHV} for liquid water product, or ΔH_{LHV} for gaseous water.

V_{cell} = Cell voltage

For this research project, a particular capacity fuel cell will be considered (35 kW). A generic way of calculating waste thermal energy for a particular capacity cell and required water to dissipate this energy will also be calculated in section 4.

2.2 Construction of PEM fuel cell stack

So far, a general description of the working principle of the fuel cell has been given. This section gives some idea about the PEM fuel cell stack and its design.

As has been already discussed, the OCV for a single cell is 1.229 V under standard conditions with liquid water product, but this voltage is never achieved due to various irreversibilities (Section 2.1.2). Typically, individual cells never generate more than 0.6-0.8 volt at a current density of 0.4-0.8 A/cm^2. Therefore, for most practical operations, a large number (a least 20 cells or higher) of individual cells are piled up together to produce the desired level of voltage and current. This stack of individual fuel cells is known as “fuel cell stack”. Figure 7 shows a PEMFC stack taken at the Center for Electrochemical Systems and Hydrogen Research.

2.2.1 Design approach for fuel cell stack

Designing a stack, that will give a desired voltage at a particular current density while maintaining a desired efficiency, is not easy. Moreover, the design approach for the stack varies greatly with the developer. But, the most common type of stacking design that is more or less universally accepted throughout the industry is “sandwich” type arrangement. In this arrangement, bipolar plates are used at two extreme ends and other components of the cell, e.g., membrane electrode assembly, flow fields, gaskets and endplates are sandwiched between them. Figure 8 is a photograph of the same PEMFC stack shown in Figure 7, only this time the stack is dismantled to give a better view of how the stack is arranged internally. It is to be noted that the stack is rather a repetitive structure with repeating elements such as bipolar plates, MEA, gaskets and flow fields.

2.2.1.1 Components of a typical PEMFC stack

The most important components of a PEMFC stack are the bipolar plates, MEA and flow fields. A brief account of each with their working principle is given below:

2.2. 1.1.1 MEA (membrane electrode assembly)

The MEA or membrane electrode-assembly is basically the most important element of a PEM stack, i.e., MEAs are the building blocks for the PEMFC. Figure 9 shows a 50 cm^2 MEA manufactured by 3M Corporation, which was previously used in experiments at CESHR.

MEA is essentially comprised of the following elements:

1. Nafion® ion exchange membrane
2. Anode catalyst layer

3. Cathode Catalyst layer
4. Gas diffusion layer (GDL)

In Figure 9, a black carbon cloth is visible. This carbon cloth is used to support a gas diffusion layer (GDL), which consist of carbon black bonded by hydrophobic PTFE.

There are two gas diffusion layers, one in the anode side and one in the cathode side. The anode and cathode catalyst layers are loaded onto the GDL on the carbon cloth via a proprietary process. At the anode side, the GDL supports the electrode structure and allows the hydrogen gas to reach the active site of the catalyst. Upon reacting, the hydrated protons migrate to the cathode side and the electrons flow perpendicularly and opposite to the direction of ion flow and eventually reach the outer circuit. Therefore GDL must be porous and electronically conductive. At the cathode, the GDL has even more complicated responsibility. Water is produced at the cathode side and its removal is challenging if not insurmountable. Product water makes their exit in liquid form if the reactant gases are saturated. In that case, there is a high probability that pores in the GDL may get blocked by water, thus preventing the oxygen-in-air reactant from coming into contact with the active sites of the cathode catalyst layer. Therefore, it is extremely important for the cathode GDL to work properly so that gas transport is not stalled in the cathode reaction zone of the PEMFC in a phenomenon called “flooding.”

2.2.1.1.2 Flow fields

The function flow field in the PEMFC is to distribute the gas and water uniformly along the surface of the MEA and conduct the current perpendicular to the surface. Various types of flow fields are currently in use. Figure 10 shows some common patterns. All flow fields are grooved or stamped into the bipolar plate. The channels that can be seen in the flow-fields act as passages to distribute the reactant gases over the surface of the MEA. The pattern in Figure 10a is known as a parallel flow-field. The problem with this type is that it is possible for a channel to become blocked by water or

reactant impurities such as nitrogen. This would result in some area of the MEA being starved for reactants. [2].

Figure 10b, called a serpentine flow-field, is an attempt to resolve the above mentioned issue. For this pattern, there are no parallel channels available and no matter what, all the reatants must flow in one particular serpentine channel. Therefore, even there is a blockage in the channel, the continuous flow of reactant gases and its pressure will move the blockage the reactants will move everywhere. But the problem in this case is that too much pressure is developed in the channels and excessive work is required to move the reactants along the channel path. Figure 10c is a compromise between parallel and serpentine pattern flow-fields [2].

The flow-field in Figure 10d is called intensely parallel or grid type flow field. Since flow passages are all over the surface, this design is believed to be a better one in terms of reactant gas delivery, although it is still possible for water or nitrogen to get accumulated in the channels.

Transport problems in the above mentioned flow-fields prompted flow-field designers to look for an alternative solution and eventually a metal foam flow-field was developed. Figure 11 shows a metal foam flow-field. These flow-fields are nothing but high porosity metal foam. They are placed between the MEA and the bipolar plate. As soon as the reactant gases come in contact with metal foam, they are distributed all over the surface of the foam and pass through the multitude of pores (flowchannels) to the surface of the MEA. Thus the gas transport becomes uniform without requiring excessive work. This type of flow field is made of nickel or tin-coated nickel. These flow fields are commonly known as Nickel metal flow field or Ni-metal flow field. In the rest of the thesis, this type of flow field will be referred to as Ni-metal flow field. In most cases their porosity is 100-110 p.p.i (pores per lineal inch). Figure 12 shows a microscopic view of Ni- metal foam, clearly showing the pores. Reactant gases and water particle pass through these pores. It is important to mention here that, this research project uses nickel metal foam as a flow-field for its superior gas and water transport capability.

2.2.1.1.3 Bipolar plates

Bipolar plates are used to connect the individual cells of a PEMFC stack. Bipolar plates are so named because one side of the plate is connected to the anode of a cell whereas the opposite side is connected to the cathode of the adjacent cell. Actually, individual cells are sandwiched between these bipolar plates in PEMFC stack. Figure 8 shows the repetitive arrangement of bipolar plates in a stack.

Bipolar plates carry out the important responsibility of collecting and conducting the current from the anode of one cell to the cathode of the next, which is why these plates have generally been made from electronically-conducting graphite. In case of flow fields being stamped in the plates (when Ni- metal foam is not used as a flow field), bipolar plates must also distribute reactant gases over the surfaces of the anode and cathode. It was mentioned early in the Introduction that, even after the significant reduction in the loading of platinum catalyst in MEA, the PEMFC FC is still very costly. One of the reasons of this high cost is bi-polar plates. With all the required function that a bi-polar plate has to perform, manufacturing of these plates becomes costly.

After the brief discussion on the design and working principle of the PEMFC stack, water and thermal management in the PEMFC requires discussion. These two topics are inherently related to the objective of this research project and therefore the next section is dedicated to the description of these two important issues.

3. WATER AND THERMAL MANAGEMENT OF PEM FUEL CELL

Water and thermal management of a PEM fuel cell are two important issues in which a lot of research is still being conducted. But before going any further, it is important to introduce these two terms and give a brief idea about what they mean.

3.1 Water management

It was stated in Section 2.1.1 that the there must be sufficient water content (hydration) in the electrolyte membrane for proper ion conductivity, which is strongly dependent on moisture content Moreover, water must be present at the anode side of the fuel cell for the formation of hydrated hydronium ion formed by combining a proton from hydrogen with water. Therefore presence of water is a must for the fulfillment of these tasks. Now, the question is how to make the water available at the anode side of the fuel cell? It must be mentioned here that the presence of too much water can cause flooding and thus blocking the pores of the gas diffusion layer. So, a balance between the two is of extreme importance.

There are several ways in which water can be supplied to the anode side of the fuel cell. The first uses water that is produced on the cathode side as a result of the overall reaction shown in Equation 3. This water can diffuse back to the anode side as a result of concentration gradient of water present in the anode and cathode. This can be an ideal method of required water transport. However, this back-diffusion is relatively slow and therefore cannot meet the demand for the total water requirement.

At this point, it is important to mention the special phenomenon occurring within the fuel cell which is known as “electroosmotic drag”. During fuel cell operation, electroosmotic drag results in water being transported through the electrolyte membrane

from anode side to cathode side by H^+ ions due to this effect. This electroosmotic drag is quantified by a quantity called "drag coefficient, K_{Drag}, defined as the number of water molecules transferred through the membrane per proton in the absence of other water transport mechanisms" [14]. This drag coefficient has been researched extensively but the measured value of this coefficient for Nafion™, the most commonly used membrane, exhibits a wide scatter [14]. La Conti et al. reported a value of K_{Drag} from 0 (in the dry state) to 4–5 (in the fully hydrated state) for Nafion™ membranes [15]. Zawodzinski et al. obtained K_{Drag} between 0.9 and 2.5 for partially and fully hydrated Nafion 117 membranes at 300 K, respectively [16]. We should note that if $H_9O_4^+$ is the vehicle for proton conduction, the value of K_{Drag} would be 4.0, whereas if the "hopping" mechanism were exclusive, it would be zero. This indicates that both mechanisms may play a part.

Electroosmotic drag at high current densities (large flow of protons) can result in depletion of the water from the anode side of the cell and thus drying it out [2]. Therefore, to keep the electrolyte membrane highly conductive, water has to be continuously supplied externally in some fashion to keep the required level of wetness in the membrane. At the same time, excess water must be removed in some way to prevent flooding in the membrane. Different water movements are shown in Figure 13. All these water movements are predictable and controllable and the quantities are directly proportional to the current density [2].

3.1.1 Typical water management methods

For practical applications, various water management techniques are used. Of them the most popular and widely accepted methods are reactant gas humidification and the wicking method. To follow is a brief description of these two mostly used water management techniques.

3.1.1.1 Reactant gas humidification

This is the most commonly used water supply method. In this method, reactant gas is bubbled through water before it makes an entry to the anode side of the PEM fuel cell thereby humidifying it with water. Although simple, this method is not free from complexity. If the temperature of the water, through which the reactant gas is bubbled, is too low, there will not be enough water vapor present in the reactant gas to provide sufficient humidification. At the same time, too high a temperature in the water bubbler can also cause problems. In that case, there is a considerable possibility that the water vapor will condense as soon as it gets in contact with the relatively cool MEA or other cell parts. Moreover, reactant gases may become diluted due to an increase in water vapor pressure, especially at high temperature and/or high current densities [17]. Even with these complications, this method is widely used to deliver water at the anode side of the cell to allow the formation of hydronium ion, as well as maintaining required moisture content in the electrolyte membrane.

3.1.1.2 Wicking method

In this methodology, reactant gas is allowed to enter dry in the cell and water is supplied from an external source using a wick. Watanabe et al. used this process in his research and found that this method reduces the membrane resistance without introducing a flooding problem [18].

3.1.2 Removal of water from the cell

Water management has direct influence on the performance of fuel cell. This is shown on the polarization curve, which is the performance indicator of the cell. Water management, therefore, poses critical performance issues such as liquid water formation,

flooding due to presence of excess water, reactant gas dilution and dehydration of polymer electrolyte membrane [17].

Condensation of liquid water can block the active sites of the electrode as a result of excess water or flooding. Moreover, excess water can block the pores of the gas diffusion layer and limit the transport of oxygen. The most common method of getting rid of this problematic excess water is to vent the vapor and water mixture to the atmosphere at the cathode. Care must be taken when this method is applied as the presence of too much water in the cathode gas stream in the exit may cause flooding.

Another method, know as wicking method, can be used for removal of water from the PEMFC. A wick can be conveniently built into the bi-polar plates of the PEMFC and remove water from inside the cell. The limitation of using wicking method is that, this method will severely complicate the bi-polar plate design and may give rise to the cost associated with it.

One other option is to run the cell without any kind of external humidification and any excess water can be evaporated in the dry cathode gas stream. The problem with this approach is that, even with external anode humidification, the moisture content of the polymer electrolyte will be so low that it will be unable to handle higher current density. Therefore, if no external humidification approach is applied, the fuel cell must be operated at a very low current density due to poor hydration of the membrane and low ion conductivity. This will result in a very low power density.

3.2 Thermal management of PEMFC

Although the PEMFC is known to be a very efficient system, a major quantity of the energy produced is wasted as excess thermal energy (40-50% of the total energy produced). This waste energy can be easily traced back to the irreversibilities discussed in Section 2.1.2. With reference to Equation 22, the Q is the waste thermal energy produced

due to the irreversibilities that occur during the operation of the cell. This waste energy must be removed in some way otherwise this excess thermal energy can easily cause the electrolyte membrane to dry out quickly and raise the temperature of the cell beyond the safe operating range (beyond 80°C). Thermal Management deals with this excess thermal energy.

There are various ways of removing excess thermal energy. One thing common to all of these methods are parasitic power losses. Most of the techniques currently in use for removing thermal energy either use air or water depending on the size or capacity of the stack. Usage of these fluids necessitates installing extra equipment such as pumps, blowers, air compressors etc and all of these means rise in extra cost due to parasitic power losses. Moreover, due to this parasitic power loss, it becomes difficult to obtain the desired power density from the stack.

From thermal management point of view, PEM fuel cell stack can be divided in four categories depending on their capacity or size:

1. Fuel Cell below 100 W
2. Fuel Cell stack between 100 W– 2,000 W
3. Fuel Cell stack between 2,000 W– 5,000 W
4. Fuel Cell stack over 5,000 W

Generally, fuel cells below 100 W in capacity are cooled by reactant air using the convection heat transfer principle. In these small-scale cells, the design structure is generally open type so that air stream can be used to transfer heat from the surface [2].

The next class of fuel cell, within capacity range of 100–1000 W, generally needs external airflow using a fan or similar arrangement. When fuel cell power goes above 100 W, some of the heat transfer is through natural convection and radiation and that is when complications begin to arise. In situations like this, although it is possible to increase the reactant air flow to a certain point to avoid drying out of the membrane [19], the most

common practice is to introduce a separate cooling air flow over and above the reactant airflow.

Using only the reactant flow to cool the cell will necessitate a large passage since a large airflow is necessary to cool any cell in this size range. Generally extra channels are made in the bipolar plates to facilitate passage of separate cooling air. Figure 3b shows extra channels made in bipolar plates for passages of air. Although common in some designs of PEMFCs, the introduction of separate air passage makes the design of the bipolar plate more complicated and expensive. As an alternative method, perhaps no less expensive, separate cooling plates can be introduced in the cell stack through which air can be blown.

For larger fuel cell stacks, it becomes difficult to carry out cooling by using air only. Although simple, it is difficult to maintain a uniform temperature throughout the stack with air cooling. In these cases, water cooling is used. While water cooling definitely makes the stack design much more complicated, in terms of water passage, temperature, pressure management, weight and size of the stack, it is very effective and has the capability of removing much more thermal energy than air due its larger heat capacity. This is why PEM fuel cell stacks over 5 kW generally use water as the cooling fluid, whereas judicious judgment is necessary as to which fluid to choose in case of fuel cell stacks between 2 and 5 kW [2]

Another strategy in thermal management was proposed by P.R. Margiott and R.D. Breault in patents [20] and [21] that make use of antifreeze or coolants. Using water as a cooling fluid can introduce significant start-up complexity on freezing. Antifreeze or coolant can be the answer to such problems.

3.3 Evaporative cooling, an innovative way of dealing the thermal management of PEM fuel cell stacks

It is obvious that most of these conventional methods of thermal management do have advantages, but also some drawbacks, in particular, their extra cost in terms of parasitic power losses and loss of power density. Evaporative cooling can be a good and innovative strategy to minimize the disadvantages posed by the above-mentioned methods. The next section will elaborate on this particular method of thermal management and on how water may be introduced inside the fuel cell to accomplish this technique for removing waste thermal energy.

4. EVAPORATIVE COOLING

4.1 What is evaporative cooling and how it can be used in PEMFC thermal management

Conventional cooling systems generally entail the use of some sort of cooling fluid and consequently necessitate the use of pumps, blowers, etc. The situation is no different when a refrigeration cycle is used. Evaporative cooling can be an innovative solution for cooling and can be applied to fuel cell systems. The basic principle of evaporative cooling is very simple. When water evaporates, the latent heat of vaporization is provided by the water as well as from the surroundings.. As a consequence, both water and the surroundings are cooled.

Evaporative cooling can be a successful and effective method for removal of waste thermal energy from the PEMFC. All that needs to be done is to introduce water (in some fashion, which is very critical to the efficacy of the whole process of removal of thermal energy) in the MEA and let the water evaporate from the surface of the MEA into the dry reactant gas stream. This evaporation of water can remove thermal energy from the reaction zone of the PEMFC. If this process can be implemented, cost may be reduced, both in terms of parasitic power loss and for additional devices like pumps, fans and heat exchangers.

The idea of the evaporative cooling gives rise to certain questions:

- How much water should be introduced to effect cooling of the fuel cell?
- How can the required water be introduced into the PEM fuel cell chamber?

These are very important and pertinent questions and need special attention if an evaporative cooling strategy is to be implemented.

4.2 Electroosmotic drag and its relevance in evaporative cooling

As already mentioned (Section 3.1) water is transported from the anode side to the cathode side due to electroosmotic drag. On average, 2.5 moles of water are transported by one H^+ ion. Therefore, for each mole of hydrogen (H_2), there will be 5 moles of water transported across the MEA. Moreover, 1 mole of water is produced at the cathode side as a consequence of the half-cell reaction there. So there are total of 6 moles of water available at the cathode for each mole of hydrogen consumed. This water may be used for evaporative cooling. Later, via calculation, it will be shown that this water is more than sufficient to carry out evaporative cooling to remove the waste thermal energy produced during the operation of a PEMFC.

At this stage one relevant issue is the quantity of the water to be supplied to the PEMFC. Although each H^+ transports 2.5 mole of water across the MEA, it is perhaps not necessary to make that much water available in the anode because of the back diffusion occurring in the PEM fuel cell due to gradient of water concentration across the MEA. Water is carried to the cathode side from the anode side in the form of hydronium ion (Section 2.1.1). Moreover, water is also produced at the cathode side due to the redox reaction there (Equation 1, 2 & 3). But the anode side remains relatively more starved of water than the cathode and therefore water diffuses back into the anode side through the MEA due to concentration gradient. Back-diffusion of water, in turn, benefits fuel cell operation, because this diffused water helps the MEA to stay wet and supplies necessary water to produce hydrated hydronium ions since the molar ratio of water to humidified reactant hydrogen is much less than 2.5: 1. In most conventional method of water management, the molar ratio of water to hydrogen is around 0.4:1 [7]. Therefore, water supplied by conventional method of humidifying the reactant gas is by no means sufficient for carrying out evaporative cooling in the PEMFC. The question now is how much water should be supplied inside the PEMFC for effective evaporative cooling to take place? In the next section we will develop equations to see how much water (in terms of molar volume) is required for evaporative cooling.

4.3 Water requirement for evaporative cooling

Supplying the right amount of water in the fuel cell anode compartment is extremely important. Insufficient water would lead to poor performance of the MEA and ineffective cooling whereas too much water will cause flooding in the gas diffusion layer pores in the MEA leading to extremely poor performance. Therefore, before water is admitted inside the fuel cell, care must be taken to calculate the correct amount of water to be delivered inside a cell. Following is an approach to calculate the amount of water required for evaporative cooling:

Starting with the basic power equation, we know:

Power = (volts) x (amps) = V x I

The maximum theoretical voltage that a fuel cell can produce cannot be obtained. This is due to the irreversibilities occurring in the cell. Therefore the difference between the observed voltage and the voltage equivalent to the ΔH_{HHV} (for liquid water product) or the ΔH_{LHV} (for vapor product) is proportional to the waste thermal energy. In an operating cell with the gases saturated, some water is produced in the liquid state and some as vapor.

So, with reference to Equation 22, we obtain:

Heat $\dot{Q} = I\left(V_{th} - V_{cell}\right)$

Here $\dot{Q}$ = Waste thermal energy

V_{th} = Thermoneutral potential or 1.253 volt

V_{cell} = Individual cell voltage

I = Current density = Ampere/cm^2

The unit of the waste power or thermal energy $\dot{Q}$ is watt or joule per second. Therefore specific waste power or waste thermal energy (q'') will have the unit $\frac{W}{cm^2}$ or $\frac{J}{scm^2}$.

Now, loss of voltage or voltage drop can be defined as,

$$\Delta V = \left(V_{th} - V_{cell}\right) \text{ ---------- (23)}$$

Therefore, the following can be written for specific waste power or thermal energy,,

$$q'' = \left(I\right)\left(\Delta V\right)\frac{J}{scm^2} \text{ ---------- (24)}$$

This gives the waste thermal energy as a function of operating voltage and operating current. As was discussed before, a polarization curve of PEMFC gives the relation between cell voltages with corresponding current density. Therefore a polarization curve like the one shown in Fig 6 can be used to obtain values of the cell voltage of a PEMFC at a particular current density. This means that, since V_{th} is already known, values of I and V_{cell} can be obtained from a polarization curve and q" can be calculated as per Equation 24.

The next step is to calculate the amount of water required to dissipate this waste thermal energy (q"). The mass flow rate of water that can be evaporated to dissipate this waste power can be calculated by dividing the specific waste thermal energy by enthalpy of vaporization of water.

$$\dot{m} = \frac{q''}{\Delta h_{vap,H_2O}} \text{ ---------- (25)}$$

Where, $\dot{m}$ = mass flow rate of water

The temperature of the PEMFC can be assumed to be 80^0C and the enthalpy of vaporization of water ($\Delta h_{vap,H_2O}$) at 80°C is $\frac{2296kJ}{kg}$. Using this information and equation 25, mass flow rate of water per cm^2 area of the MEA can be obtained.

From Equation 25, the mass flow rate of water for a particular capacity of fuel cell can be calculated. In this research project, to calculate the amount of water needed for any particular PEMFC capacity, we would try to explore a standard case and calculate the water requirement for a 35 kW capacity fuel cell and try to build our design and determine design requirements from there.

To calculate waste thermal energy as shown in Equation 24, and thereby the water required to dissipate this energy as in Equation 25, it is important at the beginning to assume specific values for current density and the cell voltage. Typically, for most practical operations, individual cell voltage ranges between 0.6-0.7 V and respective current density ranges between 0.7-0.8 A/cm^2.

Therefore, let us assume that voltage per cell = 0.6 volts and current density = 0.8 A/cm^2

Therefore, Energy Flux = 0.6 * 0.8 = 0.48 $Watts/cm^2$

Therefore total area required = 35,000 Watts/ 0.48 ≈ 73,000 cm^2

Assuming 200 cells in the stack, we get that area per cell = 73,000/200 ≈365 cm^2

Now, $\sqrt{365} \approx 20$

Therefore a 20 x 20 cm^2 cell area can be approximated for the MEA.

Now we will proceed with Lower Heating Value (LHV) for our calculation. For the LHV, the thermoneutral potential is equal to 1.253 V/cell. This is the voltage at which an electrolyzer operating on water vapor would be neither exothermic nor endothermic.

Having this, the waste heat generated can be calculated as per Equation 24,

Waste heat = 0.8*(1.253-0.6) Watts/cm^2

= 0.52 Watts/cm^2

Therefore, waste heat generated per cell = 0.52 * (20 x 20)

≈ 208 Watts/Cell

Since, in this case, we have 200 cells, total waster thermal energy generated = 208*200 Watts = 41.6 K-Watts.

Thus total waster thermal energy is calculated. Now, as per Equation 25, the total water required to be evaporated to remove the 41.6 kW of waste thermal energy can be found in the following way:

$$\text{Water required} = \frac{Total\ waste\ heat}{Enthalpy\ of\ vaporization\ of\ water}$$

$$= \frac{41.6\,K-Watts * 60 * 1000}{2296 KJ/Kg * 1000}$$

= 1087.1 gram/minute

To find the volume flow rate from the mass flow rate, following procedure can be followed:

Density of water * Volume flow rate = mass flow rate of water

Therefore Volume Flow Rate = mass flow rate of water / Density of water ---- (26)

Now density of water @ 298 K = 0.998 gm/cc

Therefore, from equation (26),

Volume flow rate = 1087.1/0.998 cc/min
= 1089.28 cc/min
= 1089.28 X 10^{-3} Liter/min
= 0.28775 US Gallon/min (gpm)

This amount of water is equivalent to 3.5 moles of water per mole of reacting H_2. This is the minimum amount of water that the water delivery system must provide.

It must be stated here that the figure of 0.28775 Gallon/min is very important. This gives the basic requirement of water to cool a 35 kW capacity PEMFC. The same procedure can be used to determine the water requirement for any PEMFC.

A very interesting observation can be made when a relation between the number of water moles required and cell voltage, stoichiometry of supplied oxygen in the PEMFC is obtained. To do this, let's start with Gibbs free energy equation,

$\Delta G_R = \Delta H - T\Delta S_R$ ---------- (27)

Or, $T\Delta S_R = \Delta H - \Delta G_R$ ---------- (28)

Now,

$\Delta H_R = T\Delta S_R + T\Delta S_{IRR}$ ----------(29)

Where,

$T\Delta S_{IRR} = \Delta G_R - nFV$ ----------(30)

Now, in a PEMFC, water in the cathode side will include water in both liquid and vapor phase. Therefore, any calculation regarding the water in the PEMFC must consider this both phase of water.

Let p be the water mole fraction of water vapor. Then if latent heat of water and enthalpy of formation are considered as [22],

$$\Delta h_{vap} = -44010 \frac{J}{mole}, \ \Delta h_l = -285830 \frac{J}{mole}$$

Then equation © can be rewritten as:

$$\Delta H_R = -285830 + 44010\, p + 2FV \quad \text{---------- (31)}$$

Where V is the cell voltage and F is the Faraday constant. Equation (31) can give us,

$$n = 6.495 - p - 4.385V \quad \text{---------- (32)}$$

Where n is the number of moles of water required to be evaporated per mole of reactant hydrogen in a PEMFC.

Before going any further, let's look back at the basic electrochemical reaction of the PEMFC. The reaction is as follows:

$$2H_2 + O_2 \rightarrow 2H_2O$$

So the product water is 2 moles. Now, it is possible to develop a relationship between the total number of moles of water required for cooling as a function of O_2 stoichiometry and operating voltage. Following paragraph shows the process of developing the said relationship.

Let, S moles of O_2 is entering the cathode. Typically, pure oxygen is not used in PEMFC. Rather air is supplied. Since air consists of mainly oxygen and nitrogen (ignoring other small percentage of inert gases) and since nitrogen is 3.76 times the

oxygen in air, it can be said that, when S moles of oxygen are being supplied at cathode, 3.762S moles of N_2 will also enter the cathode. These are the species that are entering the cathode.

Exiting the cathode is 2p moles of water vapor, (S-1) moles of O_2 and 3.762S moles of N_2. Thus the total moles exiting the cathode are $4.762S - 1 + 2p$.

Total vapor moles at cathode = $4.762S - 1 + 2p$

Total product water moles = 2

Vapor product water moles = 2p

Liquid product water moles = $2(1-p)$

Let X moles of liquid water per mole of reactant hydrogen be added. So considering the basic electrochemical reaction of PEMFC, total water moles added to the anode are 2X.

Therefore, total vapor at the cathode exit = $4.762S - 1 + 2p + 2pX$

Therefore, total water vapor = $2p + 2pX$

And total liquid water = $2(1-p)(1+X)$

From equation (f) and the above expression of total water vapor, it is quite clear that,

$(2p + 2pX)/2 = n = 6.495 - p - 4.385V$

Or, $n = 6.495 - p - 4.385V = p(1+X)$ ----------(33)

Now, water vapor partial pressure at the exit of cathode can be given by following expression:

$$\frac{V_p}{P_t} = \frac{2p(1+X)}{4.762S - 1 + 2p(1+X)} \quad \text{----------(34)}$$

Where, V_p is the water vapor pressure and P_t is the total pressure in the fuel cell.

Vapor pressure can be expressed in terms of temperature as follows:

$$V_p = \frac{10^{\left(20.9586 - \frac{2825.4}{T}\right)}}{T^{4.0843}} \text{ ---------- (35)}$$

Solving the simultaneous equations (32), (33), (34) and (35), one gets,

$$X = \frac{[2*[2.381*S-0.5]+[6.495-4.385*V-\frac{P_t*(6.495-4.385*V)}{[\frac{10^{\left(20.9586-\frac{2825.4}{T}\right)}}{T^{4.0843}}]}]}{[\frac{P_t*(6.495-4.385*V)}{[\frac{10^{\left(20.9586-\frac{2825.4}{T}\right)}}{T^{4.0843}}]}]-[2.381*S-0.5]+[6.495-4.385*V]} \text{ -------- (36)}$$

Equation (36) gives the number of moles of water per mole of hydrogen required for evaporative cooling of PEMFC at certain oxygen stoichiometry 'S' ,operating voltage 'V' and temperature T. This equation can also find temperatures of PEMFC under specific number of moles of water X supplied per mole of reacting hydrogen, oxygen stoichiometry S and cell voltage V. Table 1 shows different values obtained through using the equation (36). Table 2 depicts the effect of added water on the temperature of the PEMFC and Table 3 shows the effect posed by the total pressure on the temperature of a PEMFC.

Figure 14 shows a graph that was plotted to examine the relationship between the temperature of the PEMFC (T) and the added water (X) per mole of reacting hydrogen.

Figure 14 also unveils some interesting characteristic of the relationship between added water at anode per mole of H_2 and PEMFC temperature. To follow is a brief description of inference from the plot:

- Addition of water does cut down the temperature of PEMFC

- After 5 moles of H_2O/mole of H_2, further temperature profile keeps an asymptotic nature. This signifies that, as long as minimum continuous water supply is ensured, cooling will continue.
- Therefore, mass flow rate of water does not need a strong regulation. As long as it is possible to supply water at the rate mentioned above, the water will keep on working towards evaporative cooling. This is a very important issue from design point of view.
- As long as flooding is avoided, supplying more than 5 moles of H_2O/mole of H_2 may be helpful. This is not impossible. Laconti et. al. [15] mentioned that up to 8 moles of H_2O/mole of H_2 are possible to be moved across the ionomer membrane utilizing electro-osmotic drag. This provides the designer with a huge flexibility and convenience for water delivery system design.

Now, it pays to recover some water in the condenser for recycling them back into the PEMFC. Generally, $V_p/P = 2p(1+X)/\{4.786S–1+2p(1+X)\}$ (from Equation. 34) and the amount of liquid water is $2(1–p)(1+X)$. At the condenser exit, we need to recover 2X moles of liquid. So, $2X = 2(1–p^*)(1+X)$, where p^* is the value at the condenser exit, so $p^* = 1/(1+X)$. This can be put into Equation 34, which gives $V_p/P = 2/\{4.786S–1+2\}$, which is obvious because at the condenser exit there are 2 moles in the vapor phase, X in the liquid. Thus, V_p and temperature only depend on stoichiometry and pressure. For S = 1.6, 2.0, 2.5, and 4.0 at 1 atm, condenser exit temp is 63.6°C, 59.2°C, 54.9°C, and 46.0°C. For S = 2.0 and P = 2 atm, temp is 74.9°C. So it pays to have low S and pressure to have a better temperature gradient and better cooling.

Up to this point, the calculations show that it was possible to determine the quantity of water required to be evaporated for dissipating a particular amount of waste thermal energy. However, the basic challenge for satisfying the objective of the research still remained. A water delivery system had to be designed which was capable of delivering the required amount of water for evaporative cooling (amount calculated above) in such a way that the distribution of water is uniform over the surface of the reaction zone of the PEMFC. The step by step design methodology towards attaining the

desired design for a water delivery system that meets the objective of the research project is described in the following section.

4.4 Design approach to attain a realistic design solution for water delivery system

In the previous section, the quantity of water required to be evaporated to dissipate the waste thermal energy was calculated. This quantity of water, in some fashion, has to be introduced inside the PEMFC. The way in which this water is delivered determines whether evaporative cooling will be successful or not. It was already mentioned that, since this research project is concerned with the delivery of water and its pattern of distribution in the Ni- metal foam flow field, it is not necessary to incorporate it into an actual fuel cell. Rather a physical model of a PEMFC was used. Although a detailed description will be given in a later section (Section 5.3.1), for the time being, it is important for the reader to know that the water delivery system will include two different types of nozzles. PJ type nozzles for producing finely atomized conical fog flow and BJ type nozzle for producing flat fan strip type water flow with relatively coarse atomization.

Delivery of water was the only limitation of the previous work done at CESHR [7]. As discussed earlier, results of this work showed no signs of cooling. However, it has been shown that evaporative cooling is theoretically possible. One of the primary reasons for disappointing result of the previous CESHR work was the inability of the system to deliver the required amount of water to the reaction zone of the PEMFC. In fact, if one assumes an evaporation temperature of 70°C, and a cooling load of 30 W, the quantity of water that was deliverable with the previous CESHR system design (using an ultrasonic nebulizer) was 7 times less than that actually required by the load [7]. With that in mind, to overcome the difficulty regarding the delivery of water, the problem was treated with a step by step design methodology, including the formulation of a need statement and analysis of need to determine the necessary functions to be fulfilled to achieve the system

objectives, that is to deliver required quantity of water uniformly distributed over the active surface of the PEMFC so that evaporative cooling could take place.

4.4.1 Need Statement

As mentioned in the previous section, to follow a design methodology, the first thing to do is to come up with a need statement outlining the necessary functions to be fulfilled to attain required system design. Following is the need statement for the design of the water delivery system:

"Design a system to deliver adequate amount of water (at least 3.4-3.6 moles of water per hydrogen mole) using any method that delivers water directly into the reaction zone PEM fuel cell stack where it can be distributed evenly and where it can be evaporated to dissipate waste thermal energy produced from the operation of a PEMFC."

After outlining this need statement, the next job is to analyze this need or in other words, come up with a need analysis that explains the need statement from a functional requirement point of view.

4.4.2 Need analysis

The primary function of the design is to deliver sufficient water uniformly distributed to the PEMFC so that evaporative cooling can take place. The word "enough" means adequate water that is required to be evaporated to dissipate the waste thermal energy of the PEMFC. This adequate amount of water is calculated and found to be 3.4-3.6 moles of water per hydrogen mol of reactant gas. Therefore the proposed water delivery system needs to supply at least this quantity of water.

Moreover, for the design to be effective, water has to be delivered directly into the fuel cell reaction zone, i.e., to the MEA. The previous attempt for cooling the PEMFC via evaporation of water was by humidifying the reactant gas. This approach did not work, as

the system could not deliver adequate water into the cell. This leaves us with the notion that indirect introduction of water makes it difficult to deliver water into the cell. A more direct approach of introducing the water is probably going to be more effective. Therefore arrangements had to be made in the water delivery system so that water can be injected directly into the reaction zone of the PEMFC.

For an overall heat dissipation, it is important that water be distributed uniformly inside the PEMFC reaction zone. This will effectively improve both the water and thermal management of the PEMFC. Failure to do so may give rise to the generation of hotspots in the cell. Therefore, only delivery of the required amount of water is not going to be the only design criterion for the water delivery system design, it must also deliver the water in such a fashion that it can be uniformly distributed in the Nafion^{TM} membrane of the MEA.

From the discussion above, it can be concluded that the most important parameters that can affect the performance of the design are delivery of right amount of water in the PEMFC and a proper distribution of this water in the reaction zone of the PEMFC. Therefore these parameters can be referred to as critical parameters of the design of the water delivery system. These critical parameters are the very factors that affect the lowest level functions. Therefore they have the capability of affecting the performance of the design itself. Or more precisely, these parameters can affect the performance of the cooling fluid (water in this case). For developing an efficient design, these parameters have to be defined properly and their effect on the performance of the cooling fluid must be investigated. To accomplish this task, it is important to find out what are the operating and design parameters that can affect these critical parameters and in what ways. There will be an experimental set-up to investigate the effect of these design parameters on the critical parameters which in turn affect the total design. Section 4.6 goes through these critical parameters in details and also investigates if any further design or operating parameter can affect these critical parameters and in what ways.

4.5 Means to supply water to the Fuel Cell

There are some important aspects of this design and these should be discussed in details. The most important of all the issues is the problem of delivering water into the PEMFC reaction zone. Getting the water inside the cell properly was the most challenging problem for the water delivery system design. In CESHR's previous design, an effort was made to humidify the reactant gas to deliver water to the reaction zone of the PEM Fuel Cell. However, the reactant gas (hydrogen) could not carry enough water with it and therefore the scarcity of water inside the PEMFC did not allow successful evaporative cooling. Consequently, it followed that water should be introduced directly inside the PEMFC rather than using the reactant gas as a carrier of water. A design employing nozzles to deliver water directly into the reaction zone seemed very promising and this was the route investigated.

One more issue regarding the delivery of water should be clarified here. First of all, it has been repeatedly stated and also mentioned in the function structure that water needs to be delivered in the reaction zone of the PEM fuel cell. Actually the water delivery system will not deliver water directly in the MEA. Rather the water is sprayed on the surface of the Ni-metal foam, which is the flow field for reactant gases in a PEMFC, and which is located in a very close contact with the MEA. Upon reaching the Ni-metal foam flow field, the reactant gas (H_2) is distributed along the surface of the Ni-metal foam by flowing through its pores. Therefore, if it is possible to deliver water to the Ni-flow field, the reactant gas (H_2) will ultimately end up in transporting the water through the MEA from the anode side to the cathode side utilizing electroosmotic drag. At the cathode side, water will be evaporated and will thereby absorb the excess thermal energy. If water, in the right quantity, can be delivered uniformly in the Ni-metal foam, it is ensured that it will diffuse to the cathode side and evaporative cooling will be possible. Therefore, the bottom line is, in order to provide a uniform water distribution inside the PEM FC, water has to be delivered in such a way that it gets distributed

evenly along the surface area of the Ni- metal foam. In other words, if water is distributed uniformly in the Ni- metal foam, it can be said that water will also be distributed evenly in the MEA of the PEMFC.

The next step for the design of the water delivery system is to consider the critical parameters that have direct influence on the design and performance of the delivery system. A brief description of the critical parameters crucial for this design follows.

4.6 Critical parameters and their influence on the design

In the process of analyzing the need, critical parameters were identified that would have an influence on the performance of the water delivery system. This section gives a detailed overview of the critical parameters for the water delivery system design. This section also investigates if any further parameter (design or operating) imposes any effect on the critical parameters.

From the need analysis (section 4.4.2), it is clear that the following parameters are crucial to investigate the research objective:

I. Mass Flow rate of water at the exit point of the nozzle to ensure the right/desired amount of water coming out of the nozzle tip

II. The distribution of water inside the Ni-Metal flow field. This parameter is vital, since uneven distribution may give rise to poor water distribution in the Nafion™ membrane resulting poor water and thermal management for the MEA. Uneven water distribution may give rise to hot spots in the PEMFC membrane and inside

the cell compartment. Therefore, water distribution in the Ni-metal flow field is extremely important and is a vital design issue.

It occurred that to the author that the distribution of water inside the Ni-metal foam might be affected by several design and operating parameters. These parameters needed to be investigated individually to see what effect they might pose on the distribution of water in the foam flow-field. A brief discussion of these parameters and how they may affect the distribution of water in the Ni-metal foam is given below:

4.6.1 Design parameters

The design parameters that might have direct effect on the distribution of water in the Ni-metal foam were identified as type of the water spray pattern, height of the nozzle and area of the nozzle. To follow is a brief description of all of these design parameters.

4.6.1.1 Type of water spray pattern

The spray pattern deemed to have a have a great impact on the distribution of water on the Ni-metal foam flow-field. That's why it was decided that two different water spray patterns would be used to study the impact of the spray pattern of water on the distribution of water in the Ni-metal foam. To facilitate this investigation, the experimental model would have two compartments simulating two cells of a PEM fuel cell stack. In these two compartments two different spray patterns of water injection (conical fog spray and flat fan spray) were employed to investigate the effect of water spray pattern on the distribution of water in the Ni-Metal flow field. A critical decision at this point was the choice of the nozzles since they would determine the flow pattern

which is important for an even distribution of the water inside the reaction chamber of the cell. As already mentioned, an attempt would be made to try to utilize nozzles available off-the-shelf. This would give a basic starting point. The main difference between the two types of flow patterns selected are the shape of the water spray (one has a conical shape and the other has a flat fan shape) and the water droplet distribution (one has a fog type water distribution with very fine water droplet size and the other has a continuous flat fan type water distribution). Below is brief discussion about the water spray pattern from the nozzles:

4.6.1.1.1 Flat fan flow pattern

It was anticipated that the flat fan spray pattern would provide an even distribution across the surface of the Ni-Metal flow field. This particular type of spray pattern, which can be viewed as a strip of water flow (flat strip), has the capability to cover the top edge of the foam and thereby was expected to deliver water along the edge. Commercially available Bete BJ type Nozzles (Bete Fog Nozzle Inc., Greenfield, MA) can produce such a flat spray pattern. Figures 15 and 16 show the configuration of flat fan spray.

It was important that the flat fan flow covered the length of the Ni-metal foam used in the experiment. Figure 17 shows a datasheet provided by the manufacturer that shows the values of the flow rates that can be obtained under different pressures and nozzles areas.

4.6.1.1.2 Finely atomized conical spray pattern

This type of flow is obtained from the commercially available Bete PJ type nozzle. In this case, the spray pattern would be a little conical in shape. Therefore, unlike the previous flat fan flow discussed above, this type would cover a wider area, as is shown schematically in Figure 18.

Moreover, water would be sprayed as very finely atomized droplets. These finely atomized water droplets would help the water particles penetrate the Ni-metal foam flow-field very easily. Figure 19 shows an actual picture of the mist or fog generated by these finely atomized water droplets:

The datasheet in Figure 20 shows the nozzle to be used in the design for conical pattern flow. The datasheet also shows the values of the flow rates that can be obtained under different pressures and different flow rates.

4.6.1.1.3 Atomization of water

An important issue that needs to be addressed here is whether atomization of water will have any effect on the performance of the design. Actually it will not. It does not matter actually how one delivers water in the reaction zone of the PEMFC. This water will be injected at the anode side of the PEMFC and will eventually get transported to the cathode side via electroosmotic drag. And the state of the water at the cathode will be same irrespective of whether they are introduced as finely atomized water or coarsely atomized water droplets.

4.6.1.2 Height (H) of the nozzle

The height H is defined as the vertical distance between the nozzle exit and the top edge of the Ni-metal foam (Figures 16 and 18). This is another design variable. Depending on the different values of H (that is, different vertical locations of the nozzle), there was a possibility that the water might be distributed differently in the Ni flow-field. Therefore, an investigation was required to determine what impact the variable H would have on the water distribution in the Ni-metal foam.

4.6.1.3 Area of the nozzle orifice

This is another design variable that was deemed to potentially have impact on the distribution of water in the Ni-Metal flow-field. Therefore the effect of the orifice of the orifice area of the nozzles to be used for each particular type of water spray was investigated.

4.6.2 Operating parameters

In the previous paragraph, it was discussed how the design parameters could the affect the distribution of water in the Ni-metal foam flow field. These design parameters must be investigated thoroughly as they will have a direct impact on the cooling fluid performance (water) and also on the stack design.

Just like the design parameters, there were certain operating parameters that could have affected the performance of the water delivery system. After careful judgment, it was determined that the most crucial operating parameter that could have an effect on

the distribution of water in the flow-field was the reactant gas flow (H_2 gas flow). A description of this parameter and its probable impact measurement follows.

4.6.2.1 Reactant gas flow

It was of concern whether the reactant gas flow in a fuel cell would affect the water droplet flow exiting the nozzle and influence the water distribution in the Ni-metal flow-field. Therefore, for this research project, it was decided that this issue would be investigated. To do that, it was necessary to find out for our test case of a 35 kW PEMFC how much hydrogen we needed and what the expected velocity was. Next, it was important to find out what was the water particle velocity. If the water particle velocity was greater than hydrogen velocity, water particles would not be entrained by hydrogen and water particle distribution would not be affected by hydrogen flow, i.e., reactant gas flow. The equations necessary to investigate this issue were developed in the following section.

4.6.2.1.1 Calculation of velocity of hydrogen in the PEMFC

From equation (1), we know hydrogen dissociates at the anode:

$$H_2 \longrightarrow H^+ + 2e^-$$

2 electrons are transferred for each mole of hydrogen

Therefore, charge = 2 x F x amount of H_2 used

Therefore, amount of H_2 used = Charge / (2xF) moles/sec

$$= I / (2 \times F) \quad \text{moles/sec} \quad \text{---------- (37)}$$

Where I = Charge.

Now, Power, $P_e = V_c \times I \times n$ ---------- (38)

Where, V_c = Voltage of each cell

n = number of individual PEM FC in a stack

F = Faraday's Constant

= 96,485 C

From Equations (37) and (38),

H_2 usage = $P_e / (V_c \times n \times 2F)$ ---------- (39)

This is for individual cell.

Now, Molar weight of hydrogen = 2.02×10^{-3} kg/mol

Therefore, total H_2 usage in kg = $(P_e \times 2.02 \times 10^{-3}) / (V_c \times 2 \times F)$ ----------(40)

Here, P_e = 35 KW = 35,000 Watts = 35000 J/Sec

V_c = 0.7 Volts = 0.7 J/Sec

Therefore, from equation (40),

Total H_2 mass flow rate = 0.523397×10^{-3} kg/sec

$= \dot{m}_{H_2}$

Now, Volume flow rate Q = V x A

Where V = Velocity of H_2

A = Area available for H_2

Now, $\dot{Q}_{H_2} = \dot{m}_{H_2} / \dot{\rho}_{H_2}$ ---------- (41)

Where, $\dot{m}_{H_2}$ = mass flow rate of H_2 (total)

$\dot{\rho}_{H_2}$ = density of H_2

= 0.0000899 gm / cc

So from Equation (41), we get the total volumetric flow rate of H_2,

$\dot{Q}_{H_2}$ = 5821.99 cc/sec

≈ 5822 cc / sec

This is total H_2 flow.

Therefore, for individual cell, H_2 flow can be given as,

$\dot{Q}_{ind,H_2}$ = 5822 / 200 cc/sec = 29.11 cc/sec

Therefore, for a PEMFC that contains a 20 x 20 cm^2 membrane will have an approximately 2 x 20 x 25 cm^3 chamber. So the cross sectional area would be 2 x 25 cm^2. This means that the velocity of the hydrogen gas inside the cell will be,

$\dot{V}_{H_2}$ = $\dot{Q}_{ind,H_2}$ / Area available for H_2

= 5.822 cm/sec.

Next, the terminal velocity of water particles must be calculated.

4.6.2.1.2 Calculation of terminal velocity of the water particle

To do this, the first thing that must be done is to find out what will be the Reynolds number for the water particle if the water particles flow in hydrogen.

Reynolds Number $N_{Rep} = (D_p \times U_o \times \dot{\rho}_{H_2}) / \dot{\mu}_{H_2}$ ---------- (42)

Where, N_{Rep} = Particle Reynolds Number

D_p = Particle diameter = 80 x 10^{-6} meter (on average)

U_o = Relative Velocity of Water Particle in H_2

ρ_{H_2} = density of H_2 = 0.089 kg/m^3

μ_{H_2} = Viscosity of Hydrogen = 0.0000097 kg/m-s

Now, $U_o = U_p - U_g$ ---------- (43)
= particle velocity – gas velocity

Where U_g = H_2 gas velocity that was calculated in section 4.6.2.1.1.

Next, the water particle velocity was calculated. The velocity of a water particle depended on the orifice size of the nozzles. As was previously discussed, the two types of nozzles selected for this project were Bete Nozzle type PJ and Bete Nozzle Type BJ. In case of both BJ and PJ nozzles, three different orifice sizes were used. A brief description of both types of nozzles used in the investigation can be found in Tables 1 and 2.

Orifice sizes of these nozzles can also be obtained from Figures 16 and 19. To calculate the particle velocity, first generic equations were used and then the specific particle velocity for different size of PJ Nozzle was calculated. Lastly, particle velocity of each size of PJ Nozzle was used to calculate the terminal velocity of water particle for respective nozzles. As was previously mentioned, if these terminal velocities of water particles were found to be greater than the reactant gas velocity, it could be assumed that reactant gas flow would not affect the water distribution pattern in the Ni-metal foam.

To begin with the calculations, lets assume that the orifice diameter = D_o

The required amount of water to dissipate waste heat generated in a 35 kW PEM FC was calculated to be 1089.28 cc/min.

Also, $\dot{Q}_{H_2O}$ = U_p x Area of the orifice

= U_p x Π x D_o^2 ---------- (44)

Where, $\dot{Q}_{H_2O}$ = Volume flow rate of water

U_p = Water Particle Velocity

Π = 3.14

From Equation 44, we get,

$U_p = \dot{Q}_{H_2O} / (\Pi \times D_o^2)$ ---------- (45)

Next, the terminal velocity of water particle was calculated. It was known that water particles would travel a certain distance to reach the Ni-Metal foam and in this gap, hydrogen would also be moving. So, it was important to find out if the water particles were going to be entrained or affected in any other way by the reactant gas flows. To accomplish this, it was important to derive equations for the motion of water particles in a fluid (H_2 in this case), which will be conducted in the next paragraph.

4.6.2.1.3 Equations for water particle motion moving in a fluid

Theoretically, it was important to find out the motion and velocity of water particles in the hydrogen environment as it was known that water particles in PEM FC would have to move in a PEMFC chamber that would be occupied by reactant hydrogen

gas. Therefore, in this section, a mathematical approach was applied to quantitatively determine the water particle velocity in hydrogen gas environment.

Let us now consider a particle of mass m is moving through a fluid under the action of an external force Fe (Figure 21)

Let U_o = particle velocity with respect to the moving fluid (reactant gas in this case)

$= U_p - U_g$

If, m = mass of the particle

ρ_{H_2} = density of the fluid medium

ρ_p = density of the particle

F_e = External Force = $(m \times a_e) / g_c$ ---------- (46)

F_b = Buoyant Force = $(m \times \rho_{H_2} \times a_e) / (\rho_p \times g_c)$ ---------- (47)

F_d = Drag Force = $(C_d \times U_o^2 \times \rho_{H_2} \times A_p) / (2 \times g_c)$ ---------- (48)

Where, a_e = acceleration due to external forces

A_p = Projected area of the particle

C_d = Drag Co-efficient

Now, acceleration of the = dU_o/dt

Therefore, $m/ g_c \times dU_o/dt = F_e - F_b - F_d$ ---------- (49)

From Equations (46), (47), (48) & (49), we get,

$dU_o/dt = a_e \times (\rho_P - \rho_{H_2}) / \rho_P - (C_d \times U_o^2 \times \rho_{H_2} \times A_p)/2m$ ---------- (50)

If the external force is due to gravity, then,

$a_e = g$

From (49) and (50),

$dU_o/dt = g \times (\rho_P - \rho_{H2}) / \rho_P - (C_d \times U_o^2 \times \rho_{H_2} \times A_p)/2m$ ---------- (51)

At the terminal velocity,

$dUo/dt = 0$ ----------(52)

Therefore, from (52),

$U_o = U_t = [\{2g \times (\rho_P - \rho_{H2}) \times m\} / \{C_d \times \rho_{H_2} \times A_p \times \rho_P\}]^{1/2}$ ---------- (53)

(Assuming that the water particle is spherical:

m = Volume of the particle x ρ_P

$= 4/3 \times \Pi \times (r_p)^3 \times \rho_P$ where r_p = radius of particle

$= 4/3 \times \Pi \times (D_p/2)^3 \times \rho_P$

$= 1/6 \times \Pi \times (D_p)^3 \times \rho_P$ ---------- (54)

$A_p = (\Pi \times D_p^2)/2$ ---------- (55)

From (53), (54) and (55),

Terminal Velocity, $U_t = [\{4g \times (\rho_P - \rho_{H_2}) \times D_p\} / \{3 \times C_d \times \rho_{H_2}\}]^{1/2}$ ------ (56)

$g = 9.81\ m/s^2$

$\rho_P = 998.23\ kg/m^3$

$\rho_{H_2} = 0.0899\ kg/m^3$

$D_p = 80 \times 10^{-6}$ meter (on average)

C_d = Coefficient of drag

The value of C_d depends on the Reynolds Number (N_{Rp}) of the particle. The following is a brief outline of the determination of the appropriate C_d [23]

- For small Reynolds Numbers (i.e., Re < 0.5), viscous effects dominate and no separation is observed. Therefore an analytical solution for the drag co-efficient is possible, as proposed by Stokes:

$$C_d = 24/ N_{Rp}$$

- In the transition region (i.e., $0.5 < N_{Rp} < 1000$) inertial effects become of increasing importance. Above N_{Rp} of 24, the flow around the particle begins to separate. For this region, following correlation is used:

$$C_d = 24/ N_{Rp} (1+0.15 \times N_{Rp}^{0.687})$$

- Above $N_{Rp} = 1000$, the drag coefficient remains almost constant up to a critical Reynolds Number and C_d is given a constant value as follows:

$$C_d = 0.44$$

Now, the particle velocities and their terminal velocities are calculated according to the relations developed above for conical fog flow and they are given in the Table 2. Table 3 shows the water spray particle velocity calculated for flat fan type flow.

One can see that the terminal velocities of all water particles out of all the types of nozzles used are greater than the reactant gas (hydrogen) velocity. This gives a clear indication that water particles are not going to be entrained by the reactant gas flow and water should get distributed without being affected by gas flow. Although, theoretically, that is the case, the question of whether the water particles are entrained by reactant gas or whether the distribution of water is affected by gas flow will be investigated through experiment.

5. EXPERIMENTAL SET-UP AND PROCEDURES

5.1 General description

The objective of this investigation was to design a water delivery system that could deliver enough water directly inside a PEMFC so that evaporative cooling could take place and also to investigate what design and operating parameters affect the performance of the cooling fluid, i.e., water. To accomplish this task, it was important to decide what performance metrics would be used to evaluate the design performance. This decision would facilitate the design of the experimental set-up.

With reference to the discussion regarding the need analysis and critical parameters (Section 4.6), one can easily see that the most important parameters for this design are mass flow rate of the cooling fluid (water) that is introduced into the PEMFC and the distribution of this water over the surface of the Ni-metal flow-field. The mass flow rate of water will determine the maximum amount of waste heat that can be removed from a PEMFC and the distribution of water in the Ni-metal flow-field will indicate whether water eventually becomes uniformly distributed in the MEA. As soon as the reactant gas arrives at the MEA, it will be dissociated into H^+ and e^-. Electrons will pass through the external circuit and the H^+ will form the hydrated H_3O^+ (hydronium) ion, which carries the water to the cathode side where it eventually evaporates. If the distribution of water is uniform over the Ni-metal foam, that is if hydrogen can contact water uniformly in the foam, hydronium ions can be produced uniformly and water will therefore be carried throughout the whole surface of the MEA. This will result in improved performance of the Nafion® membrane because it will remain hydrated and maintain the proper operating temperature.

Moreover, uniform water distribution also obviates the possibility of any hot spots generated within the cell. Therefore, distribution of water in the Ni-metal foam flow field is an important performance metric.

As mentioned before, the maximum amount of waste thermal energy removal depends mainly on the amount of water input at the anode side of a PEM fuel cell. Therefore it is necessary to measure the mass flow rate of water from the nozzles used in the investigation. The Bete Type PJ nozzles produces very fine conical fog type flow and Bete type BJ nozzles produces flat fan type flow as seen in Figures 15 and 19. Their flow rate depends on both pressure and the nozzle area. Specifications of these nozzles can be obtained from Figures 17 and 20. To verify their performance, it was decided that mass flow rate from each of these nozzles would be recorded and that data would be matched against those provided by Bete Fog Nozzle Inc. This would ensure that the nozzles would discharge water according to the manufacturer's specification and that the required water was supplied to the PEMFC. That is, for for evaporative cooling to take place, at least 3.4-3.6 mols of water per mol of reacting hydrogen is required to be injected inside the PEMFC (as mentioned and calculated in the section 4.3). Therefore, it is important to measure the mass flow rate of each type of the nozzle so that a minimum water flow of 3.4-3.6 moles of water per mol of reacting hydrogen are actually obtained.

As for the distribution, it was very difficult to measure or quantify the distribution of water over the surface of the Ni-metal foam. However, a distribution parameter" was defined to quantify the distribution of water over the surface of the Ni-metal foam. The "distribution parameter" was defined as a ratio of the area of the Ni-metal foam covered by the impinged water (wet area) to the total area of the metal foam surface. Hence, the distribution of water can be expressed as:

$$\text{Distribution of water (\% of area)} = \frac{\text{wet area}}{\text{Total area of the Nickel Metal Foam}} \quad \text{---------- (57)}$$

Figure 22 schematically shows the areas used to define the distribution parameter.

After the water was sprayed over the Ni-metal foam, water covered a certain area of the foam. An outline of the two areas (wet area and the total area) was drawn by putting a clear tracing paper on top of the wet Ni-Metal foam after water had penetrated into it. Once these areas were measured, the distribution parameter could be calculated. The distribution parameters for various cases were calculated using Equation 57. This procedure is explained in detail in the experimental procedure section (section

A concern here was how the wet areas would be measured as these areas were rather irregular in shape. However, the solution was easy. The outlines of the areas were drawn on a sheet of tracing paper. The area where water could not penetrate were colored as black leaving the rest of the area white. These tracing papers were then scanned and formatted as digital image. From those images, digital software was used to determine the area of the black areas (that is, the areas where water could not penetrate) by calculating the white and black pixels.

One other important issue about the distribution was whether the water distribution would be affected by the reactant gas (hydrogen) flow. Calculations showed that the terminal velocity of water particles were higher than the hydrogen gas velocity for the all the applicable cases in the PEMFC chamber. This velocity comparison indicated that there will not be any effect on water distribution imposed by the hydrogen flow. To corroborate the results obtained from the equations, an experiment was conducted where the reactant gas was simulated with air. Air was allowed to flow into the prototype structure of the PEMFC (a detailed description of the prototype structure is given in Section 5.31). For a particular pressure and flow rate, water was sprayed through nozzles in the Ni-metal foam and the distribution was recorded. The same experiment was conducted with air flowing in the PEMFC prototype structure. These

two distributions were then compared to determine if there was any effect of gas flow on the water distribution.

At this point, it is important to discuss the issue of using air as a simulator of hydrogen. Hydrogen is the reactant gas for PEMFC anode and therefore it is more appropriate to use it for the experimental model of this research project. But hydrogen is highly flammable, very light, and diffuses and floats upward when leaked. The prototype structure of the PEMFC, which was used in this project, contains some open areas which might cause hydrogen to leak and accumulate in the laboratory. Therefore, in this environment, the use of hydrogen might have serious safety consequences. Moreover, in the experimental study, the aim was to investigate the how the distribution of water in the Ni-metal foam flow-field gets affected by the flow of reactant gas only and therefore it was decided to use air to examine the effect of reactant gas flow on water distribution. To accomplish this particular goal, air flow at the rates of 1.71 slm (standard liter per minute) and 3.0 slm were flown into the prototype structure simultaneously with water flow from the nozzle. 1.71 slm was the amount of hydrogen that was required by the 35 kw stack PEMFC, whereas, 3 slm was even a higher order of reactant flow. Distribution pattern by using air flow at these rates were observed and distribution parameters were calculated. Then these distribution parameters were compared with the water distribution obtained by using water only with no air flow. It is common knowledge that air is 14 times more dense than hydrogen. So if these air flows, which were flown at the same or higher rate than that of the actual hydrogen flow, didn't affect the water distribution in the Ni- metal foam, it could be concluded that hydrogen flow in PEM FC would not affect the distribution in Ni- metal foam either.

The remaining portion of this section is divided in two parts. In the first part, the experimental set-up is described and in the second part, experimental procedures are described for the two sets of experiments involving the mass flow rate of water and the the distribution of water over the surface of the Ni-metal foam flow field. Apart from the

experimental set-up, a detailed description of the apparatus used for all the experiments is also given in the first part of this section. The second part will include a thorough description of the experimental procedures.

5.2 Experimental set-up

The following is a description of the experimental set-up used in this project to conduct experiments. This section will also include a description of the apparatus used in all the experiments.

5.2.1 Description of experimental set-up to measure the average water mass flow output of the nozzles

Figure 23 is a schematic representation of the experimental setup used to measure the mass flow rate of the nozzles used in this project. This consisted of the following apparatus:

BETE Fog Nozzles: PJ Type
BETE FOG nozzles: BJ Type
Water supply (from city line)
Pressure Gauge
PEMFC model structure
Water Collector
Electronic Analytical Balance

To measure the mass flow rate of water, the water collector was used to collect the water that comes out of the nozzle. The water collector contained Drierite™ desiccant

which can trap water. The nozzle line was fully inserted in the collector bottle to prevent any loss of water.

As was previously noted, the importance of measuring the mass flow rates of water out of the nozzles is twofold. First, the mass flow rate of water will verify the data provided by the manufacturer, and second, the mass flow rate data will enable the author to quantify the maximum expected evaporative cooling possible.

It is also important to mention here that the water was supplied at constant pressure (40 psi) for all the nozzles used. This means that pressure was not considered as a variable in the design of the water delivery system. This allowed the author to measure mass flow rate of a particular type of nozzle for various areas at constant pressure. Description of the experimental procedure will be given in section 5.4.

5.2.2 Description of experimental set-up to determine the water distribution over the surface of the Ni-metal foam flow field

The following apparatus was used to measure the distribution of water on the Ni-metal foam flow-field:

BETE Fog Nozzles: PJ Type
BETE FOG nozzles: BJ Type
Water supply (from city line)
Pressure Gauge
PEM FC prototype structure
Ni-metal foam flow field
Eosin Dye
Tracing paper

MKS Flow mass flow meter
Compresses Air Cylinder

Figure 24 is a schematic diagram of the experimental set-up used for finding the water distribution pattern.

Water from the nozzles is sprayed directly on top of the Ni-metal foam placed inside the PEMFC model structure in the same way inside an actual fuel cell with vertically placed Ni-metal flow field and MEA. Water flows down the flow-field and penetrates through its porous structure. To track the water inside the flow field, eosin dye was used. This non-toxic dye readily dissolves in water, and is used by public works departments to trace water leaks. Some tablets of this dye, which has a very strong red color, were placed in the tubing that holds the nozzles. When water was passed through the tubing, the eosin dye tablets were dissolved in water to give a clear bright red color. This allowed the water distribution to be traced.

As mentioned in Section 4.9.2.1, it is important to examine whether the water distribution is affected by reactant gas flow. As stated in Section 5.1, for safety reasons, reactant gas (hydrogen) was simulated with air to discover the effect of reactant gas flow on water distribution in Ni-metal foam. Figure 24 schematically shows the arrangement and direction of air flow. Air was passed through MKS mass flow meter (a description of this equipment is available in Section 5.2.3) before it enters the PEM FC prototype structure. This allowed a metered flow of air in the structure.

As soon as a distribution pattern was traced in the Ni-metal foam, tracing papers were used to draw an outline of the water distribution pattern on the foam. Later these tracing papers were scanned for determining the wet and dry area digitally. A description of this tracing process will be given in the experimental procedure in section 5.4.

5.3 Apparatus

This section is dedicated to the description of all the apparatus used in all the experiments conducted in this research project.

5.3.1 PEMFC model structure

As mentioned earlier, the goal of the project was to determine what and how the design and operating parameters affect the performance of a water supply system for evaporative cooling of a PEM fuel cell in terms of proper distribution and successful delivery of right amount of water. Therefore, in the early stage of the research project, it was decided that it was not necessary to employ a real PEM fuel cell system, and a model structure or mock-up would suffice for the experimental objectives. Therefore, a model structure of a PEMFC was constructed where water can be impinged directly by using nozzles. Figure 24 shows the prototype structure used in this research project.

As can be seen from Figures 24 and 25, the structure has two compartments simulating two individual cell compartments in a PEM FC Stack. The structure is made of Plexiglas so that water patterns can be visually observed as water flows. There are two stainless steel 303 tubes entering each compartment through the top lid, one for holding the nozzle and one for delivering air. There are screw arrangements made in the top lid such that the steel tubes can be moved up and down (Figure 26). This allowed changing the height of the nozzles from the top edge of the Ni-metal foam. The top lid is arranged such that it can be easily opened whenever required. This allowed easy replacement of the nozzle whenever that became necessary during the course of experiments. This also made it easy to make connections of the tubes to the water supply line.

It should be mentioned here that most of the dimensions of this model structure were obtained from an actual fuel cell stack design by Stren Mechatronics Inc., Houston built for Reliant Energy (Houston) in 2002 under license from Texas A&M University and Lynntech Inc. (College Station). The actual design of Stren cannot be outlined here for proprietary reasons, but the approximate dimension and the idea of the location of the Ni-metal foam inside the prototype structure and reactant gas supply were basically inspired by the Stren design.

The inner walls have four screws to hold the Ni-metal foam upright. The front walls of both the compartments are screwed to the side walls. This arrangement allowed removal of the front walls whenever it was necessary to put a new Ni-metal foam inside the structure. The edges of the front walls contain an o-ring to ensure that they are tightly attached to the structure and there is no air or water leakage.

5.3.2 Nozzles

As previously discussed, the water delivery system that was devised to deliver water in the PEMFC for this research project employs direct injection of water through nozzles (as seen in Figure 27). Two different types of nozzles were used, Bete type PJ and Bete type BJ nozzles for producing finely atomized conical fog flow and flat fan flow respectively. A brief description of the nozzles may be found in Figures 17 and 20.

PJ type nozzles generate conical fog comprised of very fine water droplets (average size within 50 microns), as seen in Figure 19. They are highly energy efficient. They are one piece compact construction and include no whirl vanes or internal parts. They can be connected to either $1/4^{//}$ or $1/8^{//}$ male connections. There is a 100 mesh screen, 10 micron paper filter included in each nozzle. The ones selected for this project are made of Stainless Steel 303. A summary of the PJ type nozzles is given below:

Design Features

- High energy efficiency
- One-piece, compact construction
- No whirl vanes or internal parts
- 1/8" or 1/4" male connection
- 100-mesh screen, 10 micron paper filter or polypropylene filter

Spray Characteristics

- Finest fog of any direct pressure nozzle
- Produces high percentage of droplets under 50 microns

Spray pattern: Cone-shaped Fog

Spray angles: 90°.

Flow rates: 0.013 to 1.4 gpm (0.043 to 5.34 L/min)

The other type of nozzle used in the project is BJ type. Unlike PJ type, which is of one-piece construction, BJ type is of a three-piece construction. Figure 298 shows the various parts of a BJ type nozzle, which are assembled to produce the final piece. This type of nozzle generates a thin strip fan type flow as shown in figure 14, with relatively coarse atomization. A wide range of spray angle is possible ranging from 0° to 110°.

A brief outline of the characteristics of BJ type nozzles is given below:

Design Features

- Three-piece construction

- Interchangeable spray tips
- Integral strainer
- Male and female connections

Spray Characteristics

- Relatively coarse atomization (more than 180 microns)
- Uniform distribution with tapered edges for use in overlapping sprays

Spray Pattern: Flat Fan

Spray Angles: 0° to 110°

Flow rates: 0.003 to 24.7 gpm (0.011 to 101 L/min)

5.3.3 MKS 1159B Mass flow controller

The flow rate of air was controlled via this controller equipment, which can supply any gas or air at a metered rate set in advance without any operator supervision. Figure 29 shows a photograph of a MKS 1159 b Mass Flow Controller (MFC).

Use of this controller makes the control of the air flow very easy and accurate. The maximum error that is associated with the controller is less that 0.05% of the full scale [24]. The way these controllers work is, upon entering the MFC, the gas flow is divided into two parts, the first one directed to through the sensor tube and the second goes through the changeable bypass. The two paths are then rejoined and pass through the control valve before exiting the instrument. The two paths possess an L/D ratio of 100:1, which assures laminar flow [24].

In the MFC, the resistance heaters are wound on the sensor tube and form the active legs of bridge circuits. Their temperatures are established such that a voltage change on the sensor winding is a linear function of flow change. This signal is then amplified to provide a 0 to 5 VDC output.

The flow controllers accept a 0 to 5 VDC set point signal, compare it to their own flow signal and generate error voltage. This error signal is then conditioned and amplified so that it can reposition the control valve, thus reducing the controller error to within accuracy specification of the instrument [24].

5.3.4 Watts IWTG pressure gauge

Figure 30 shows the pressure gauge used in experimental set-up. This pressure gauge was used to measure the water pressure of the water supply line. As can be seen in Figure 31, the gauge is connected in series with the nozzles. This eased the task of monitoring water pressure before it reaches nozzles. Nozzle flow rate changes with pressure and it was important that a constant pressure was maintained in the water delivery line for the nozzles to deliver a regulated water flow. The gauge is manufactured by Watts Corporation. This pressure gauge, series 276H300, IWTG, has a dial size of 2” and steel black enamel case. The connection category is hose type, which made it easier to connect it to the water supplying line in series (Figure 31). The gauge connects to the female connection. The sensing element for this gauge is a copper alloy bourdon tube. Tin is used as welding material.

5.3.5 Nickel metal foam

As discussed in section 2.2.1.1.1, the PEMFC employs some sort of flow field to distribute the flow of reactant gases inside the cell compartment. There are various types of flow fields currently in use. Nickel metal foam is one such flow field which has recently gained popularity.

One of the most crucial parts of the research objective was to measure the water distribution pattern over the surface of the Ni-metal foam. The foam that was used in this project was supplied by INCO Special Products, NJ. The trade name for the Ni-metal foam is INCOFOAM™. Figure 11 shows one of the foams that were used in this research project and Figure 12 shows a view of the microstructure of this flow field

The INCOFOAM™ is basically a porous structure of nickel metal. They are manufactured in China through a special proprietary process involving chemical vapor deposition (CVD) onto porous polyurethane, followed by electroplating and heat-treatment to remove the polymer. The porosity of the foam is 110 ppi with an area density of 400 gm/m^2. It's thickness is less than one millimeter. The intricate, lattice-like structure of INCOFOAM™ nickel foam ensures excellent conductivity, while its extraordinary porosity (up to 97%) allows for the even distribution of active material [25]. This foam is extremely light and exceptionally pure.

5.3.6 Water collector

Figure 32 shows the water collector used in this research project. The collector was such that it had a necking structure which facilitated water collection. Drierite™ was poured in so that it could trap very finely atomized water. Enough cotton was provided in the bottle opening with Teflon tape around the mouth of the bottle to ensure that no water

was lost. Figure 32 shows a photograph of the water collector used in the experiments for measuring nozzle mass flow rate for water.

5.4 Experimental procedures

This section will outline the experimental procedures for all experiments conducted in this research project. As discussed earlier, there are two fundamental sets of experiments, determination of mass flow rate for the nozzles and of the water distribution pattern in the Ni-metal foam. Therefore, this section will be divided in two subsections. The first will describe the experiments conducted to determine the mass flow rates of the nozzles while the second will describe the experiments conducted to determine the water distribution pattern in the Ni-metal foam flow-field.

5.4.1 Measurement of average water mass flow output from the nozzles

The requirement for measuring the average water mass flow rate of the nozzles was twofold:

a. Data concerning water mass flow rate of the nozzles will help verify the reliability of the nozzles as far as the manufacturer's data regarding their mass flow rate of the nozzles. It is important to ensure that the nozzles discharge the correct amount of water. Therefore as soon as experimental data concerning the mass flow rate of the nozzles were found, they were matched against the manufacturer's data.

b. By knowing the total water output mass flow rate, one can calculate the maximum evaporative cooling possible at constant water pressure. To

dissipate the waste thermal energy, it is necessary that 3.4 – 3.6 mols of water per mol of hydrogen be supplied inside the fuel cell compartments. Therefore by determining the mass flow rate of water, one can verify whether the water delivery system is actually discharging the required water flow.

A water collector (Section 5.3) was used to capture water from the nozzles. This collector bottle contained Drierite™ desiccant in tablet form, which captures water very quickly. The steel tube holding the nozzle was totally inserted in the water collector bottle. Plastic and Teflon tapes were wrapped around the mouth of the collector so that no water could escape. The water supply was then switched on and timed collection of water was performed. An appropriate question at this stage is whether we need to use Drierite™ at all since the water flow to the model structure goes to a collector. This reasoning applies for the BJ type nozzle where water droplets are coarse and flow is more or less continuous flat fan type. However, the PJ type nozzles produce very fine droplets (less than 50 micron diameter) some of which may evaporate. So it was decided to use Drierite™ desiccant so that even water evaporated in the prototype, flow could still be separately accurately measured. It is worth mentioning here that, to have meaningful results, the timed collection of water from each particular nozzle was done at least four times.

5.4.1.1 Precautions taken for the experiment

Certain precautions were taken before the start of each experiment. It was made certain that the water collector was completely dry before starting the experiment. The Drierite™ were also checked before each trial to make sure that it did not contain any water or moisture. Drierite™ desiccants change color from blue to pink as soon as they capture water, allowing their total dryness to be checked before each experiment. Before

each experiment, the water collector with the Drierite™ was weighed to record its tare weight.

5.4.1.2 Experimental procedure to measure the water mass flow rate of the nozzles

After the water collector was ready, the nozzle holding tube was inserted in the collector with proper Teflon tape and plastic wrapping and the water supply was switched on. A timer was used to conduct the timed collection of water (10 seconds for each test). After the experiment was over, the collector was removed, sealed with a cap immediately and put in the balance and weighed. The dry collector weight was then deducted from this weight of the collector and mass flow rate was calculated. As mentioned before, to have any meaningful experimental results, each trial for determining mass flow rate of water was conducted at least four times. This process had an uncertainty of +/- 0.5%.

5.4.2 Determination of the water distribution pattern over the Ni-metal foam flow field surface

This experiment was relatively easy but time-consuming. For this experiment, Ni –metal foam was attached and placed inside the model PEMFC structure. Water was sprayed through nozzles on top of the Ni-metal. The water was allowed to spread within the foam flow-field and become distributed. It was decided that water would be sprayed for 10 minutes on top of the Ni-foam to allow water to be distributed over the surface of the Ni-metal foam flow field. Ni-metal foam is a gray foamy material which is why it is easy to visualize the water distribution when water penetrates its surface. Although plain water can be traced visually in the foam, it was decided that “water tracing dye” would be used to trace water distribution in the foam. The dye that used in these experiments

was “Fluoroscent Tracing Dye” which is actually a chemical known as eosin (sodium tetrabromoresorcinolphthalein). It readily dissolves in water and is safe, which is why public works departments use it to trace water [26]. It comes in tablet form. Tablets were put in the steel tube that supplies water to the nozzles. When water flowed through the tube, the tablet dissolved quickly and water assumed the red color. This colored water was sprayed over the Ni-foam flow fields and easily traceable water distribution patterns on the surface of the Ni-foam were obtained, as can be seen in Figure 34.

As soon as the distribution pattern was obtained, a clear tracing paper was put on top of the Ni-metal foam and an outline of the dry area was drawn. Then this area was colored with black ink leaving the rest of the area as white. Therefore the black area of the tracing paper signifies dry area of the Ni-metal foam whereas the rest of the white area signifies wet area of the Ni-metal foam. This tracing was then scanned and converted to digital image. From this digital image, areas with black ink were calculated and distribution parameter was obtained for different nozzles as discussed in the general description section in the beginning of this section.

It is to be mentioned here that, the distribution patterns for both finely atomized conical fog flow and flat fan flow (from PJ and BJ type nozzles respectively) were investigated. PJ type nozzles produce a conical fog type flow whereas BJ type nozzles generate flat fan type flow. Table 1 gives a brief outline of all nozzles used in this experiment.

In the early stages of the research project, it was anticipated that some design and operating parameters might affect the water distribution pattern. This is why a decision was made that water distribution pattern for all these parameters would be investigated thoroughly. The following is a description of the experimental procedure conducted to investigate the effect of these parameters on the distribution.

5.4.2.1 Experimental procedure to investigate the effect of nozzle distance (H) from the Ni-metal foam on water distribution over the Ni-metal foam surface

The parameter H is defined as the distance between the top edge of the Ni-metal foam and the nozzle tip as shown in Figures 15 and 17. For a particular flow pattern (flat fan or fog) and pressure, the distance (H) from which the water is sprayed on the Ni-foam might have some effect on the water distribution pattern. To measure the effect posed by distance H on the distribution of water in Ni-foam, the water spray from all the nozzles was tested at varying distances H. The side wall of the prototype structure had a scale attached which was used to set the distance between the nozzle tip and the top edge of the Ni-metal foam. All the distributions so obtained were recorded and were plotted against the distance parameter H. The dependent variable in this case was the water distribution pattern and the independent variable was distance H. The water pressure was maintained constant

5.4.2.2 Experimental procedure to determine the effect of the nozzle area on the water distribution over the Ni-metal foam surface

Like the distance parameter (H), experiments were conducted to see if the area of nozzle affected the distribution parameter while keeping the pressure and the flow pattern constant. For this experiment, all that was required was to change the nozzles (which changes the its orifice size) and record their individual flow pattern. In this case, the dependent variable was water distribution pattern and independent variable was nozzle area.

5.4.2.3 Experimental procedure to investigate the effect of reactant gas flow on the water distribution over the Ni-metal foam surface

In Section 4.6.2.1.1, equations were developed to examine if the reactant gas flow might have an effect on the water distribution in the Ni-metal foam. It was found that reactant gas flow should not have any effect on the water distribution since terminal velocities of water particles for all the nozzles were found to be greater than reactant gas flow velocity. Hence, water particles should not be entrained by the gas flow. To corroborate this finding, it was decided that experiments would be conducted to see if the water distribution in the Ni-metal foam indeed remained unaffected by the gas flow.

As discussed in Section 5.1, for safety reasons, hydrogen could not be used for this experiment. Instead, air would be used to simulate the hydrogen flow effect. From Section 4.9.2.1.1, the calculated hydrogen was found to be 29.11 cm^3/sec, which is equivalent to 1.7 slm (standard liter per minute). To investigate whether reactant gas flow has any effect on the distribution of water in the Ni- metal foam flow field, air flow at a rate of 1.71 slm and 3 slm were flown in to the prototype along with each type water flow from the nozzles. Hydrogen is about 14 times lighter that air. Hence, if 1.71 slm and 3 slm (the latter is even greater than the required hydrogen flow) of air flow do not affect the distribution of water in the Ni- metal foam, reactant hydrogen will not do it either. The MKS mass flow controller was employed to meter the air flow rate.

This was an easy experiment to perform. All that was necessary was to re-run one of the earlier experiments conducted for investigating the effect of distance H on water distribution at a constant nozzle area and pressure. Unlike the previous occasion, this time the experiment was conducted by supplying air into the prototype PEMFC chamber. The distribution was recorded and was compared with case of the similar experiment performed without air.

6. RESULTS AND DISCUSSION

6.1 Introduction

There were two basic aspects of the experiments conducted in this research project. The first one was to measure the mass flow rate of water to make sure that the water delivery system discharged water at least at the required rate. The second aspect was to determine the distribution of water in the Ni- metal foam. This second part of experiments was carried out to determine the distribution of water in the Ni-metal foam under various cases. The interest was in finding out how various design and operating conditions affect the distribution of water in Ni-metal foam. Therefore water distribution under the influence of following parameters was investigated:

a. Type of flow; conical fog flow or flat fan flow (design parameter)
b. Height of nozzle tip from the top edge of the Ni- foam (design parameter)
c. Orifice areas of the nozzle (design parameter)
d. Effect of reactant gas (operating parameter)

Distributions of water in the Ni- metal foam flow field under the influence of all these parameters were recorded. The experiments were organized such that the above mentioned variables were changed before the start of each experiment; the variables were never changed while the experiments were in progress. This enabled each experiment to be established as a separate case.

The following is a description of the results obtained through the experiments conducted in the research project. The results section will consist of two parts. The first will describe the experiment on the mass flow rate of water and discuss issues related to the results obtained. The second will discuss the distribution of water under the influence

of the above design and operating parameters. This second section will also consider the interpretations of various water distribution patterns in Ni-metal foam obtained through conducting experiments varying the above-mentioned design and operating parameters.

6.2 Mass flow rate of water from the nozzles

The use of direct spray nozzle system for delivering water for evaporative cooling largely depends on whether the nozzles can discharge the required quantity of water to the Ni-metal foam. The design in this research project employs off the shelf nozzles that flow a particular amount of water at a particular pressure. The manufacturer provides data that specifies mass flow rate of these nozzles for various areas at a constant pressure. It was important for the author to verify the manufacturer's data to ensure that the nozzles were actually discharging water at rates they were supposed to. This quantity of water will ultimately determine the amount of thermal energy that can be absorbed through evaporative cooling. In fact, it is highly recommended that this investigation of mass flow rate be done with nozzles when this water delivery system is installed in an actual fuel cell to make sure that the fuel cell will receive the correct amount of water.

Figures 35 and 36 show the comparison between the measured mass flow rate and values specified by the manufacturer, for nozzles of each type of flow (PJ and BJ). It needs to be mentioned here that these mass flow rate values were collected at a constant water supply pressure of 40 psi. To have any meaningful comparison, it was imperative that the manufacturer's supplied values of mass flow rate for nozzles with various areas were also obtained under 40 psi pressure.

From the graphical comparison (Figure 35 and 36), it is clear that both PJ (conical fog type flow) and BJ (flat fan type flow) nozzle do maintain the flow rates

specified by the manufacturer. Curves for both PJ type and BJ type nozzles coincide with the curves obtained by plotting manufacturer's specified mass flow rate data. Therefore, it can be concluded that the nozzles in the water delivery system could reliably discharge water at the proper rate.

6.3 Distribution of water over the surface of the Ni- metal foam

Distribution of water over the surface of the Ni-metal foam is the core of this research project. The water delivery sub-system is designed to deliver water in the reaction zone of the fuel cell system. One may ask, if the objective is to deliver water in the reaction zone of the fuel cell, which is MEA, then why deliver water to the Ni-metal foam? To answer this question, one must have knowledge about the operation of the PEMFC. The Ni- metal foam is always placed in the close contact with the membrane electrode assembly (MEA). Reactant gas H_2, upon arrival in the Ni-metal flow field, is distributed along its surface. This Ni- metal flow field is always placed is always placed in close contact with the MEA. Therefore, if water is available in the Ni-foam, H_2 can dissociate immediately under influence of platinum catalyst and form hydrated hydronium (H_3O^+) ion and water will be transported across the Nafion™ by electroosmotic drag to the cathode side where it can be evaporated providing cooling. Therefore, if one wants to deliver water in the reaction zone of the PEMFC, delivering water over the surface of the Ni-foam flowfield will accomplish the task. Moreover, for proper water management, uniform distribution of water in the Ni- metal foam flow field will also ensure a uniform distribution of water in the MEA of the PEM FC. Therefore, one chief objective of this research project, along with delivering water in the Ni-metal foam, was to distribute water evenly along the surface of the Ni-metal flow-field.

As already stated, the distribution of water over the Ni-foam under the influence of design and operating parameters was investigated. The following is a description of

various water distribution scenarios that were obtained by varying the design and operating parameters.

6.3.1 Influence of type of flows on the distribution of water over the surface of the Ni- metal foam

In the early stage of the research, it was decided that two different types of flow (conical fog flow and flat fan type flow) would be used to investigate which type of flow performed better as far as the distribution of water in the Ni-metal foam was concerned. Figures 37 and 38 show two distribution patterns obtained by employing two different type flows. These patterns were obtained by placing both types of nozzle at a distance (H) of 9 cm at a water supply pressure of 40 psi. Moreover the equivalent diameters for both type of nozzle were also the same (0.05 cm). The square block represents the outer boundary of the Ni-foam. The dark areas represent the dry areas of the Ni-metal foam flowfield where water could not penetrate.

It is obvious from Figures 37 and 38 that the flat fan type flow (BJ nozzle) gives a much better water distribution in the Ni- metal flow field keeping all other parameters constant. In fact, the distribution of water in the case of the PJ nozzle is rather disappointing. Some areas were quite water starved, which may ultimately give rise to uneven water distribution and cooling of the MEA.

It was important to determine the reason behind this poor distribution in case of conical fog flow (from PJ type nozzle). A logical question that needs to be addressed here is whether it is caused by the flow type or the structure of the Ni-metal foam itself. Either of the two causes can be the reason behind the poor distribution. The Ni-metal foam used in this research possesses some grease in its structure. This grease is inherent in its surface and comes from a final manufacturing process. Initially, the speculation

was that grease may be the reason that water was flowing down very quickly and Ni-metal foam pores could not contain water and a poor distribution of water occurred. In that case, the Ni-metal itself may be the reason for the poor distribution, not the flow type.

On the other hand, conical fog type flow can also be the contributing factor for poor distribution of water in Ni-foam. PJ type nozzles generate very fine water droplets with a conical coverage area. As a result, water droplets get distributed in a wide area. The Ni-flow field is a thin strip of metal. Therefore, it might well be the case that water particles were too much conically dispersed while discharged from the nozzle and fell outside the surface of the Ni-metal foam. Actually the Ni-metal foam is thin strip of metal that stands vertically in the PEMFC and therefore also in the experimental model structure. Therefore, if the water flow is too conically dispersed, it may fall outside the thin strip of Ni-metal flow field leaving some area of the Ni-metal flow field water starved.

An experiment was conducted to investigate this issue. The Ni-metal flow field was immersed in acetone to remove any grease that may have been present on the surface of the pores. This grease-free Ni-metal foam was used for the experiments. Water was again discharged from PJ type nozzle from the same distance (9 cm) at a pressure of 40 psi. The distribution parameter calculated in this case was almost equal to the previous case. This enabled the author to conclude that poor water distribution in case of PJ nozzles is not due to the Ni-metal foam's inherent grease. Rather, it was the too conically dispersed flow of PJ type nozzle that caused the irregular distribution of water.

6.3.2 Influence of nozzle tip height (H) on the distribution of water over the Ni-metal foam surface

This section is divided into two subsections. In the first section, the effect of H on the distribution of water over the surface of the Ni-metal foam for the PJ type nozzle (conical fog type flow) will be discussed and the second section, the effect of H on the distribution of water over the surface of the Ni-metal foam for BJ type nozzle (flat fan flow) will be discussed.

6.3.2.1 Dependence of water distribution over the Ni-metal foam surface for the case of conical fog flow from PJ type nozzles

Figure 39 shows the dependence of the distribution parameter on the height (H) of the nozzle tip from the top edge of the Ni-metal foam. These distribution parameters were calculated by placing the Ni-metal foam at various distances at constant water supply pressure (40 psi) with the area of the nozzle orifice constant. Therefore dependent variable here was distribution and independent variable was the distance H between the nozzle tip and the top edge of the Ni-metal foam.

It is very clear from the distribution parameter vs. distance H curve that water distribution in Ni-metal foam for conical fog flow is affected by changing distance H. Initially the distribution of the water gets better as the height H is increased. This is due to the fact that increasing H helps the conical fog flow to be dispersed in a wider area. But, as one can see from the curve, the distribution of water is reduced as the H was increased beyond 9 cm. This phenomenon can be attributed to the fact that if the nozzle is located too far from the Ni-metal foam, water becomes too dispersed and some of the water may even fall outside the Ni-metal foam. It must be remembered that this finely atomized fog flow is conical in shape and therefore too much dispersion will not allow

proper distribution in the Ni-metal foam. It is to be mentioned here that each trial at a particular H was conducted at least four times for calculating the area. This allowed the author to verify the repeatability of the data. It is also to be mentioned here that the area calculation process had an uncertainty of +/- 0.07%.

Dependence of water distribution on the nozzle height is a vital knowledge when the water delivery system is to be installed in the actual fuel cell. The nozzles and the water delivery lines will be part of an external manifold, not an integral part of the fuel cell. Therefore, distance H will definitely play a crucial role in designing the actual system and its outer manifold. For this reason, it is highly recommended that, before employing a spray nozzle system for water delivery in an actual fuel cell stack, the designer must know the distance from which the nozzle should be employed to discharge water to the Ni-metal foam.

6.3.2.2 Dependence of water distribution over the Ni-metal foam surface for the case of flat fan flow from BJ type nozzles

Figure 40 shows the dependence of the distribution of water in the Ni-metal foam (distribution parameter) on the varying distance H for the flat fan type flow from the BJ type nozzle. Like the experiments with PJ type nozzles, these distribution parameters were calculated by placing the Ni-metal foam at various distances, keeping the water supply pressure (40 psi) and the area of the nozzle orifice constant. Therefore, as before, the dependent variable here was the distribution parameter and the independent variable was the distance H between the nozzle tip and the top edge of the Ni-metal foam.

Figure 40 shows that flat fan flow is also dependent on distance. Increasing nozzle height produces a better distribution of water over the surface of the Ni-metal foam. But, some distinctive features can be observed for flat fan flow.

First, when the nozzle was placed at zero distance, the distribution is not uniform. The reason for this is that flat fan flow is discharged in a triangular shape (Figure 14). Therefore the upper two corners of the Ni-metal foam remain water starved. However, as the height H increases, the coverage D of the water spray (Figure 16) starts to cover the top edge of the Ni-foam and better distribution is obtained. This phenomenon is also noticeable in the distribution parameter vs. distance curve in Figure 40.

Another interesting observation from Figure 40 is that after 5 cm mark, the distribution seems to be very less sensitive to the increase in height H (as the reader may observe that the curve is almost asymptotic). The reason behind this type of behavior of the distribution is that after 5 cm mark, the coverage D of the flat fan type flow covers almost the full edge of the Ni-metal foam and further increase of height does not greatly increase the amount of impinged water on the Ni-foam. Therefore it can be concluded that once the coverage D of the flat fan flow covers the top edge of the Ni-metal foam, a further increase in height does not contribute greatly towards the distribution of water in the Ni-metal foam flow field.

From a comparison between -Figures 39 and 40, it can also be concluded that dependence of water distribution by flat fan flow on H is not as strong as that of conical fog flow once the coverage D of the flat fan flow covers the top edge of the Ni-foam.

6.4 Influence of nozzle orifice area (A) on the distribution of water over the Ni-metal foam surface

It was a major concern whether the nozzle area affects the distribution of water in the Ni-foam. An investigation was therefore performed where PJ and BJ nozzles with

four different areas were used and the water distribution in the Ni-foam was observed and distribution parameters were calculated. In each case, the height of the nozzle tip from the top edge of the Ni-metal foam (H) and the water supply pressure were kept constant so that distribution parameters for various areas could be compared. Therefore, in this case, the dependent variable was distribution parameter and the independent variable was nozzle area.

This section is divided into two subsections, the first describing the distribution patterns obtained by varying A for the PJ type nozzle (conical fog type flow), the second describing the distribution patterns obtained by varying A for BJ type nozzle.

6.4.1 Influence of nozzle orifice area (A) on the distribution of water over the Ni-metal foam surface for conical fog flow pattern from PJ nozzles

Figure 41 shows the water distribution parameter as a function of area for conical fog flow from PJ nozzles. It can be seen that increasing nozzle area improves the distribution. This outcome was more or less expected. At a constant pressure, if the area of the nozzle is increased, mass flow rate is also increased. The increased flow of water results in better distribution. In fact, it is not very difficult to see why better distribution of water over the surface of the Ni-metal foam is obtained for the case when area was increased. If two nozzles are employed with one having larger area than the other, then the nozzle with bigger area will definitely have higher mass flow rate discharging more water than the other for a particular time. It is no wonder that higher volume of water will cover more area of the Ni-metal foam than a lower volume of water. That's why in the experiment, when area was increase, higher mass flow rate of water was obtained meaning more water was discharged from the nozzle with bigger area. This increased water covers more area in the Ni-metal foam than whatever water is obtained from comparatively smaller area of the nozzle.

Now, it should be clarified here that, when the water delivery system will be installed in an actual PEMFC - stack, one cannot afford to keep on increasing the nozzle area infinitely to improve the distribution of water in the Ni-foam. There is a limit up to which this area can be increased. The reader may recall that, for accomplishing evaporative cooling, at least 3.4-3.6 moles of water per mol of reactant hydrogen are required. The Nafion™ membrane can transport a maximum of 5 moles of water per mol of reactant hydrogen gas across its surface from the anode side to the cathode side. So, while choosing the area of the nozzle for water delivery, the designer must make sure that the chosen nozzle areas do not discharge more than 5 moles of water per mol of H_2. Otherwise, too much water may clog the pores in the GDL (gas diffusion layer). This phenomenon is known as flooding. This flooding causes blockage in the GDL and prevent proper flow of reactant gases in the MEA. Therefore, reactant gas will not be able to reach the active sites (that contains platinum catalyst) of the MEA. This whole thing will seriously hamper the performance of the PEMFC.

6.4.2 Influence of nozzle orifice area (A) on the distribution of water over the Ni-metal foam surface for flat fan type flow pattern from BJ nozzles

A similar outcome, to that found for the conical fog flow, was found in the case of the BJ type nozzle with flat fan type flow. A change of nozzle area directly affected the water distribution in the Ni-metal foam for flat fan type flow. Figure 42 shows the effect of the change in nozzle area in the distribution of water in the Ni-metal foam when flat fan type flow was used. As may be seen, as in the case with conical fog flow from PJ nozzles, increasing the nozzle area improved the water distribution. However, the curve in this case is a little flatter than that with conical fog flow. This means that flat fan flow is less sensitive to nozzle area change than conical fog flow.

The reason for decreased sensitivity of the flat fan flow can be attributed to the fact that this type always creates a strip of water flow. This strip of water coincides with the flat surface of the Ni-metal foam which is also a strip. No matter how small or big the nozzle area is, the water strip from the BJ nozzle will always impinge as a flat strip of water. However, in the case of conical fog flow from PJ nozzles, an increase in area means a wider water flow (up to a certain level), which improves the water distribution in the Ni-metal foam.

6.5 Influence of reactant gas flow on the distribution of water over the Ni-metal foam surface

As was stated earlier, there was a concern whether the reactant gas flow would affect the distribution of water in the Ni-metal foam, which is why an investigation was required to clarify this issue. Again, due to safety reasons, hydrogen could not be used for this experiment. Instead air flow was used to simulate the effect of hydrogen. It was calculated before that hydrogen requirement for a 35 kilowatt PEM FC is 29.11 cc/ sec or 1.71 slm. Therefore, to see whether reactant gas flow has any effect on the distribution of water in Ni-foam, air was flown into the prototype PEM FC structure at a flow rate of 1.7 slm and 3 slm. Since air is about 14 times heavier than hydrogen, if 1.71 slm and 3 slm (which is even higher flow rate than actual hydrogen flow) does not affect the water distribution, hydrogen flow in the PEMFC will not affect the water distribution either.

For this experiment, water was discharged from both the BJ and PJ type nozzles keeping the distance and the nozzle area constant. In both the cases, distance H was kept constant. The water supply pressure was also kept constant. Then air was flowed together with water spray from both PJ and BJ type nozzles. For both conical fog and flat fan flow, distribution parameters were obtained with air flowing at 1.71 and 3 slm

and plotted on a graph. Distribution parameters for both types of flows at zero air flow (i.e., no air flow) were also plotted in the same graph. Figures 43 and 44 graphically shows the results obtained from this experiment. One can see that the curves in Figures 43 and 44 are almost flat. This means that air flow had no effect on the water distribution.

Experimental proof of this non-existing effect of air flow simulating hydrogen was not unexpected. It was calculated before that reactant gas velocity is much less than the water particle velocity or water flow velocity. However, it was desired to verify the calculations results by conducting experiments.

7. FINDINGS

After the considering all the experimental results, the findings of the research project can be summarized as:

1. Delivery of required amount of water for evaporative cooling was possible by using a spray nozzle system.
2. Distribution of water over the surface of the Ni-metal foam from both types of water flow seemed fairly good (over 93% area of the Ni-metal foam flow field was covered by both types of flows)
3. Flat fan type flow was found to be more effective in covering the surface of the Ni-foam flow field than conical fog flow for distribution of water in Ni-metal foam. In other words, flat fan type of flow gives a better distribution of water in Ni-foam flow field than finely atomized conical fog flow.
4. Distribution of water over the surface of the Ni-metal foam flow field caused by both conical fog flow and the flat fan type flow depends on the location and area of the nozzle. The distribution of water also depends on the type of flow pattern.
5. For all cases, improved distribution of water over the Ni-metal foam flow field was observed by increasing the orifice area of the nozzles.
6. Distribution of water by flat fan type flow found to be less sensitive to location and area of the nozzles used than finely atomized conical flat fan flow.
7. Distribution of water in the Ni-metal foam by conical flow was not as uniform as the flat fan type flow. Keeping the area, the height of the nozzle and the water supply pressure constant for both types of water flow, the average percentage area covered by conical fog flow was 93% and for flat fan flow was 97%.
8. Reactant gas flow did not have any effect on the water distribution pattern over the surface of the Ni-metal foam.

8. CONCLUSIONS

Considering all the findings of the research project, following conclusions can be drawn:

1. It is possible to employ a spray nozzle system to deliver the required amount of water into the PEMFC for evaporative cooling
2. Distribution of water over the surface of the Ni-metal foam will depend on the types of the flow, for example, conical or flat fan type flow.
3. Distribution of water over the surface of Ni-metal foam flow field will also depend on design parameters, such as, the area and location of the nozzle from which the water flow is generated.
4. If a spray nozzle system is used to deliver the required amount of water into the PEMFC for evaporative cooling, the distribution of water over the surface of the Ni-metal foam flow field will not be affected by operating parameter, such as, reactant gas flow.

9. RECOMMENDATIONS

From the findings and conclusions of the research project, the author would like to propose the following recommendations:

1. The first recommendation the author wants to propose is that this water delivery system needs to be installed in a real PEMFC stack and investigate its thermal management capability using evaporative cooling.

2. Further research is required for distribution of water in case of small capacity fuel cells (in the range of 50-100 W). The size of an individual fuel cell of this range is relatively small. It is therefore required to investigate whether it is possible to use an external manifold to arrange the water delivery system or machine the nozzles directly in the bi-polar plates.

REFERENCES

[1] K. Prater, The renaissance of the solid polymer fuel cell, Journal of Power Sources, 29 (1990) 239-250.

[2] J. Larminie, A. Dicks, Fuel Cell Systems Explained, 2nd Edition, John Wiley and Sons Publishing, Chichester, England, 2003.

[3] K. Prater (1994), Polymer electrolyte fuel cells: a review of recent developments, Journal of Power Sources, 51 (1994) 129-144.

[4] R. Cohen, United States Patent 4,994,331, February19, 1991

[5] J. F. McElroy (Suffield, Connecticut), United States Patent *4,795,683,* January 3, 1989

[6] A. Hamada (Sanyo Electric Corporation), European Patent EP0,743,639, 1996.

[7] L. Snyder, A feasibility study of internal evaporative cooling for proton exchange membrane fuel cells, Masters of Science Thesis, Texas A&M University, College Station, December, 2004.

[8] D. Wood, III, Jung S Yi and Trung V. Nguyen, Effect of direct liquid water injection and interdigitated flow field on their performance of proton membrane fuel cell, Electrochemical Acta Journal, 24 (1998) 3795-3809.

[9] A. J. Appleby and F. R Foulkes, Fuel Cell Handbook, Krieger Publishing Company, Malabar, Florida, 1993.

[10] G. Hoogers, Fuel Cell Technology Handbook, CRC Press LLC, Boca Raton, Florida, 2003

[11] K. D. Kreuer, W. Weppner, and A. Rabenau, Vehicle mechanism, a new model for the interpretation of the conductivity of fast proton conductors, Angew. Chem. Int. Ed. Engl., 21, (1982), 208

[12] B.E. Conway in Modern aspects of electrochemistry, Vol 3, Eds J. O'M Bockris and B. E. Conway, Butterworths, England (1964).

[13] A. J. Appleby and E. B. Yeager, Assessment of research needs for advanced fuel cells, Energy International Journal 11, (1986), 137-151

[14] G. Karimi and X. Li, Electroosmotic flow through polymer electrolyte membranes in PEM fuel cells, Journal of Power Sources, 140 (2004) 1-11.

[15] A.B. LaConti, A.R. Fragala, J.R. Boyack, D.E. McIntyre, S. Srinivasan, E.G. Will (Eds.), Proceedings of the Symposium on Electrode Materials and Processes for Energy Conversion and Storage, 77 (1977) 354.

[16] T. A. Zawodzinski, S. Radzinski, R.J. Sherman, V.T. Smith, T.E. Springer and S. Gottesfeld, A comparative-study of water-uptake by and transport through ionomeric fuel-cell membranes, J. Electrochem. Soc. 140 (1993), 1981-1985

[17] D. P Wilkinson, H. H. Voss and K. Prater, Water management and stack design for solid polymer fuel cells, Journal of Power Sources, 49 (1994) 117-127.

[18] R. Mosdale and S. Srinivasan, Analysis of performance and of water and thermal management in proton exchange membrane fuel cells, Electrochimica Acta, 40 (1995), 413 – 421.

[19] A.Faghri, Z. Guo, Challenges and opportunities of thermal management issues related to fuel cell technology and modeling, International Journal of Heat and Mass Transfer, 48 (2005), 3891-3920.

[20] P.R. Margiott, US Patent No. 6365291, 2002.

[21] R.D. Breault, US Patent No. 6548200, 2003.

[22] Y. A. Cengel, M. A. Boles, Thermodynamics: An Engineering Approach, 5th Edition, McGraw-Hill Higher Education, Boston, Massachusetts, USA, 2006.

[23] I. M. Sommerfeld, Theoritical and experimental modeling of particulate flows, Lecture Series 2000-2006, Von Karaman Institute For Fluid Dynamics, Brussels, Belgium, April 3-7, 2000

[24] Product information on MKS Mass Flo™ Controller (1159B) found at Instructional manual for Types 1159B/2159B, 1160B/2160B, 1162B/2162B, 1163B/2163B by MKS Instruments, Inc., Massachusetts, USA (MKS Instruments Inc. is a leading manufacturer of flow control and measurement devices), 1995.

[25] Product information on INCOFOAM TM found at Inco Special Products, New Jersey, USA. (Inco Special Products is the world's leader in specialty nickel products) website: http://www.incosp.com/pdf/sp_incoFoam_en.pdf, 1999.

[26] D. D. Susong**,** Use of fluorescein dye tracing to determine ground-water flow in a glaciated, Alpine Valley, Sylvan Pass, Yellowstone National Park, Wyoming, Paper No 204-1, 2005 Salt Lake City annual meeting (2005).

APPENDIX A

FIGURES REFERRED TO FROM TEXT

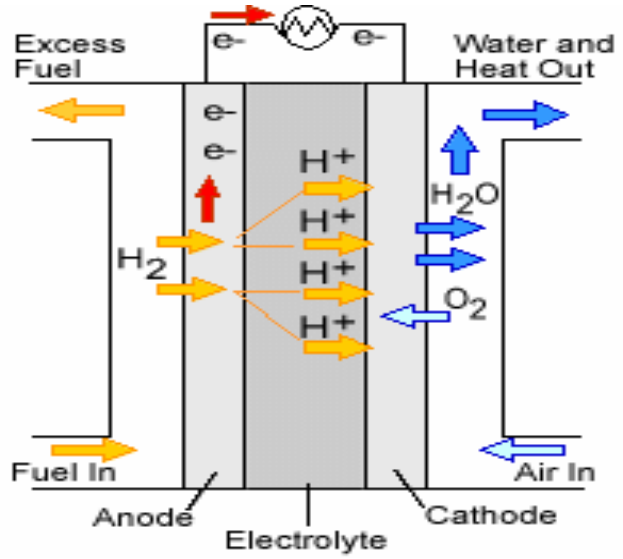

Figure 1: A typical PEM fuel cell and its working principle.

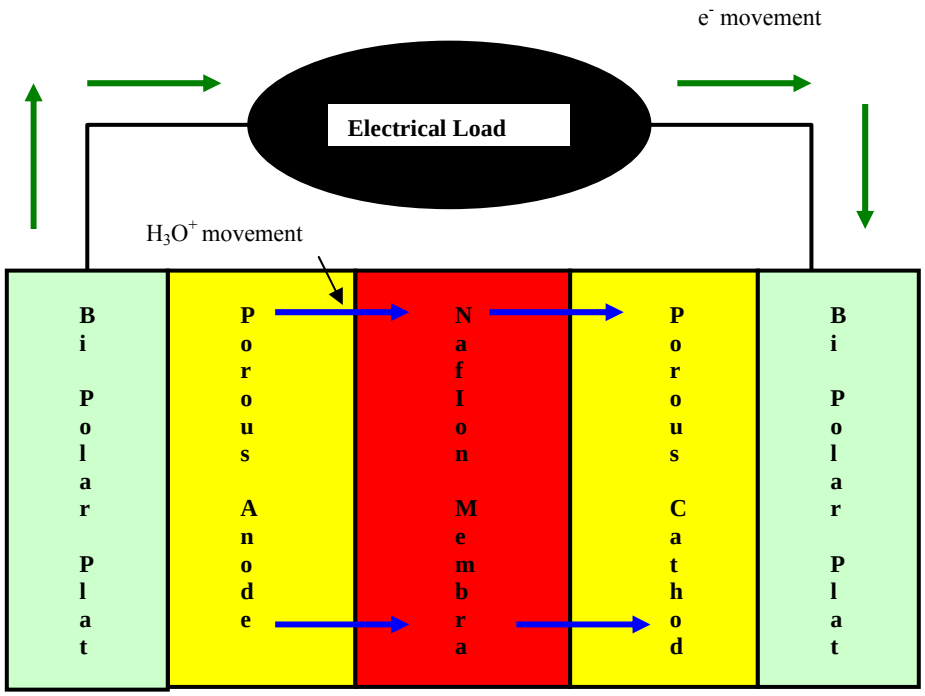

Figure 2: Schematic representation of PEMFC.

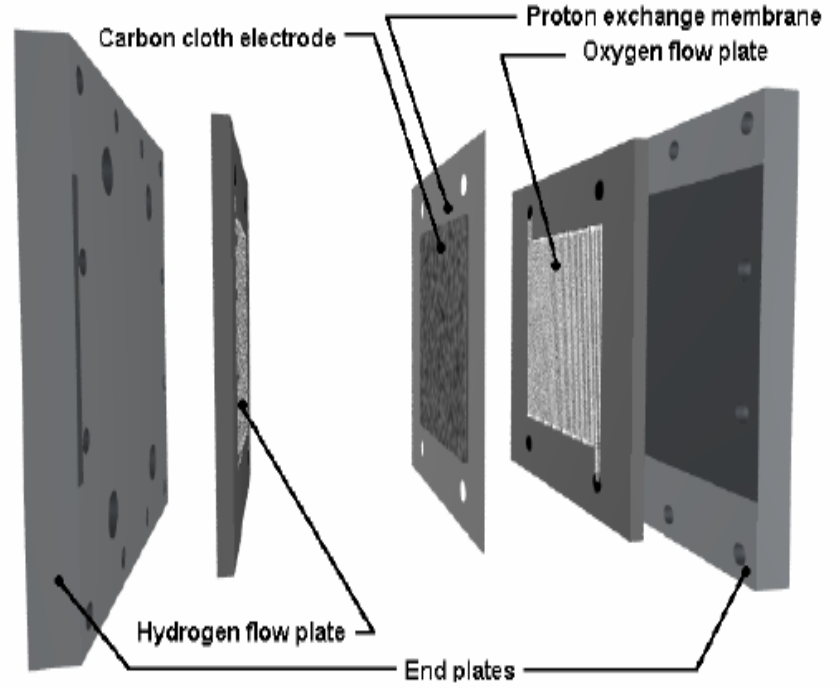

Figure 3a: Components of a typical PEMFC.

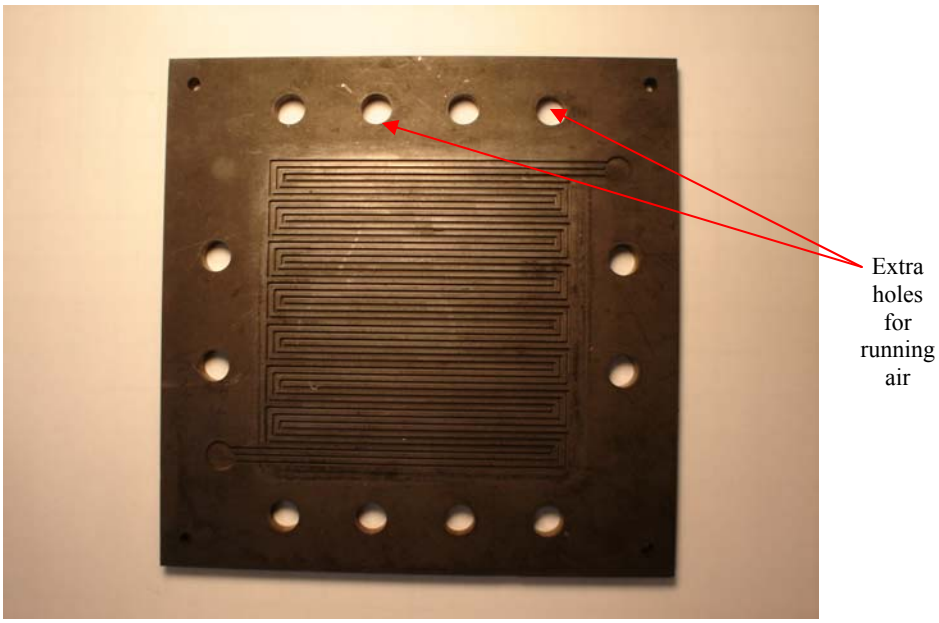

Figure 3b: Extra holes in bipolar plate for running cooling air.

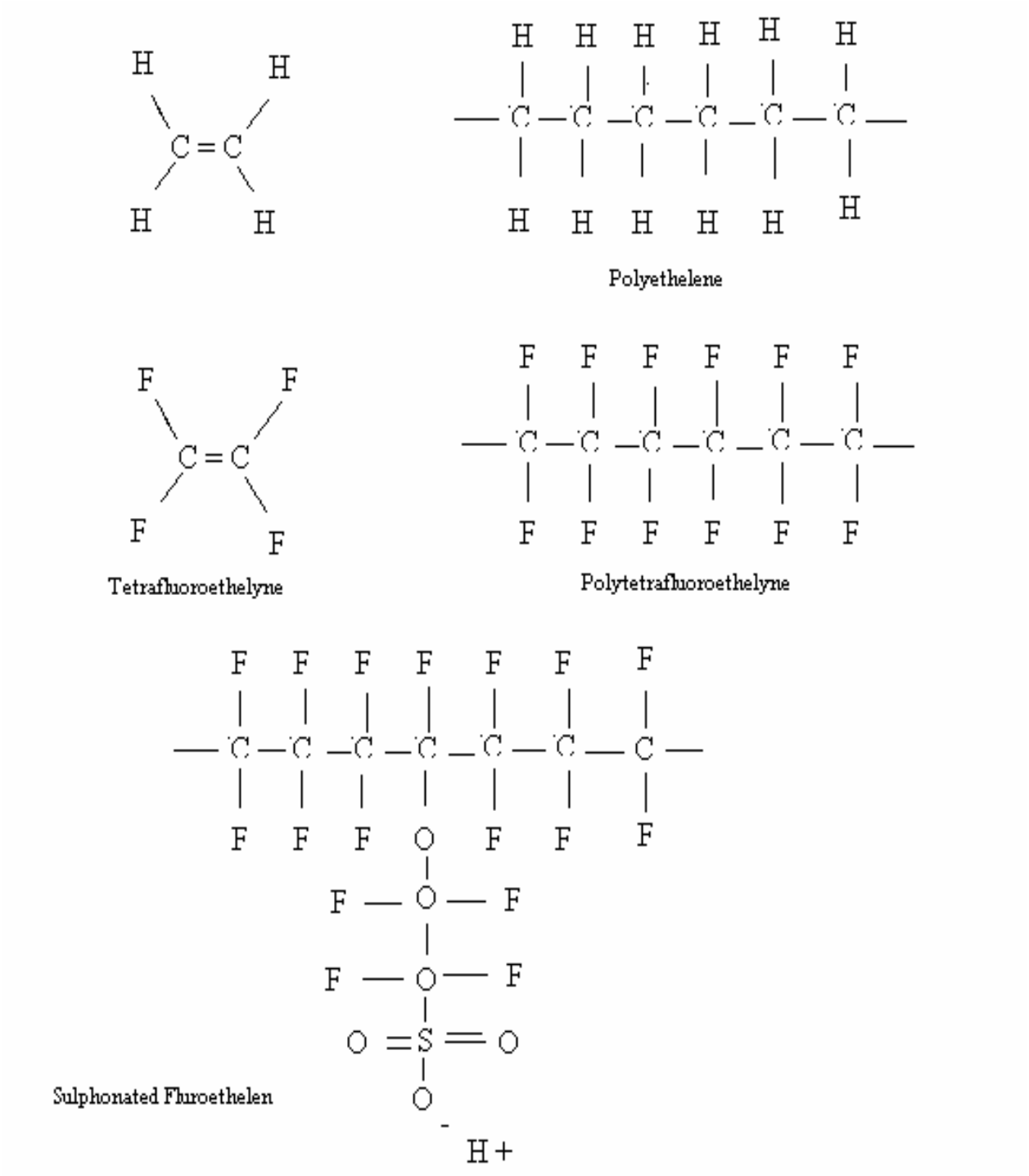

Figure 4: Structures of sulphonated fluoroethylene.

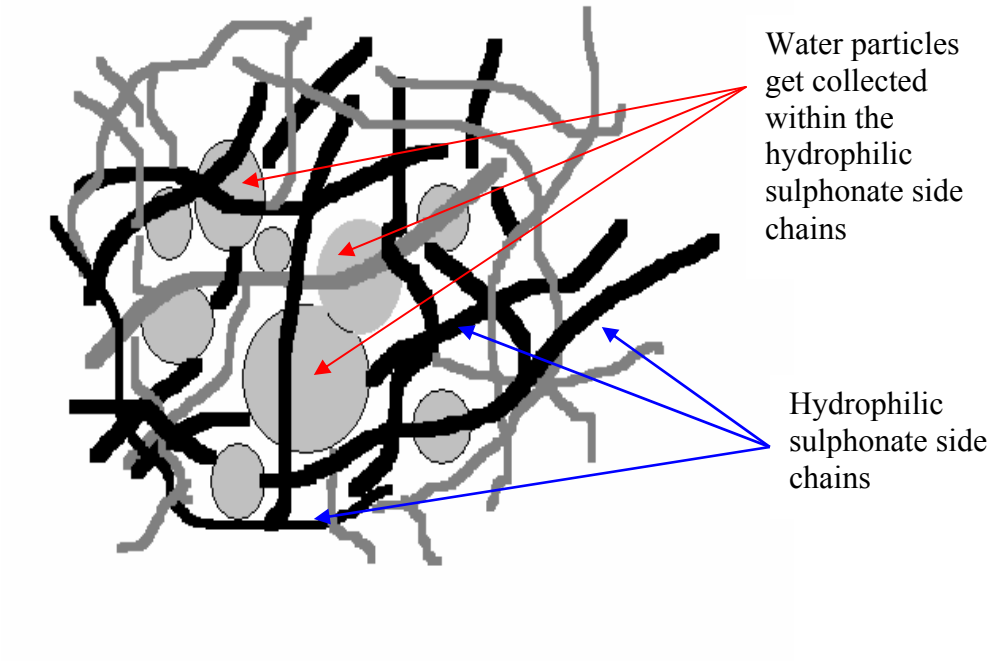

Figure 5: Structure of Nafion™ membrane and the movement of water particles in it.

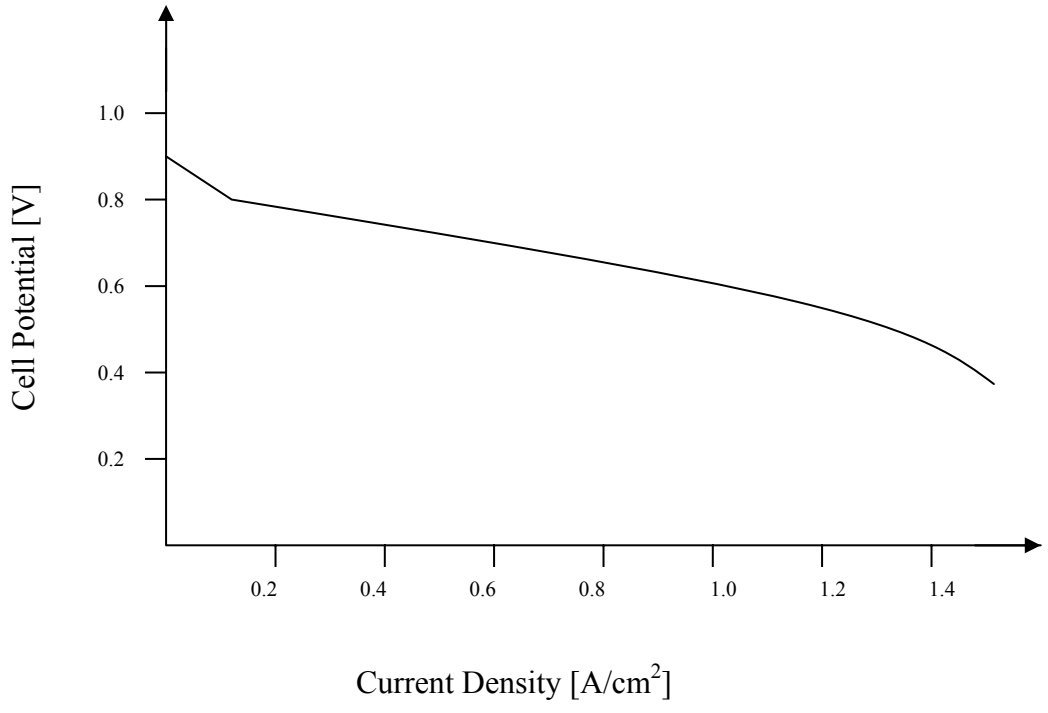

Figure 6: A typical polarization curve for a PEMFC.

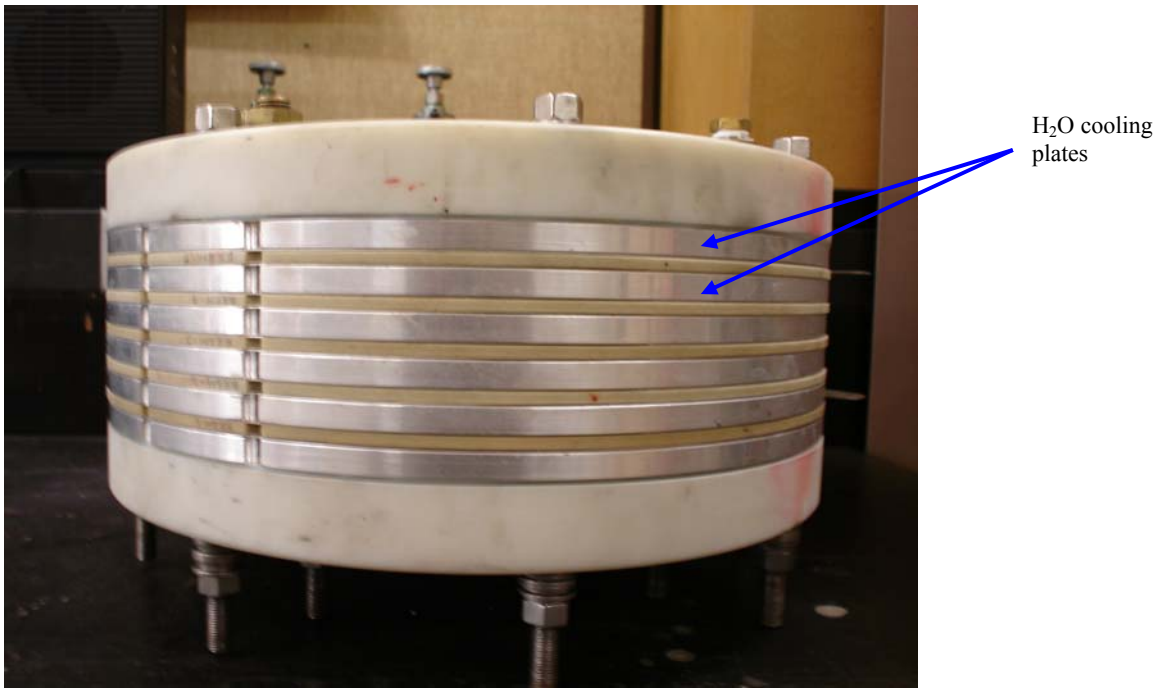

Figure 7a: Side view of water cooled PEMFC stack.

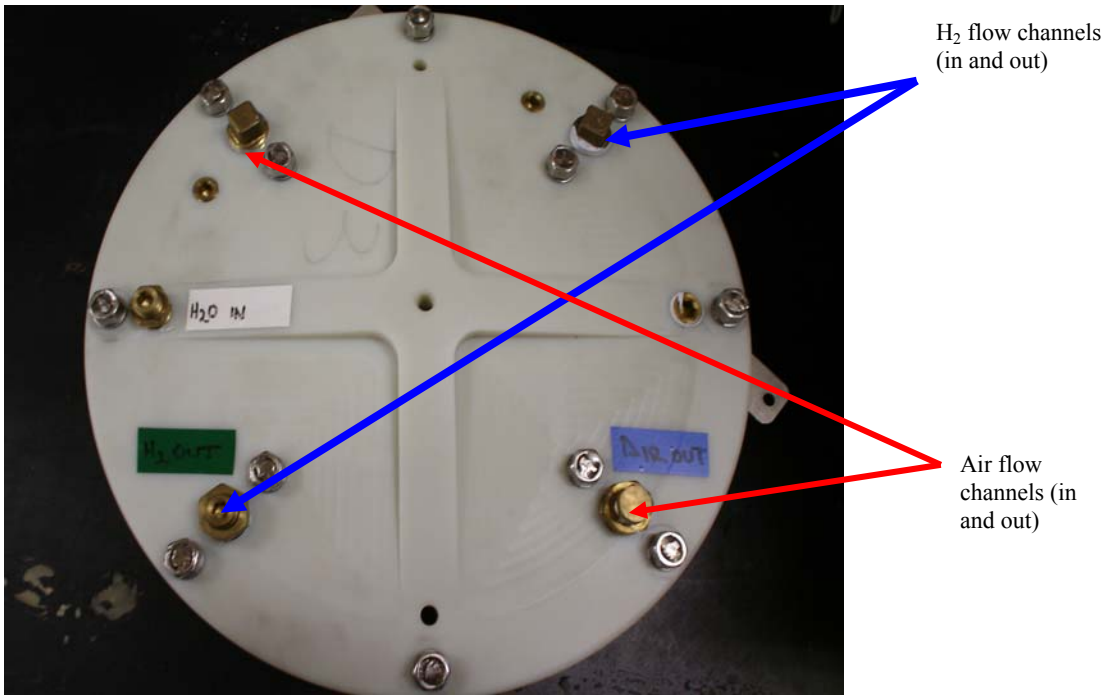

Figure 7b: PEMFC stack. Top view.

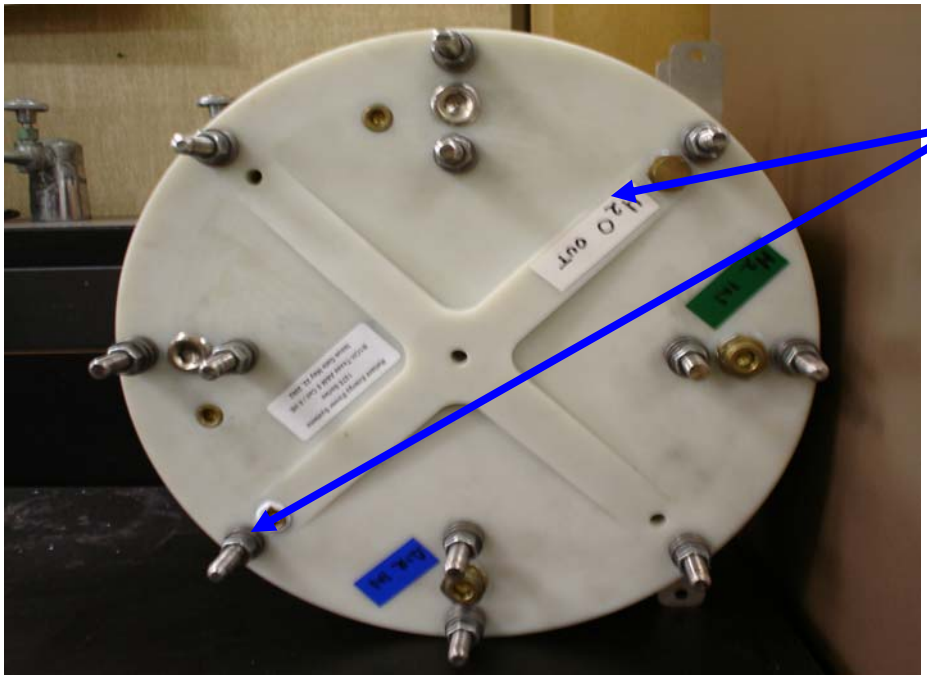

Figure 7c: PEMFC stack. Bottom view.

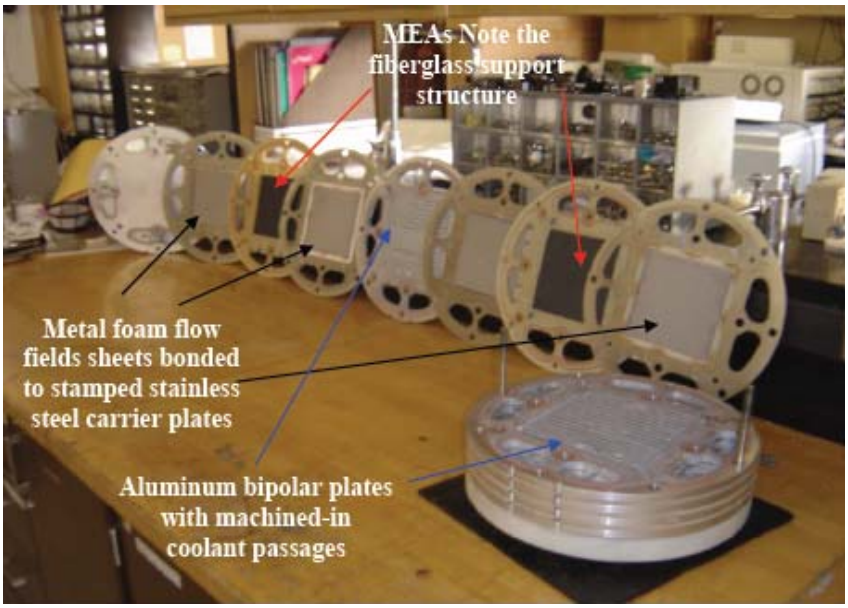

Figure 8: Dismantled PEMFC stack.

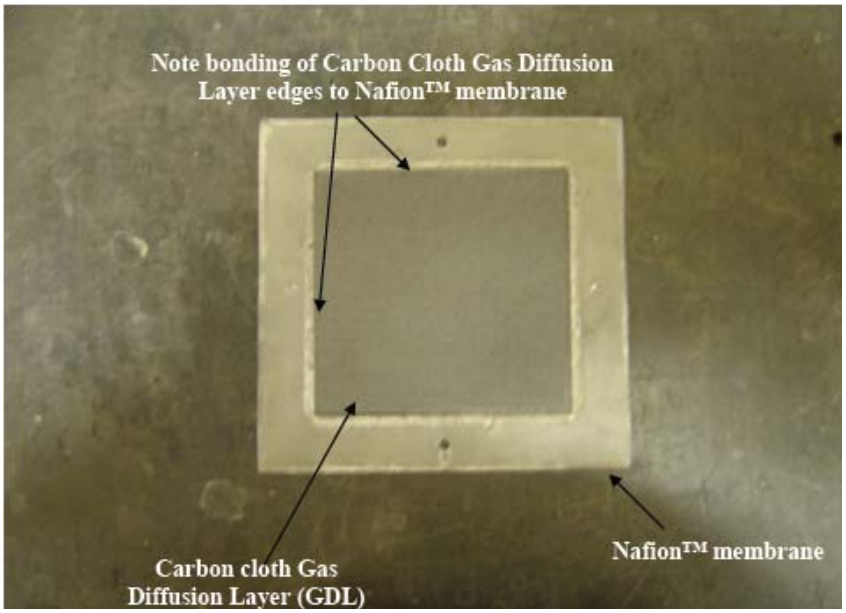

Figure 9: Membrane electrode assembly by 3M Corporation.

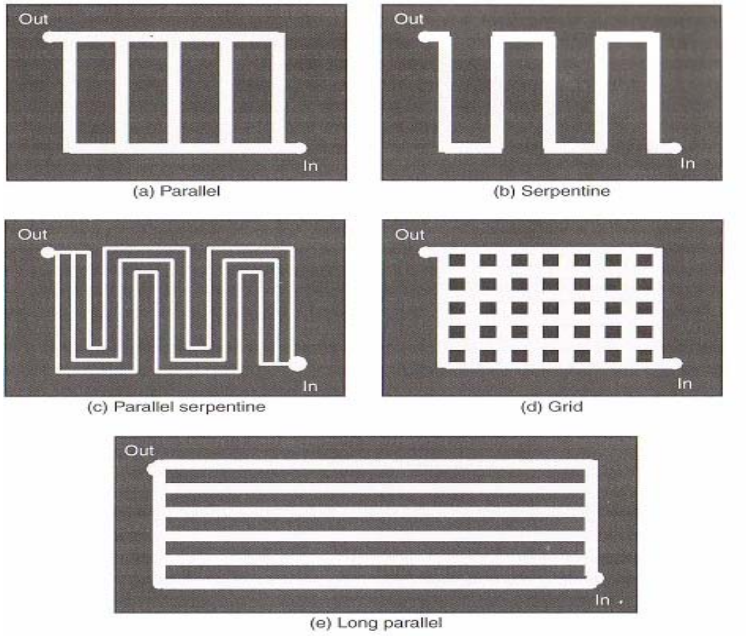

Figure 10: Various patterns of flow fields. Source: J. Larminie and A. Dicks, "Fuel Cell System Explained", 2nd Edition, John Wiley and Sons Publishing, Chichester, England, 2003.

Figure 11: Ni-metal foam flow field used in this research project.

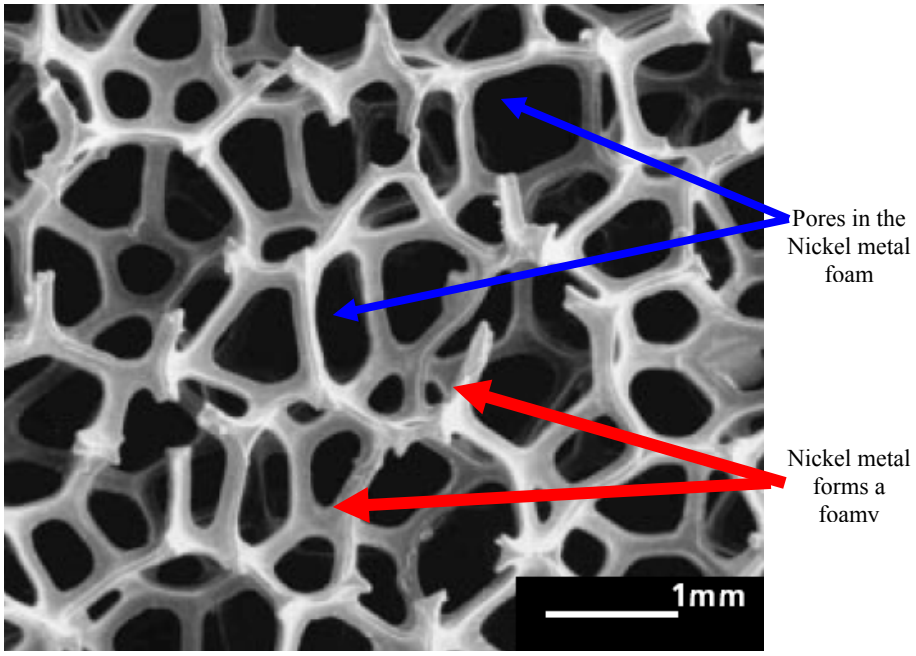

Figure 12: A microscopic view of the Ni-metal flow field used in this research project. Source: http://www.incosp.com/

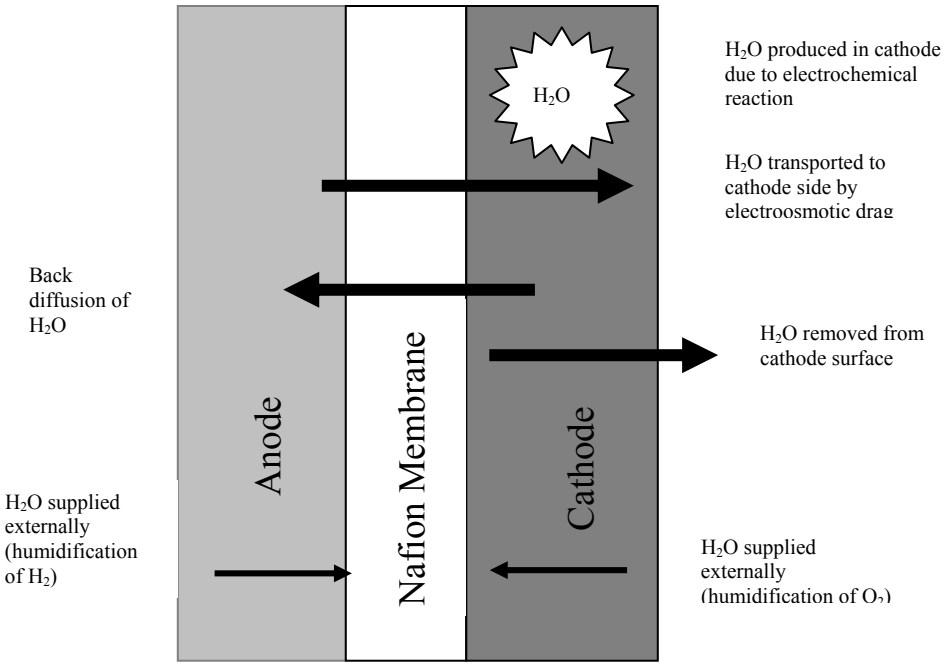

Figure 13: Various water movements in MEA.

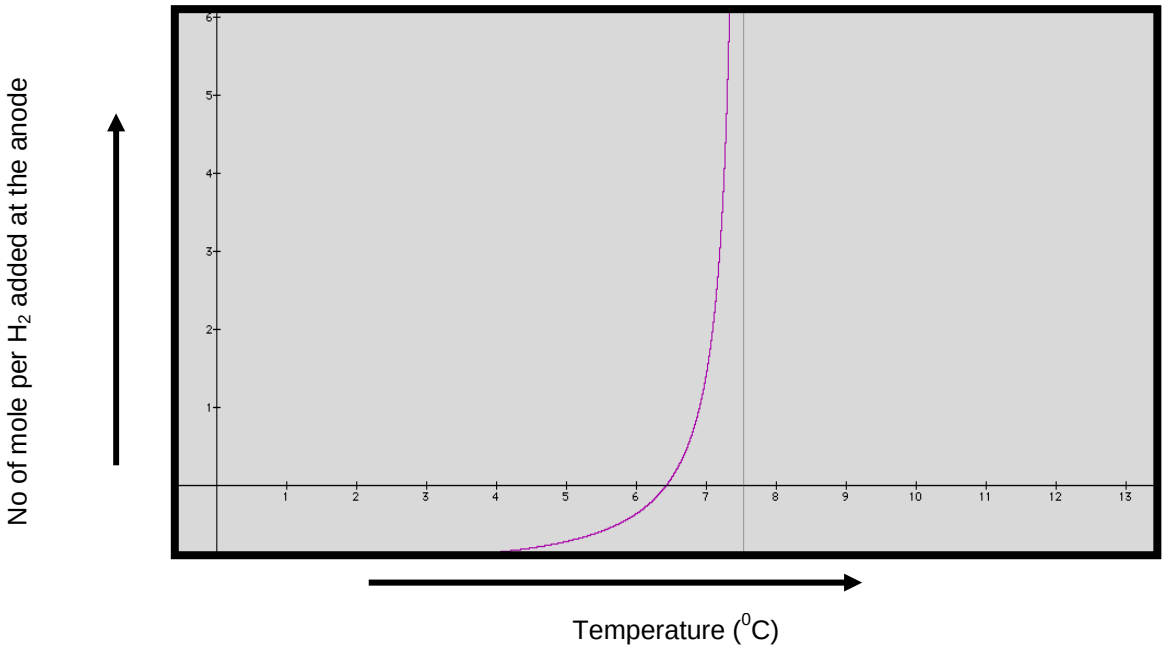

Figure 14: Temperature vs. moles of water added per mole of H_2 curve. For this plot, S = 2.5, V = 0.8 and Pt =1 atm.

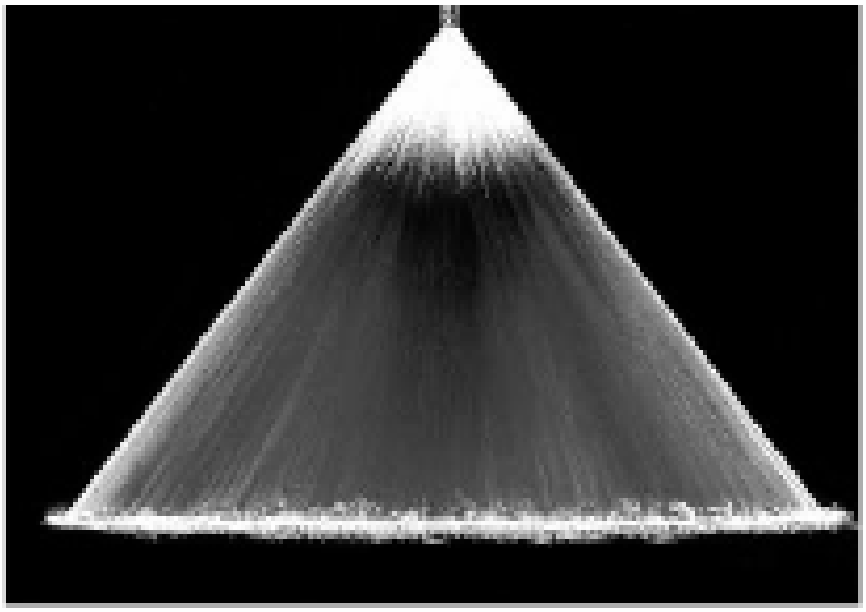

Figure 15: Flat fan type water spray from BJ type nozzles used in this research project. Source: http://www.bete.com

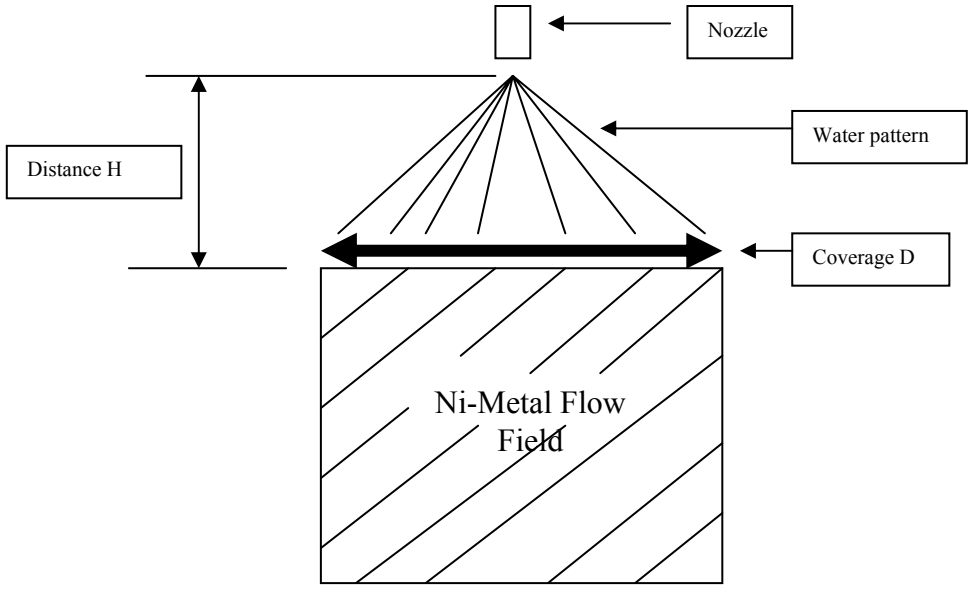

Figure 16: Schematic of a flat fan spray pattern used in this research project.

BJ

Low Flow

DESIGN FEATURES
- Three-piece construction
- Interchangeable spray tips
- Integral strainer available (refer to page 118 for more information)
- Male and female connections

SPRAY CHARACTERISTICS
- Relatively coarse atomization
- Uniform distribution with tapered edges for use in overlapping sprays

Spray pattern: Flat Fan
Spray angles: 0° to 110°
Flow rate: 0.003 to 24.7 gpm

Metal

FAN

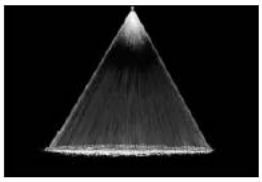

Fan 50°

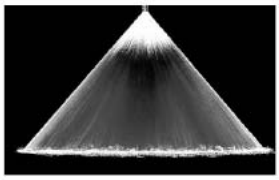

Fan 80°

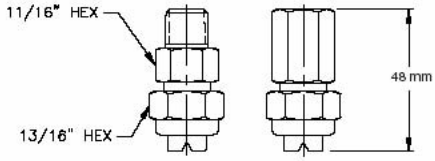

BJ Spray Angles and Weights

Fan, 0° to 110° Spray Angles, 1/8", 1/4" and 3/8" Pipe Size, Male and Female

Pipe Size	Nozzle Number	Flow Rate @ 40 psi	Available Spray Angle 0°	15°	25°	40°	50°	65°	73°	80°	95°	110°	Optional Strainer Mesh Size	Wt. (Oz.)
	BJ 0009	0.009	0°											
	BJ 0012	0.012	0°											
	BJ 0017	0.017		15°	25°	40°	50°	65°						
	BJ 0019	0.019	0°										200	2
1/8	BJ 0021	0.021	0°											
	BJ0023	0.023							73°					
	BJ 0025	0.025		15°	25°	40°	50°	65°						
	BJ 0033	0.033		15°	25°	40°	50°	65°						
	BJ 0039	0.039							73°					
OR	BJ 005	0.050	0°	15°	25°	40°	50°	65°		80°				
	BJ 0067	0.067	0°	15°	25°	40°	50°	65°						
	BJ 0077	0.077							73°				100	2
	BJ01	0.10	0°	15°	25°	40°	50°	65°		80°	95°	110°		
	BJ 0116	0.12							73°					
1/4	BJ 015	0.15	0°	15°	25°	40°	50°	65°		80°	95°	110°		
	BJ 0154	0.15							73°					
	BJ 02	0.20	0°	15°	25°	40°	50°	65°		80°	95°	110°		
	BJ 0231	0.23							73°					
	BJ 03	0.30	0°	15°	25°	40°	50°	65°		80°	95°	110°		
OR	BJ 0308	0.31							73°					
	BJ 0385	0.39							73°					
	BJ 04	0.40	0°	15°	25°	40°	50°	65°		80°	95°	110°	50	2
	BJ 0462	0.46							73°					
	BJ 05	0.50	0°	15°	25°	40°	50°	65°		80°	95°	110°		
3/8	BJ 06	0.60	0°	15°	25°	40°	50°	65°		80°	95°	110°		
	BJ 0616	0.62							73°					
	BJ 077	0.77							73°					
	BJ 08	0.80	0°	15°	25°	40°	50°	65°		80°	95°	110°		
	BJ 0924	0.92							73°					
	BJ 10	1.0	0°	15°	25°	40°	50°	65°		80°	95°	110°		
	BJ 15	1.5	0°	15°	25°	40°	50°	65°		80°	95°	110°		
	BJ 20	2.0	0°	15°	25°	40°	50°	65°		80°	95°	110°		
	BJ 30	3.0	0°	15°	25°	40°	50°	65°		80°	95°	110°		
	BJ 40	4.0	0°	15°	25°	40°	50°	65°		80°	95°	110°		
3/8	BJ 50	5.0		15°	25°	40°	50°	65°		80°	95°	110°	50	2
	BJ 60	6.0		15°	25°	40°	50°	65°		80°	95°	110°		
	BJ 70	7.0		15°	25°	40°	50°	65°		80°	95°	110°		

TO ORDER: specify pipe size, connection type, nozzle number, spray angle, and material.

Figure 17: Datasheet containing the various aspects of the nozzle utilized for the flat fan flow pattern. Source: http://www.bete.com

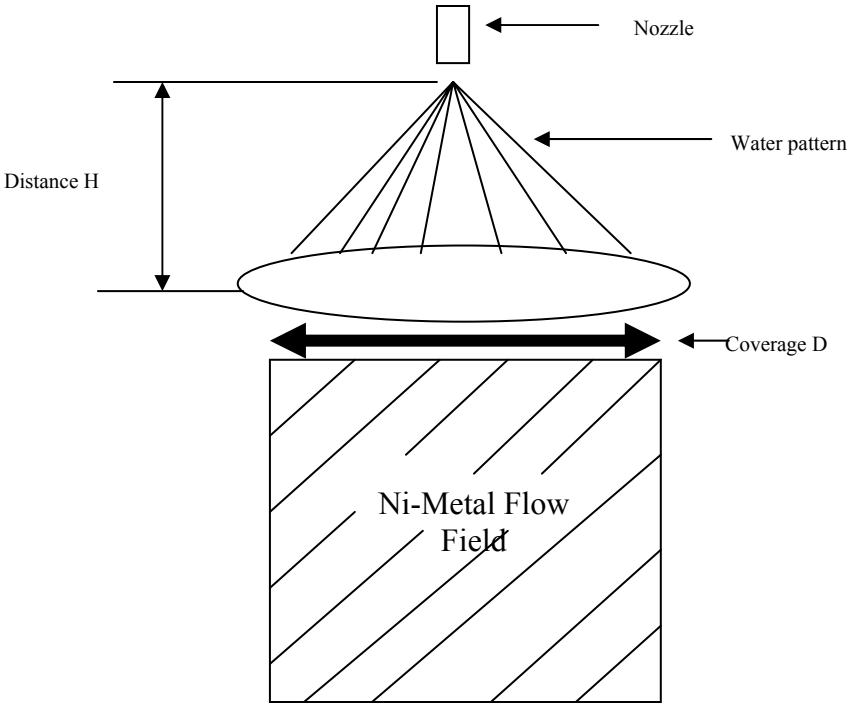

Figure 18: Finely atomized conical fog spray pattern of water.

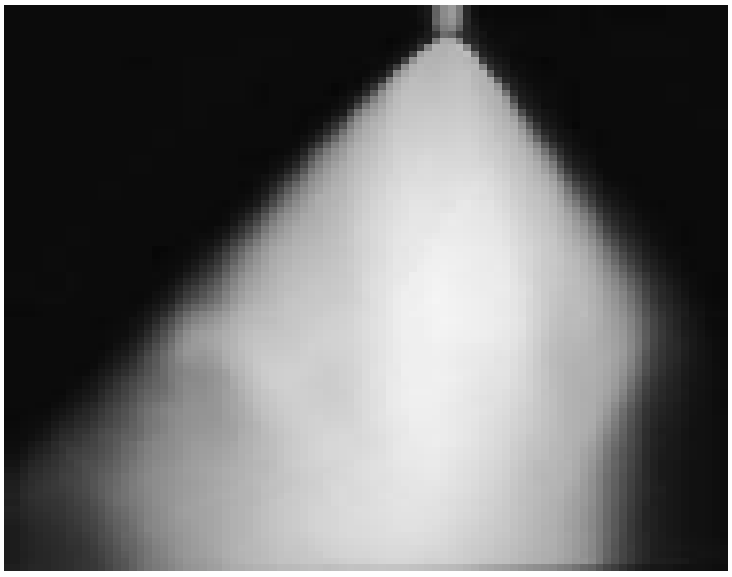

Figure 19: conical fog/mist created by the finely atomized water droplets. Source: http://www.bete.com

PJ

Smallest Physical Size

DESIGN FEATURES
- High energy efficiency
- One-piece, compact construction
- No whirl vanes or internal parts
- 1/8" or 1/4" male connection
- 100-mesh screen, 10 micron paper filter or polypropylene filter optional

SPRAY CHARACTERISTICS
- Finest fog of any direct pressure nozzle
- Produces high percentage of droplets under 50 microns

Spray pattern: Cone-shaped Fog
Spray angle: 90°. For best 90° pattern, operate nozzle at or above 60 psi
Flow rates: 0.013 to 1.4 gpm

Metal

IMPINGEMENT

TO ORDER: specify pipe size, connection type, nozzle number, spray angle, and material.

Fog

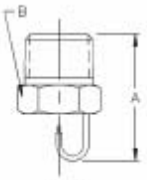

Male

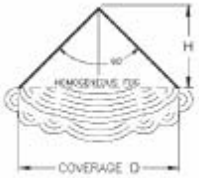

Fog Pattern

PJ with polypropylene filter

PJ Flow Rates and Dimensions

Impingement, 90° Spray Angle, 1/8" or 1/4" Pipe Sizes

Male Pipe Size	Nozzle Number	K Factor	GALLONS PER MINUTE @ PSI 30 PSI	40 PSI	50 PSI	60 PSI	80 PSI	100 PSI	200 PSI	400 PSI	1000 PSI	Approx. Orifice Dia. (in.)	Approx. Coverage (inches) D	Approx. Spray Height H (in.)	Pipe Size	Approx. Dim. (in.) A	Approx. Dim. (in.) B	Wt (oz.) Metal
	PJ6	0.00095			0.006	0.007	0.008	0.010	0.013	0.019	0.030	0.006	10	5				
	PJ8	0.00180			0.013	0.014	0.016	0.018	0.025	0.035	0.057	0.008	10	5				
1/8	PJ10	0.00269		0.017	0.019	0.021	0.024	0.027	0.038	0.054	0.085	0.010	10	5	1/8	0.75	0.44	
	PJ12	0.00364		0.023	0.026	0.028	0.033	0.036	0.051	0.073	0.115	0.012	10	5				
	PJ15	0.00585	0.032	0.037	0.041	0.045	0.052	0.059	0.083	0.117	0.19	0.015	10	5				
OR	PJ20	0.0105	0.058	0.067	0.075	0.082	0.095	0.11	0.15	0.21	0.34	0.020	12	6				0.25
	PJ24	0.0155	0.087	0.10	0.11	0.12	0.14	0.16	0.22	0.32	0.50	0.024	15	8				
	PJ28	0.0205	0.11	0.13	0.15	0.16	0.18	0.21	0.29	0.41	0.65	0.028	15	9	1/4	0.97	0.56	
1/4	PJ32	0.0255	0.16	0.18	0.20	0.22	0.25	0.28	0.40	0.57	0.90	0.032	22	11				
	PJ40	0.0443	0.24	0.28	0.31	0.34	0.40	0.44	0.63	0.89	1.40	0.040	24	12				

Flow Rate (GPM) = K √PSI

Standard Materials: Brass, 303 Stainless Steel and 316 Stainless Steel. See chart on page 21 for complete list.

Figure 20: Datasheet containing the overview of the nozzle used for producing finely atomized conical flow pattern (PJ type nozzle). Source: http://www.bete.com

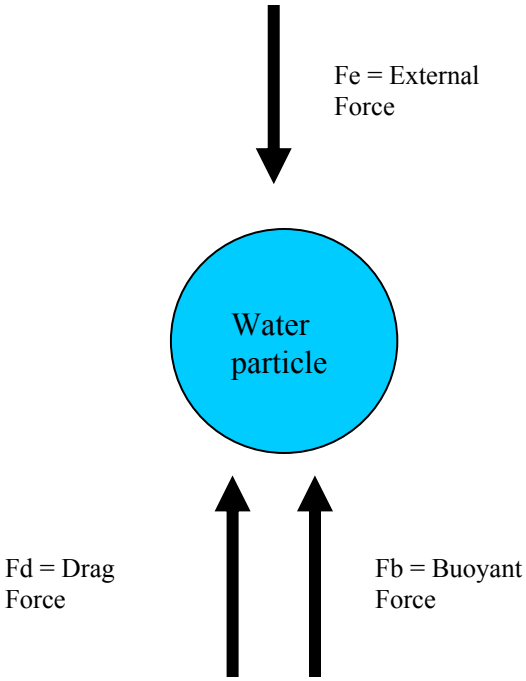

Figure 21: Schematic diagram of various forces acting on a water particle in reactant gas (H_2) environment.

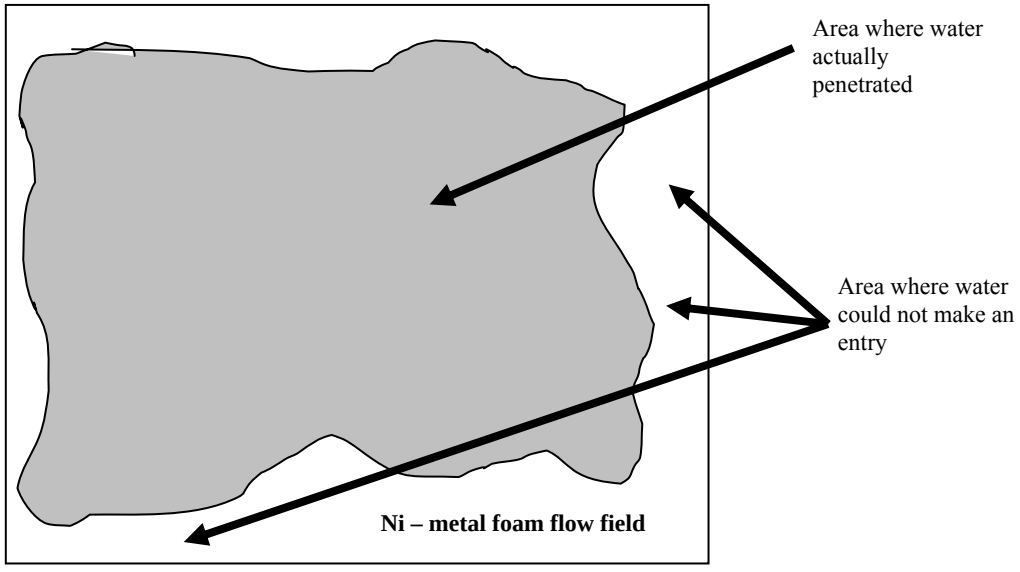

Figure 22: A schematic representation of the areas used for the calculation of distribution parameter.

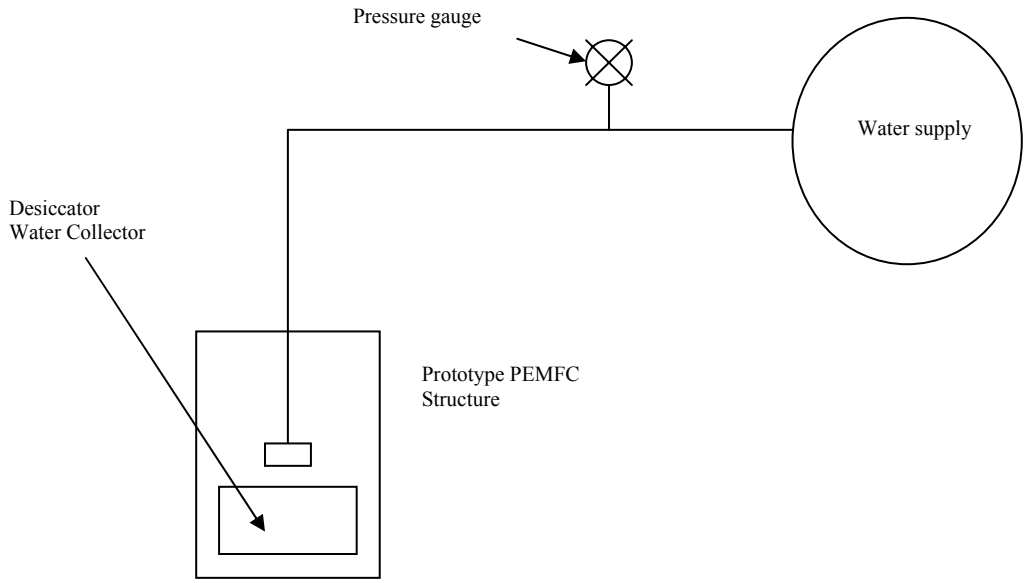

Figure 23: Schematic diagram of the experimental set-up to measure the average water mass flow output of the nozzles.

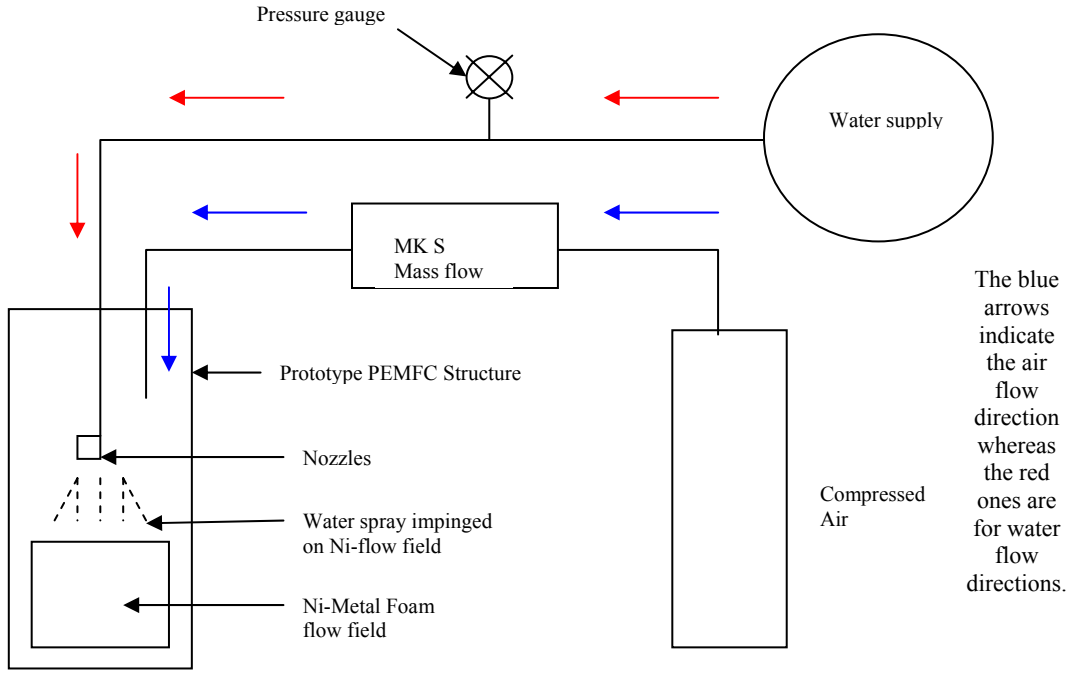

Figure 24: Schematic diagram of experimental set-up to find out the water distribution over the surface of the Ni-metal foam flow field.

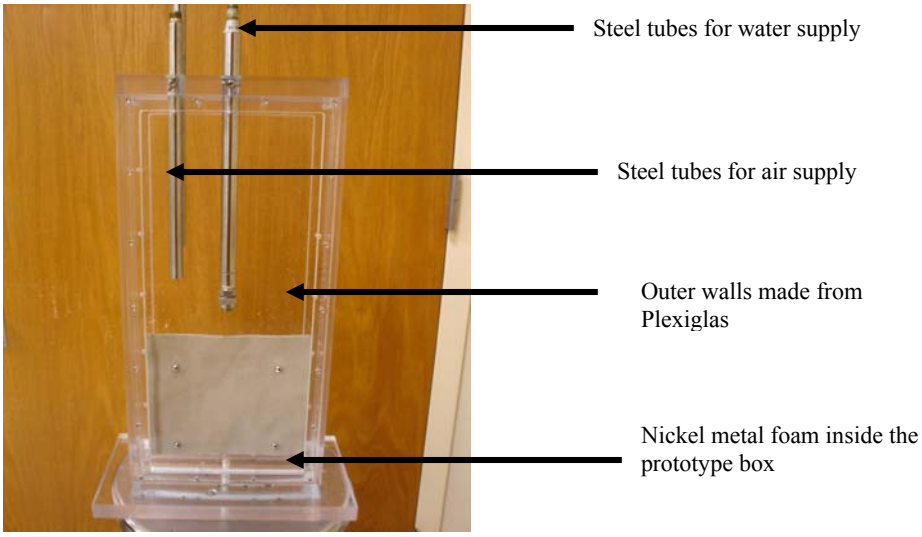

Figure 25: Front view of the model structure used in this research project.

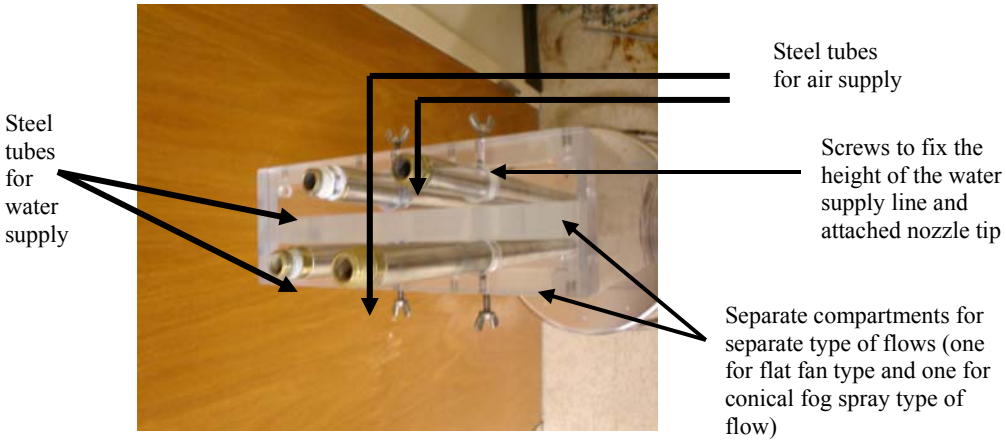

Figure 26: Top view of the model structure used in this research project.

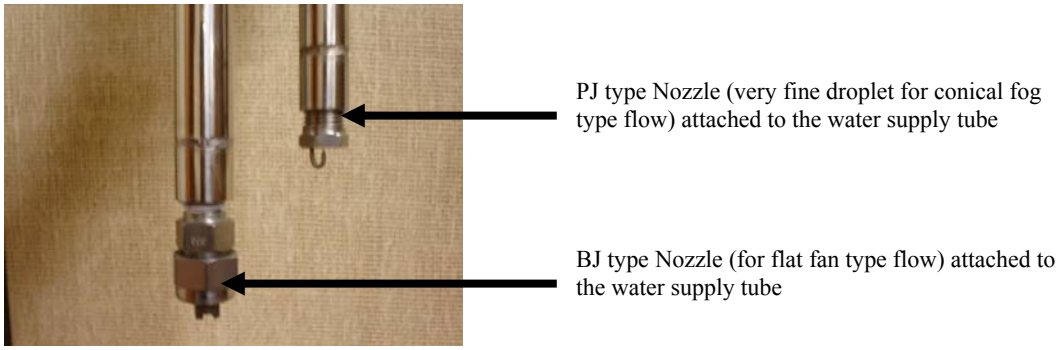

Figure 27: Nozzles in the model structure.

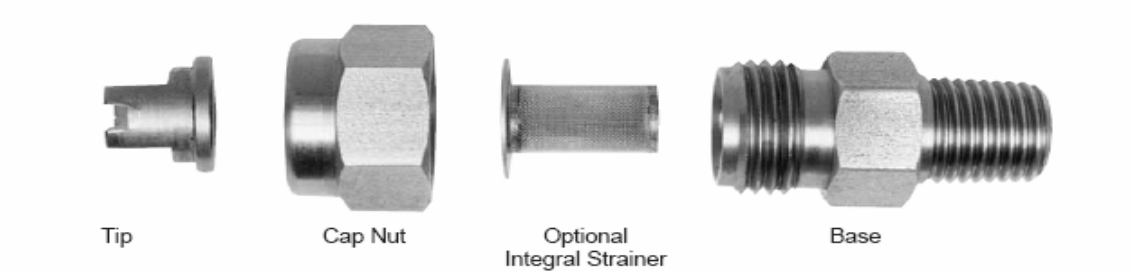

Figure 28: Various parts of a single BJ type nozzle. They are assembled to produce the final piece.

Figure 29: PID mass flow controller.

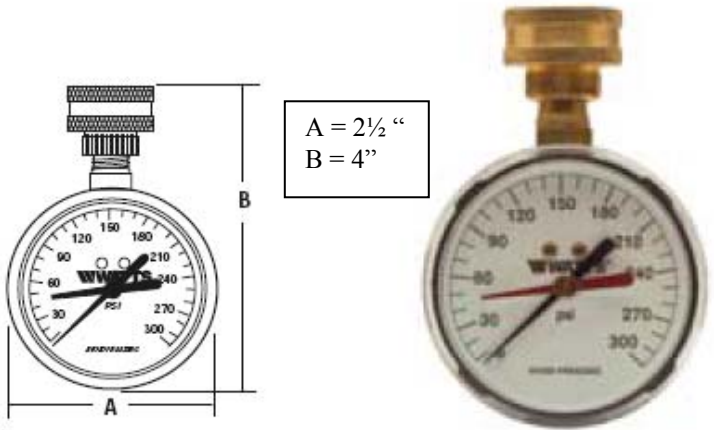

Figure 30: Watts pressure gauge.

Figure 31: Hose pressure gauge connection.

Figure 32: Water collector used in the experiment.

Figure 33: Tracing paper image imported in the Photoshop. The black areas represent dry zones.

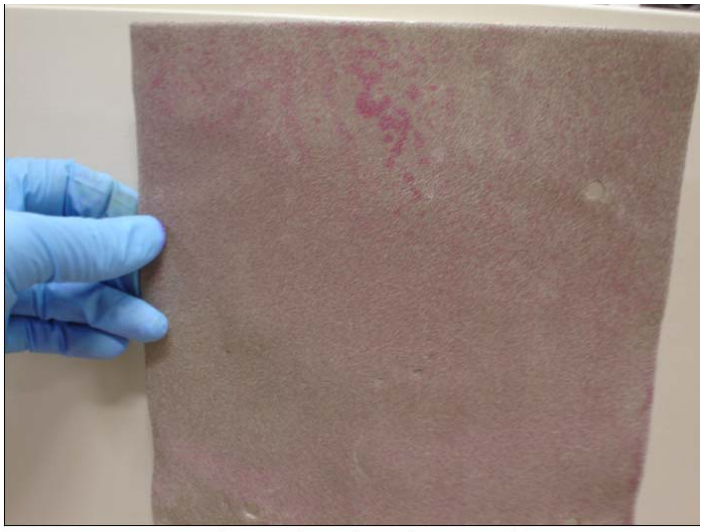

Figure 34: Colored water distribution in the Ni-metal foam.

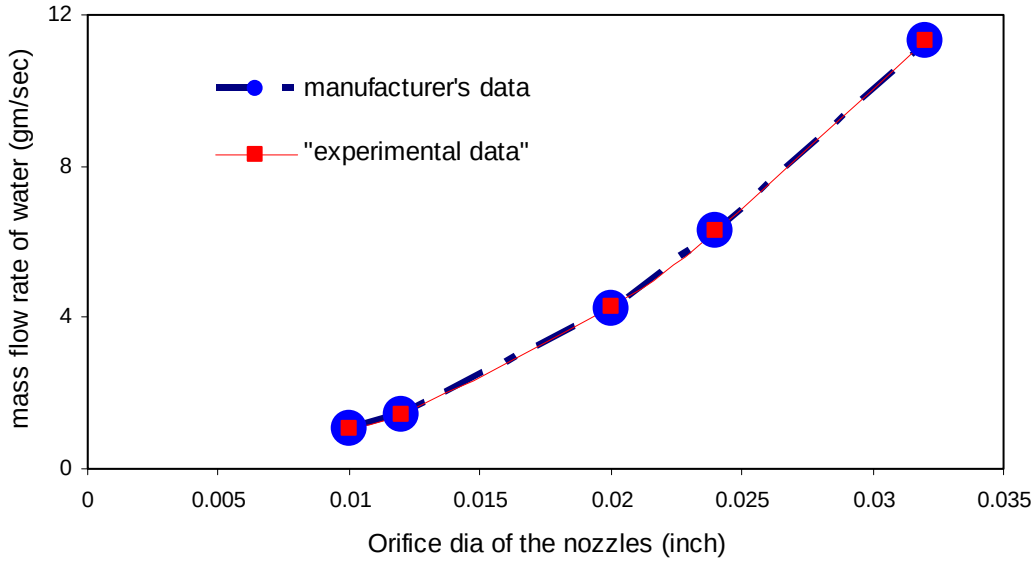

Figure 35: Comparison between the experimentally obtained mass flow rate values with those of supplied by the manufacturer for conical fog flow nozzles (PJ type nozzles with various areas).

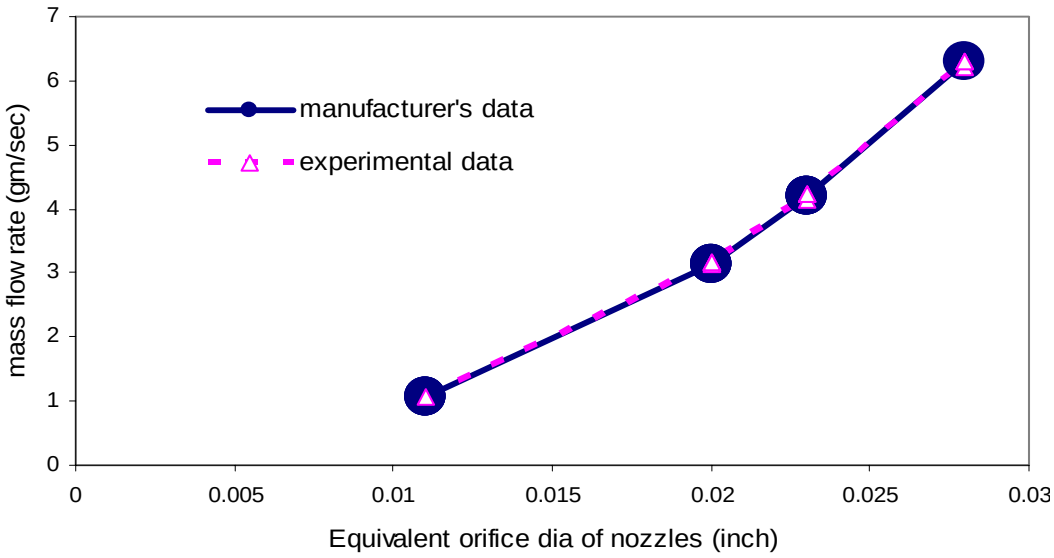

Figure 36: Comparison between the experimentally obtained mass flow rate values with those of supplied by the manufacturer for flat fan flow nozzles (BJ type nozzles with various areas).

Figure 37: Distribution of water over the Ni-metal foam surface obtained by using finely atomized conical flow (PJ nozzles).

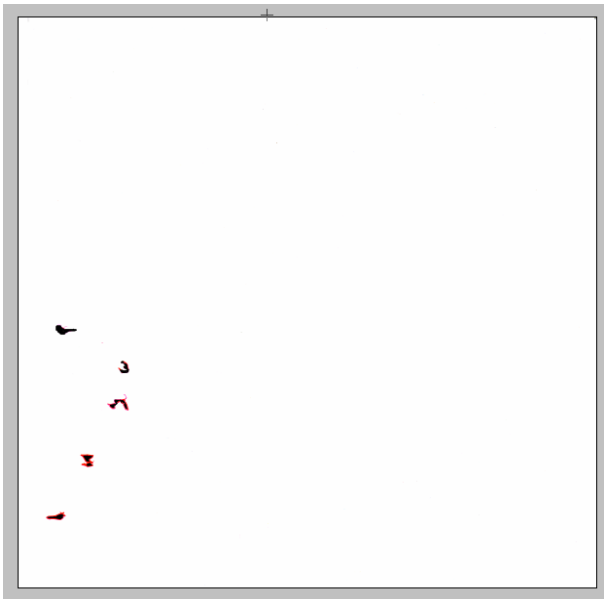

Figure 38: Distribution of water over the Ni-metal foam surface obtained by using flat fan flow (from BJ nozzles).

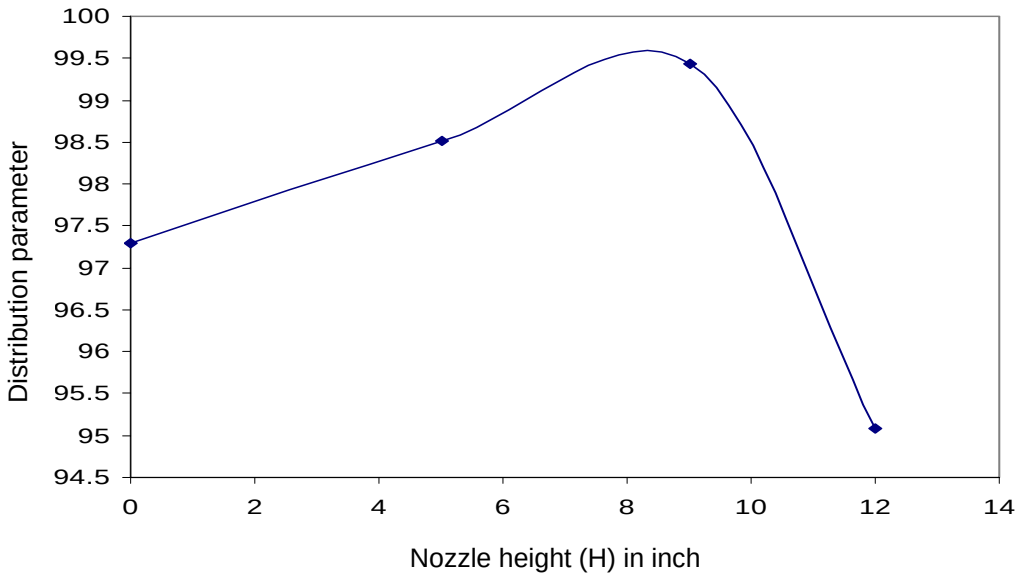

Figure 39: Effect of nozzle height from the top edge of the Ni-metal foam for the finely atomized conical fog flow (PJ type nozzle).

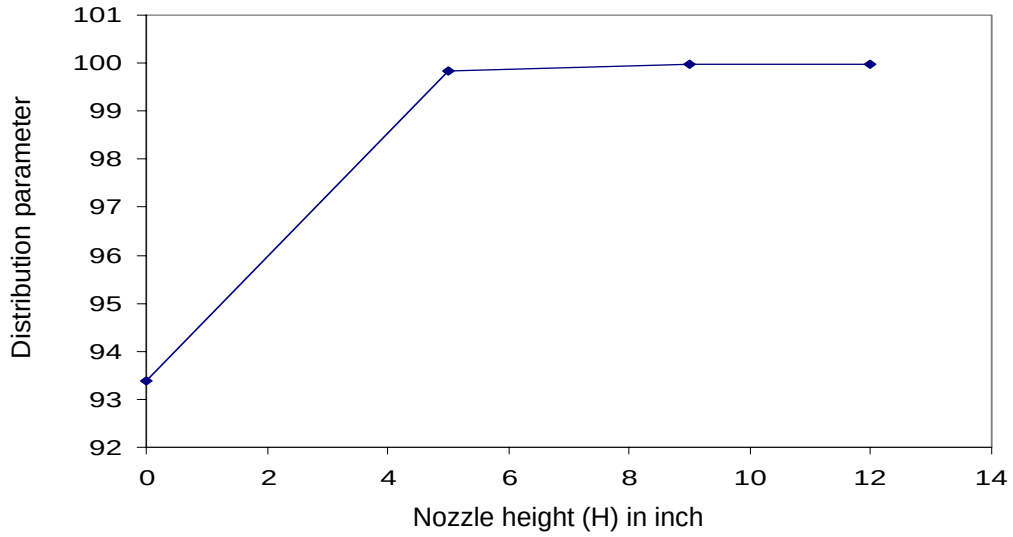

Figure 40: Effect of nozzle height from the top edge of the Ni-metal foam for the flat fan flow (BJ type nozzle).

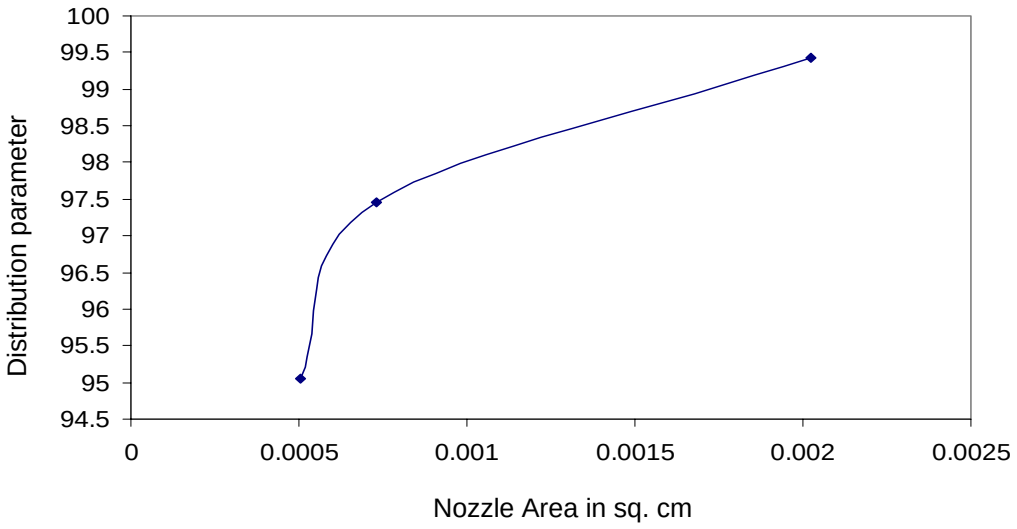

Figure 41: Effect of nozzle area on the distribution of water over the Ni-metal foam surface for the conical fog flow (PJ type nozzle).

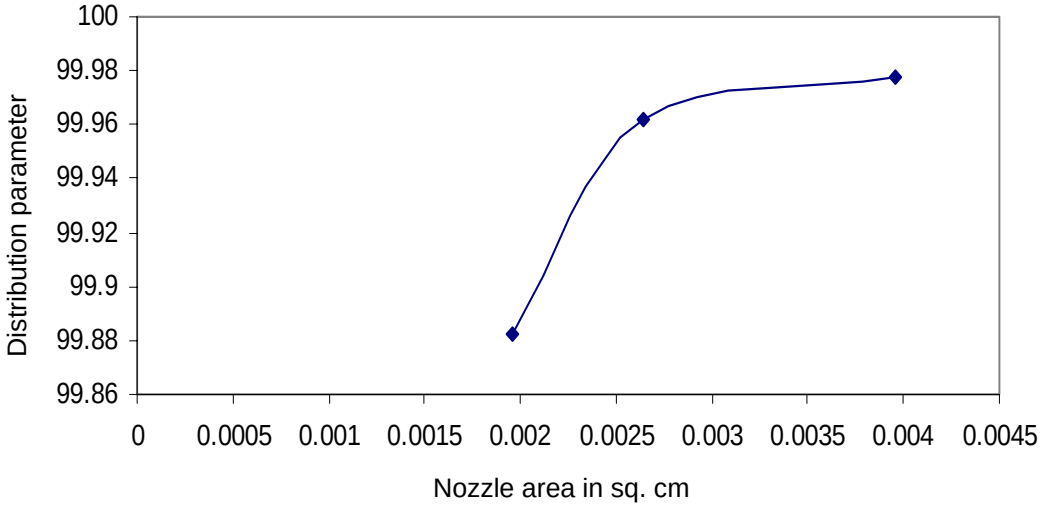

Figure 42: Effect of nozzle area on the distribution of water over the Ni-metal foam surface for the flat fan flow (BJ type nozzle).

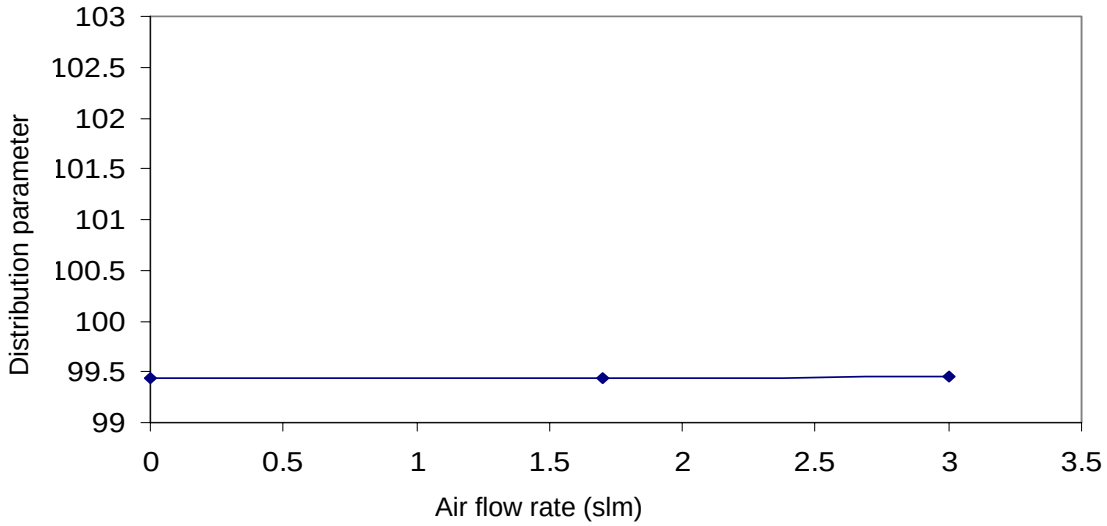

Figure 43: Effect of reactant gas flow (simulated by air) on the distribution of water over the Ni-metal foam surface for finely atomized conical fog flow (PJ Nozzles).

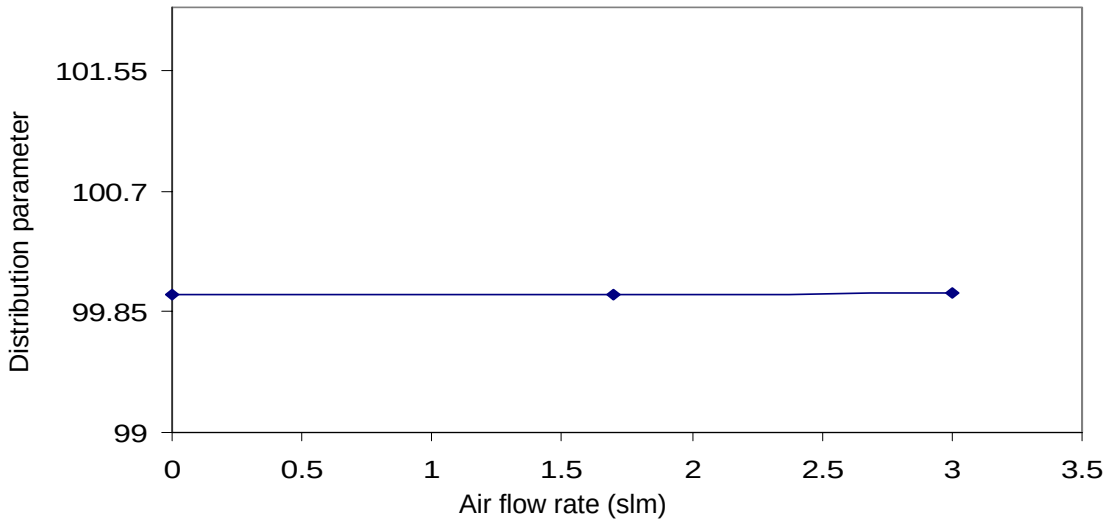

Figure 44: Effect of reactant gas flow (simulated by air) on the distribution of water over the Ni-metal foam surface for flat fan flow (PJ Nozzles).

APPENDIX B

TABLES REFERRED TO FROM TEXT

Table 1: Different values of temperature of PEMFC obtained through using the correlation between water added at anode, cell voltage, oxygen stoichiometry and atmospheric pressure.

Voltage (V)	Stoichiometry (S)	Temperature (T)	Moles water/H_2 at anode (X)	Absolute Pressure (Pt)
0.8	4.0	62.5313	5.00097	1.0
0.8	2.5	70.8438	4.98780	1.0
0.8	2.0	74.6254	4.99495	1.0
0.8	1.6	78.2500	5.01341	1.0
0.7	4.0	64.8438	4.97352	1.0
0.7	2.5	72.9688	4.9754	1.0
0.7	2.0	76.625	5.00804	1.0
0.7	1.6	80.0938	5.0415	1.0
0.6	4.0	66.875	5.02973	1.0
0.6	2.5	74.8125	5.06029	1.0
0.6	2.0	78.3125	5.01483	1.0
0.6	1.6	81.625	5.02713	1.0

Table 2: Effect of moles of water added on the temperature of PEMFC.

Voltage (V)	Stoichiometry (S)	Temperature (T)	Moles water/H_2 at anode (X)	Absolute Pressure (Pt)
0.7	2.5	71.9219	3.01058	1.0
0.7	2.5	73.5313	6.99932	1.0

Table 3: Effect of varying total pressure on the temperature and the water requirement per mole of reactant hydrogen for evaporative cooling.

Voltage (V)	Stoichiometry (S)	Temperature (T)	Moles water/H_2 at anode (X)	Absolute Pressure (Pt)
0.7	2.5	82.8281	5.00000	1.5
0.7	1.6	90.4063	4.99311	1.5
0.7	2.5	90.2188	5.00539	2.0
0.7	1.6	98.1719	5.01032	2.0
0.7	2.5	72.9688	4.9754	2.0
0.7	2.5	96.2031	5.01902	2.5
0.7	1.6	104.453	4.99349	2.5
0.7	2.5	101.250	4.99761	3.0
0.7	1.6	109.781	5.00551	3.0

Table 4: Terminal velocities of water particles in the hydrogen gas environment for the conical fog type flow from PJ nozzles.

Water flow and Nozzle Type	Orifice Dia (cm)	Reynolds Number N_{Rp}	Coefficient of drag C_d	U_t (Terminal Velocity) (cm/sec)	Reactant gas (hydrogen) velocity in the PEM FC (cm/sec)
Finely atomized Conical fog flow (PJ Nozzles)	0.02032	1.27	19	77	5.822
	0.0254	0.86	28	64	
	0.0508	0.28	85	36.9	
	0.0609	0.19	129.35	29.9	
	0.08128	0.0857	279	21.1	

Table 5: Terminal velocities of water particles in the hydrogen gas environment for the flat fan type flow from BJ nozzles.

Water flow and Nozzle Type	Orifice Dia (cm)	Reynolds Number N_{Rp}	Coefficient of drag C_d	U_t (Terminal Velocity) (cm/sec)	Reactant gas (hydrogen) velocity in the PEM FC (cm/sec)
Flat fan flow (BJ Nozzles)	0.0508	0.52	46	65	5.822
	0.05842	0.37	65	58	
	0.07112	0.28	79	41	

Table 6: List of nozzles used in the research and their orifice diameters.

Nozzle Type	Orifice Diameter (cm)
PJ 12	0.0254
PJ 20	0.0508
PJ 24	0.0609
BJ 005	0.0508
BJ 0067	0.05842
BJ 01	0.07112

VITA

Name:

Dawood Khaled Abdullah Al-Asad

Address:

293 New Park Place

Columbia, SC-29212.

Education:

B.S. Mechanical Engineering, Bangladesh University of Engineering and Technology, Dhaka, Bangladesh.

MS Texas A&M University, College Station, TX